NASA LEWIS SEMI-ANNUAL STATUS REPORT
NAG 3-67 (6/1/81–12/1/81)

PREDICTION OF SOUND RADIATION FROM DIFFERENT PRACTICAL JET ENGINE INLETS

By

Ben T. Zinn
William L. Meyer

GEORGIA INSTITUTE OF TECHNOLOGY
A UNIT OF THE UNIVERSITY SYSTEM OF GEORGIA
SCHOOL OF AEROSPACE ENGINEERING
ATLANTA, GEORGIA 30332

1982

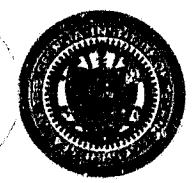

NASA LEWIS SEMI-ANNUAL STATUS REPORT

NAG 3-67 (6/1/81-12/1/81)

PREDICTION OF SOUND RADIATION FROM DIFFERENT PRACTICAL JET ENGINE INLETS

BY

Ben T. Zinn

and

William L. Meyer

SCHOOL OF AEROSPACE ENGINEERIG

GEORGIA INSTITUTE OF TECHNOLOGY

ATLANTA, GA 30332

ABSTRACT

This report summarizes the work performed duirng the third six-month period of the NASA Lewis sponsored research program (Contract Number NAG 3-67) entitled, "Prediction of Sound Radiation from Different Practical Jet Engine Inlets". The work done during the first year of the contract may be summarized as follows. During the initial six-month period the computer codes necessary for this study were developed and checked against exact solutions generated by the point source method using the NASA Lewis QCSEE inlet geometry. During the second half year, these computer codes were used to predict the acoustic properties of the following five inlet configurations: the NASA Langley Bellmouth, the NASA Lewis JT15D-1 Ground Test Nacelle, and three finite hyperbolic inlets of 50, 70 and 90 degrees.

During the past six months, 35 computer runs were done for the NASA Langley Bellmouth. For each of these computer runs, the reflection coefficient at the duct exit plane was calculated as was the far field radiation pattern. These results are presented in both graphical and tabular form in this report with many of the results cross plotted so that trends in the results verses cut-off ratio (wave number) and tangential mode number may be easily identified.

Table of Contents

	Page
Introduction	1
Numerical Considerations	3
The Computer Runs	4
Reflection Coefficients	6
Radiation Patterns	8
References	10
Tables	12
Figures	15

Introduction

During the first year of this contract, the two developmental tasks associated with this project were completed. Firstly, existing computer codes for the calculation of the sound radiated from axisymmetric bodies were upgraded and refined so that calculations could be made having non-dimensional wave numbers (based on duct radius) of up to 20. This initial development work was accomplished using the NASA Lewis QCSEE inlet of Ref. 1. The results of this initial development work are presented in the NASA Lewis Semi-Annual Status Report (6/2/80-11/20/80) for this grant (Number NAG 3-67). Secondly, many small satellite programs were developed to do such things as calculate the cut-off wave numbers for various modes, calculate the modal source inputs for the other computer programs, and plot the data generated in the field. These and the two main programs, for calculating the surface distributions and field distributions of the acoustic quantities of interest, were then combined into a coherent package of programs (i.e. the data file structure for each is the same so that only a single set of data files is required). This package of programs was then used to investigate the acoustic behavior of five different inlet configurations, namely: the NASA Langley Bellmouth[2,3], the NASA Lewis JT15D-1 ground test nacelle[4,5], and three finite hyperbolic inlets similar to those of the Y.C. CHO[5,7] study of 50, 70 and 90 degrees. Comparisons were made between the results generated by the integral technique [8-10] used in this study and those of other experimental and theoretical studies for

the five inlet configurations. Both reflection coefficients and radiation patterns in the field were compared for various modal inputs at various wave numbers. These results are presented in the NASA Lewis Semi-Annual Status Report (12/1/80-5/30/81) for this grant.

During the past six months, 35 computer runs were done for the NASA Langley Bellmouth. These runs form a parametric study for this geometry which consists of five different input modes and six cut-off ratios plus five special runs at other cut-off ratios done at the sponsors request. For each run, the reflection coefficient at the duct exit plane is calcualted along with the distribution of the acoustic sound power level (SPL) in the field. These results are plotted and cross plotted holding either the input mode or the cut-off ratio constant.

Numerical Considerations

Since the required computer runs for the parametric study for this inlet geometry cover a wide range of input modes and cut-off ratios (i.e. wave numbers) the same number of calculational points on the body was not used for all of the runs. In Table I is found the range of values of the input parameters for which the different numbers of points along the body and in the θ (tangential) direction are used. As the wave number (cut-off ratio) is increased, more points must be used on the body to accurately describe the distribution of the acoustic quantities on the surface of the body as is indicated in Table I. Also, as the input mode number (M) is increased, the number of points used in the θ integration must be increased to accurately describe the variations of the acoustic quantities in that direction.

In Figs. 1-3, the distributions of calculational points on the surface of the body are presented. The arrows represent outward normals from the body as these plots represent a visual check of the geometric input data for the acoustic calculation programs. It will be noted here that if the driver plane, which doubles here as the duct exit plane as there is no straight duct section connected to the inlet lip, is non-dimensionalized as 1.0 then the nominal point spacings on the driver plane and the inner bellmouth are 0.04, 0.025, and 0.02 respectively. The bellmouth geometry is terminated in all cases by a 2:1 ellipse as the theory requires a closed body.

The Computer Runs

In Table II, a matrix of all of the computer runs done for the Langley Bellmouth is presented along with the five special runs done at the request of the contractor. This table also relates the cut-off ratios for the various modes run to the corresponding non-dimensional wave numbers at which the runs were performed. A standard plot of the sound pressure level calculated in the field is generated with each computer run. These plots are presented as Figs. 4-38. These figures are grouped according to the input mode used at the driver and are presented in ascending wave number order. Thus Figs. 4-12 are for an input mode of M=1, Figs. 13-20 for M=2, Figs. 21-26 for M=4, and Figs. 27-32 for M=8. All of these are done for the first radial mode input at the driver plane. The final set of these plots, Figs. 33-38 is for a tangential mode of M=4 and the third radial mode input at the driver plane. For these plots, the data is calculated at 46 points in the field on a quarter circle having a radius of 20.36a. These points are evenly spaced from 0^{o}, the centerline of the duct, to 90^{o} in 2^{o} increments. This is actually a rather course mesh when looking at higher radial modes as in Figs. 33-38 run for an input mode of (M,N)=(4,3) and this is why the valleys between the three lobed radiation pattern in the field are somewhat indistinct. Also, the points are calculated 20.36 radii from the duct entrance as this is where they are measured in Refs. 2 and 3

If we now look at the "concept of angular location of the predominant acoustic radiation" we find that in general, this radiation peak moves towards the centerline of the duct for increasing wave numbers and

away from the duct centerline for increasing tangential mode numbers. These results, for all of the runs done for this inlet, are presented in Table III. For the modal input (4,3) the lobe that carries the maximum SPL in (dB) changes from the first (counted from the centerline of the duct) to the third at a cut-off ratio of 1.305. Thus, the bracketed values in Table III follow the first lobe even though it is no longer the predominant one (See Figs. 33-38.). It will be noted here again that since the acoustic quantities were only calcuated at 2^{o} increments from the centerline of the duct to 90^{o} that the angular values in Table III are probably only good to $\pm 1^{o}$.

Reflection Coefficients

Since there is no straight duct section connected to the inlet, the driver plane is the same as the duct exit plane. Therefore, the reflection coefficient defined as

$$R = \frac{ik\phi - \frac{\partial \phi}{\partial n}}{ik\phi + \frac{\partial \phi}{\partial n}} \qquad (1)$$

where k is the wave number, ϕ is the acoustic potential, and $\frac{\partial \phi}{\partial n}$ is the normal acoustic velocity (defined with an outward normal to the body), can be calculated directly from the results of the surface acoustic program without using the field program. Since the reflection coefficient is complex, it is plotted as a modulus and a phase (in degrees) in two separate graphs with the same figure number.

In Figs. 39 and 40, the reflection coefficient is plotted for an input mode of (1,1) for all of the wave numbers (cut-off ratios) run. Some of the individual cases run are repeated in both figures for ease of comparison. Similarly, in Figs. 41 and 42, the reflection coefficient at the duct exit plane is plotted for an input mode of (2,1) at the driver plane for all of the cases run. Also, Figs. 43 and 44 are for input modes of (4,1) and (8,1) respectively. For an input mode of (4,3) the results are plotted in six graphs designated as Fig. 45. Since the input mode has two zero crossings for the acoustic potential specified, the reflection coefficient has a discontinuity at these points. This is shown in Fig. 45 by artifically extending the data to the plot boundaries in the direction it was headed at these points. Since the trends were not always in the same direction at these points, the data was plotted in separate graphs for clarity.

In the next set of figures, the reflection coefficient is plotted for input modes of (1,1), (2,1), (4,1) and (8,1) for constant cut-off ratio. As before, each figure consists of two plots, one for the modulus of the reflection coefficient and one for the phase. Figures 46-51 are for cut-off ratios of 1.005, 1.015, 1.064, 1.155, and 1.305 and 1.556 respectively.

It will be noted here that the reason for the seemingly strange behavior of the reflection coefficient in Figs. 44 and 51 for an input mode of (8,1) at a wave number of 15.01 (i.e. a cut-off ratio of 1.556) is that this is above the second radial mode cut-off wave number which is ka=14.12 for (8,2). This is significant as the integral technique employed in the calculation of these values automatically considers all radial modes for the tangential mode specified. Thus, even though the pressure (i.e. potential) specified at the driver plane is for the (8,1) mode, the solution is picking up the effect of the (8,2) mode as well as for this wave number it is cut-on and has a cut-off ratio of 1.063. It is not possible to separate out this effect with this formulation of the problem as this would require the over specification of the boundary conditions on the driver plane. That is, it would require the specification of both the acoustic potential (i.e. pressure) and the normal acoustic velocity on the driver which cannot be done for an elliptic problem.

This is also why the principle radiation peak shifts from the first to the third for an input mode of (4,3) (See Figs. 33-38 and Table III.). In this case, the (4,4) mode is cut-on at a wave number of 15.96 so that the last two wave numbers, 16.55 and 19.73, have this mode cut-on with cut-off ratios of 1.037 and 1.236 respectively.

Radiation Patterns

The radiation patterns are presented in Figs. 4-38 for the 35 runs done for the Langely Bellmouth. Since in this form the results are not easy to compare, the relative SPL (Sound Pressure Level) in decibels and phase in degrees have been cross plotted so that trends can be seen more easily. The plots are of the relative values referenced in all cases to the point in the field where the maximum SPL occurs for each case.

In Figs. 52 and 53, the results are plotted for all of the runs done for an input mode of M=(1,1). Each figure consists of three plots: two for the relative SPL in dB and one for the phase. Note that the phase plot in Fig. 52 has an expanded scale as compared to the phase plot in Fig. 53. This was done simply for the sake of clarity. This is also done in Fig. 54. As with the reflection coefficient plots some of the runs are repeated in Figs. 52 and 53 for ease of comparison. Similarly, the results of all of the runs done for a modal input of M=(2,1) are presented in Figs. 54 and 55. Also, the results for input modes of (4,1) and (8,1) are presented in Figs. 56 and 57 respectively. As mentioned before, the seemingly aberrant behavior of the results for a modal input of (8,1) at a non-dimensional wave number of ka=15.01, clearly visible in Fig. 57b, is due to the fact that the (8,2) mode is cut-on at this frequency. This is one of the reasons why the results for an input mode of (4,3) for the last two wave numbers run, 16.55 and 19.73, are presented in separate plots in Fig. 58. Also, the valleys between the lobes in these plots would be more distinct if more points had been used in the field.

Finally, in Figs. 59-64, the relative results in the field are presented for modal inputs of M=(1,1), (2,1), (4,1) and (8,1) while the cut-off ratio is held constant as was done for the reflection coefficient plots. Again, the relative SPL in dB is plotted in two ways in each figure.

References

1. "Effect of Entry-Lip Design on Aerodynamics and Acoustics of High-Throat-Mach-Number Inlets for the Quiet, Clean, Short-haul Experimental Engine," B. A. Miller, B. J. Dastoli and H. L. Wesoky, NASA TM X-3222, May 1975.

2. "Inlet Contour and Flow Effects on Radiation," J. M. Ville, and R. J. Silcox, AIAA Papaer Number 80-0966, June 1980.

3. "Experimental Investigation of the Radiation of Sound from an Unflanged Duct and a Bellmouth Including the Flow Effect," J. M. Ville nd R. J. Silcox, NASA Technical Paper 1697, August 1980.

4. "Analysis of Radiation Patterns of Interaction Tones Generated by Inlet Rods in the JT15D Engine," M. F. Heidmann, A. V. Saule and J. G. McArdle, AIAA Paper Number 79-0581, March 1979.

5. "Analysis of Radiation Patterns of Interaction Tones Generated by Inlet Rods in the JT15D Engine," M. F. Heidmann, A. V. Saule and J. G. McArdle, NASA TM-79074, March 1979.

6. "Sound Radiation from Hyperboloidal Inlet Ducts," Y. C. Cho, AIAA Paper Number 79-0677, March 1979.

7. "Rigorous Solutions for Sound Radiation from Circular Ducts with Hyperbolic Horns or Infinite Plane Baffle," Y. C. Cho, Journal of Sound and Vibration, Vol. 69, No. 3, pp. 405-425, 1980.

8. "Predicting the Acoustics of Arbitrarily Shaped Bodies Using an Integral Approach," W. A. Bell, W. L. Meyer and B. T. Zinn, AIAA Journal, Vol. 15, No. 6, pp. 813-820, June 1977.

9. "Boundary Integral Solutions of Three Dimensional Acoustic Radiation Problems," W. L. Meyer, W. A. Bell, M. P. Stallybrass and B. T. Zinn, Journal of Sound and Vibration, Vol. 59, No. 2, pp. 245-262, July 1978.

10. "Prediction of the Sound Field Radiated from Axisymmetric Surfaces," W. L. Meyer, W. A. Bell, M. P. Stallybrass and B. T. Zinn, Journal of the Acoustical Society of America, Vol. 63, No. 2, pp. 631-638, March 1979.

TABLE I

Number of Points Used in the Surface Integrations

Number of Points on the Body	Range of Non-Dimensional Wave Numbers (ka)
102	0 ---> 5
155	5 ---> 12
189	12 ---> 20

Number of Points in Tangential Integration	Range of Tangential Mode Numbers (M)
32	0 ---> 3
64	4 ---> 7
76	8 ---> 11

TABLE II

Non-Dimensional Wave Numbers Used in Computer Runs

Cut-Off Ratios	(Tangential, Radial) Modes				
	(1,1)	(2,1)	(4,1)	(0,1)	(4,3)
1.005	1.850	3.069	5.345	9.695	12.74
1.015	1.869	3.100	5.398	9.792	12.87
1.064	1.959	3.249	5.658	10.26	13.49
1.155	2.127	3.527	6.142	11.14	14.65
1.305	2.403	3.985	6.940	12.59	16.55+
1.556	2.865	4.752	8.275	15.01*	19.73+
1.740		5.314			
2.040	3.756				
2.150		6.566			
2.500	4.603				
2.870	5.284				

* (0,2) Mode cut-on.

\+ (4,4) Mode cut-on

TABLE III

The Concept of Angular Location of Predominant Acoustic Radiation

Mode (M,N)	Wave Number (ka)	f/f mn	Ψ_{MIN} (-6dB) (Degrees)	Ψ_{MAX} (-6dB) (Degrees)
(1,1)	1.850	1.005	12	89
(1,1)	1.869	1.015	12	88
(1,1)	1.959	1.064	12	85
(1,1)	2.127	1.155	11	76
(1,1)	2.403	1.305	11	72
(1,1)	2.865	1.556	10	66
(1,1)	3.756	2.040	8	55
(1,1)	4.603	2.500	7	49
(1,1)	5.284	2.870	7	44
(2,1)	3.069	1.005	21	82
(2,1)	3.100	1.015	21	81
(2,1)	3.249	1.064	20	80
(2,1)	3.527	1.155	19	76
(2,1)	3.985	1.305	17	69
(2,1)	4.752	1.556	16	62
(2,1)	5.314	1.740	15	58
(2,1)	6.566	2.150	14	50
(4,1)	5.345	1.005	28	79
(4,1)	5.398	1.015	28	78
(4,1)	5.658	1.064	27	77
(4,1)	6.142	1.155	26	74
(4,1)	6.940	1.305	25	66
(4,1)	8.275	1.556	23	58
(8,1)	9.695	1.005	36	77
(8,1)	9.792	1.015	36	76
(8,1)	10.26	1.064	35	74
(8,1)	11.14	1.155	34	70
(8,1)	12.59	1.305	31	63
(8,1)	15.01	1.556	28	56
(4,3)	12.74	1.005	13	27
(4,3)	12.87	1.015	13	27
(4,3)	13.49	1.064	13	26
(4,3)	14.65	1.155	12	24
(4,3)	16.56	1.305	40(11)	62(22)
(4,3)	19.73	1.556	33(9)	49(19)

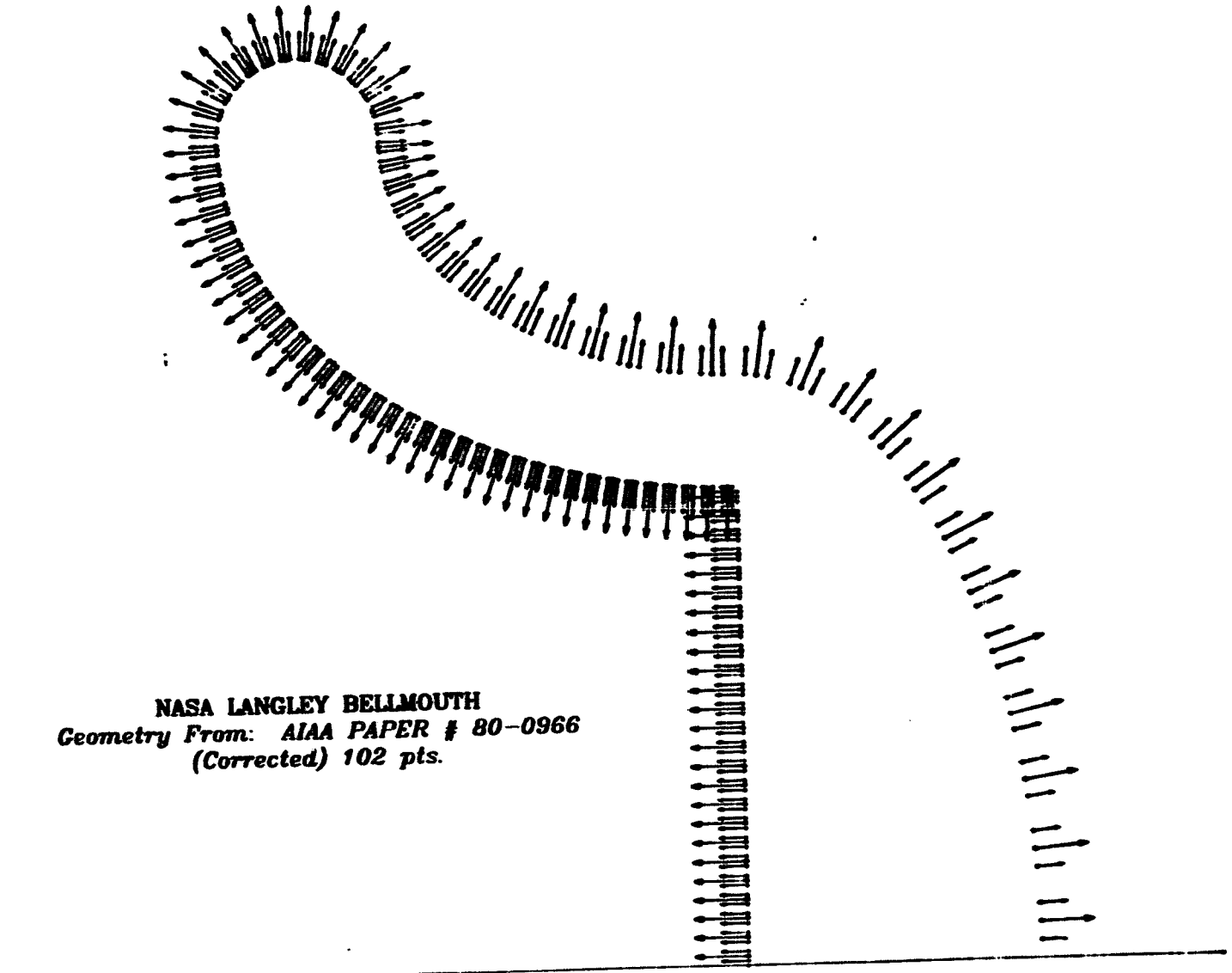
NASA LANGLEY BELLMOUTH
Geometry From: AIAA PAPER # 80-0966
(Corrected) 102 pts.

Fig. 1

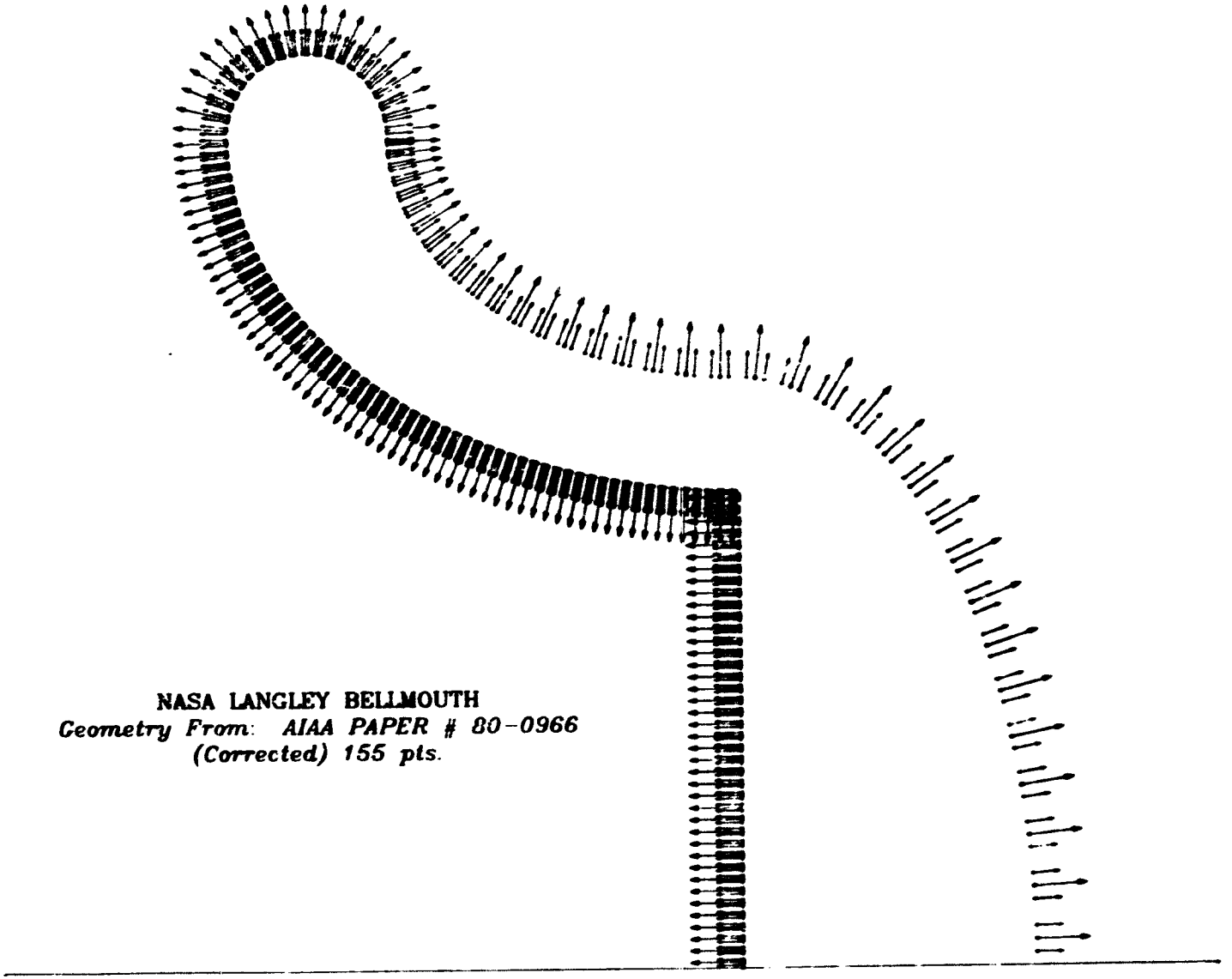
NASA LANGLEY BELLMOUTH
Geometry From: AIAA PAPER # 80-0966
(Corrected) 155 pts.

Fig. 2

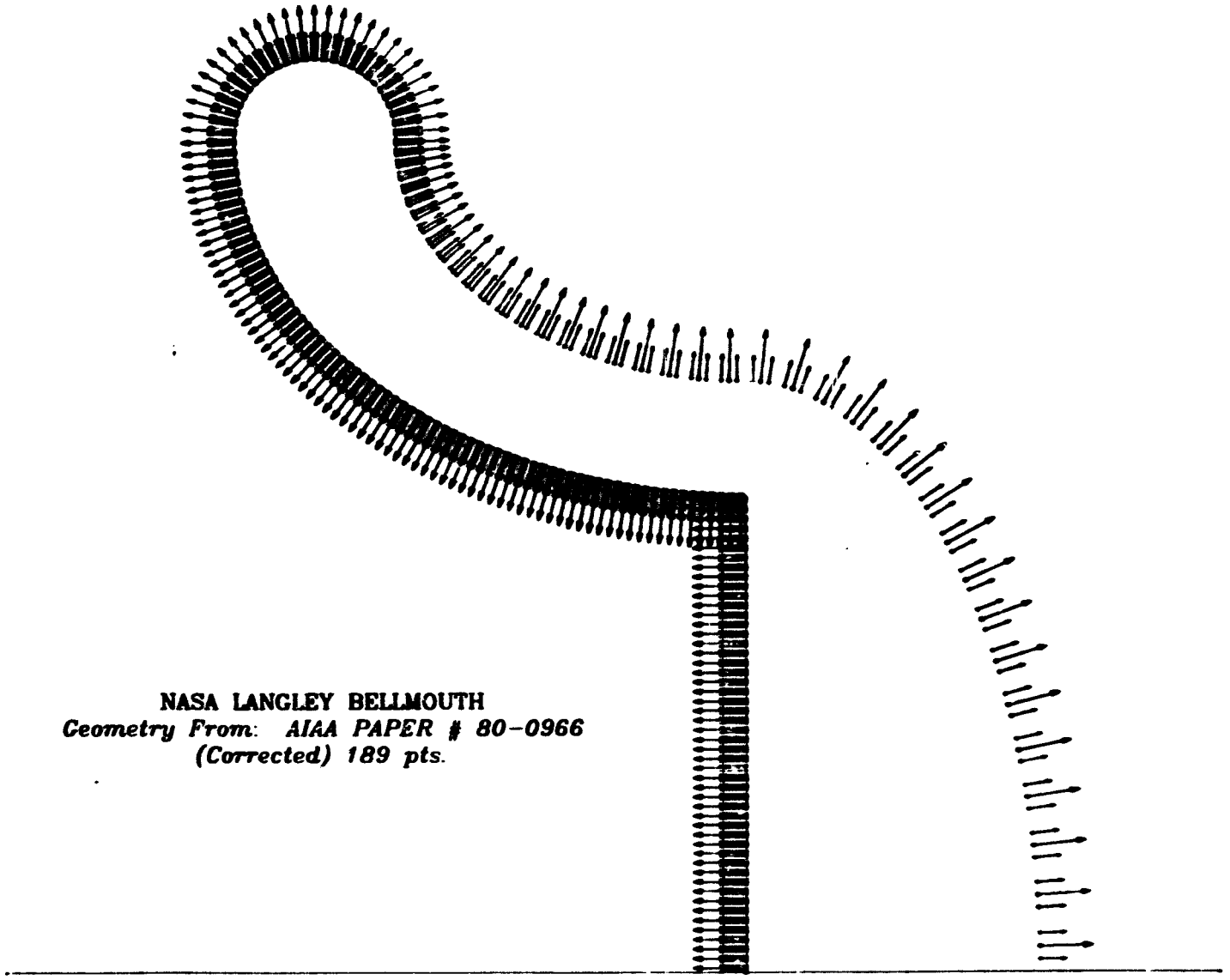
NASA LANGLEY BELLMOUTH
Geometry From: AIAA PAPER # 80-0966
(Corrected) 189 pts.

Fig. 3

LANGLEY BELLMOUTH

Deg	SPL	Deg	SPL
0	0	46	107
2	85	48	106
4	91	50	106
6	95	52	106
8	97	54	106
10	99	56	106
12	101	58	105
14	102	60	105
16	103	62	105
18	104	64	105
20	104	66	104
22	105	68	104
24	105	70	104
26	106	72	103
28	106	74	103
30	106	76	103
32	106	78	103
34	107	80	102
36	107	82	102
38	107	84	102
40	107	86	101
42	107	88	101
44	107	90	101

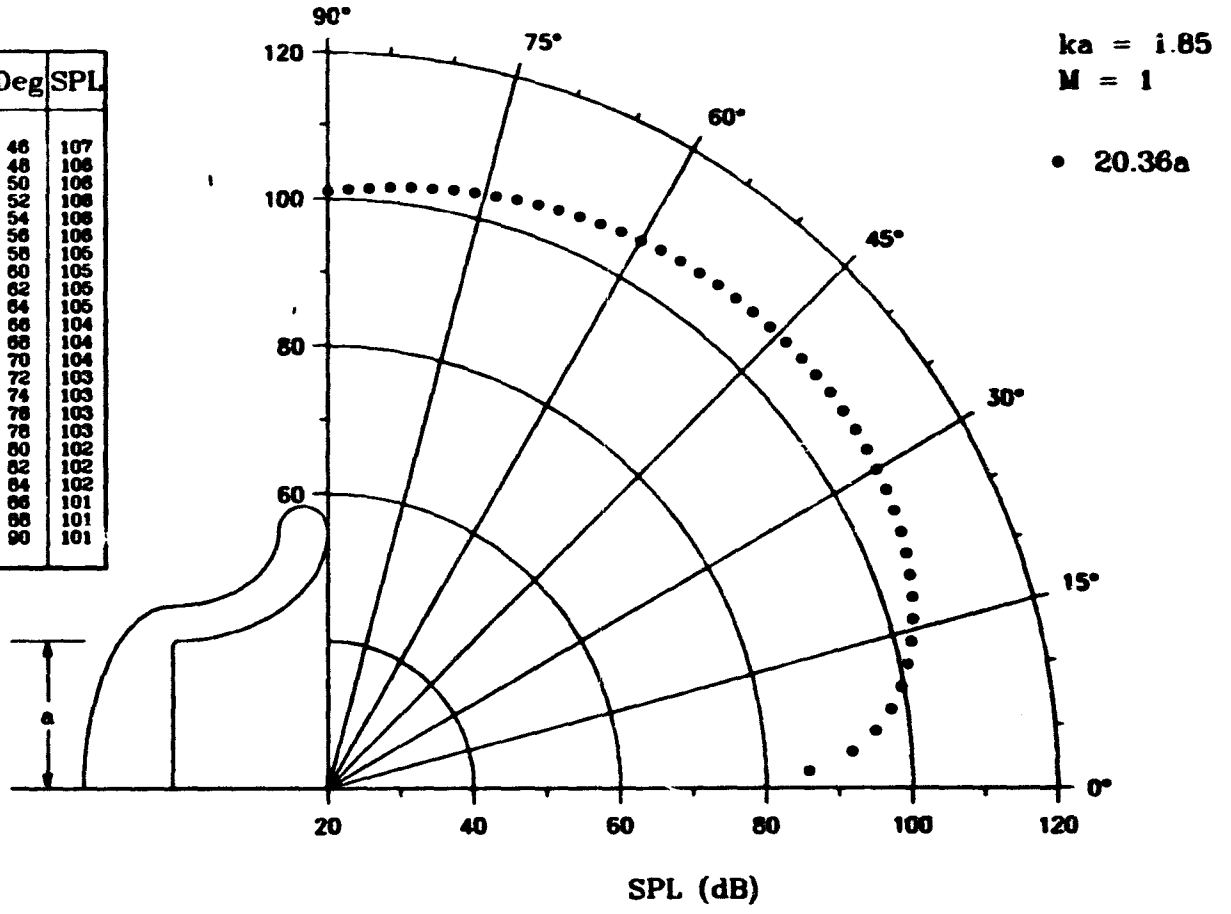

Fig. 4 (M,N) = (1,1)

LANGLEY BELLMOUTH

Deg	SPL	Deg	SPL
0	0	46	107
2	88	48	107
4	92	50	107
6	96	52	106
8	98	54	106
10	100	56	106
12	101	58	106
14	102	60	106
16	103	62	105
18	104	64	105
20	105	66	105
22	105	68	104
24	106	70	104
26	106	72	104
28	106	74	103
30	107	76	103
32	107	78	103
34	107	80	102
36	107	82	102
38	107	84	102
40	107	86	101
42	107	88	101
44	107	90	101

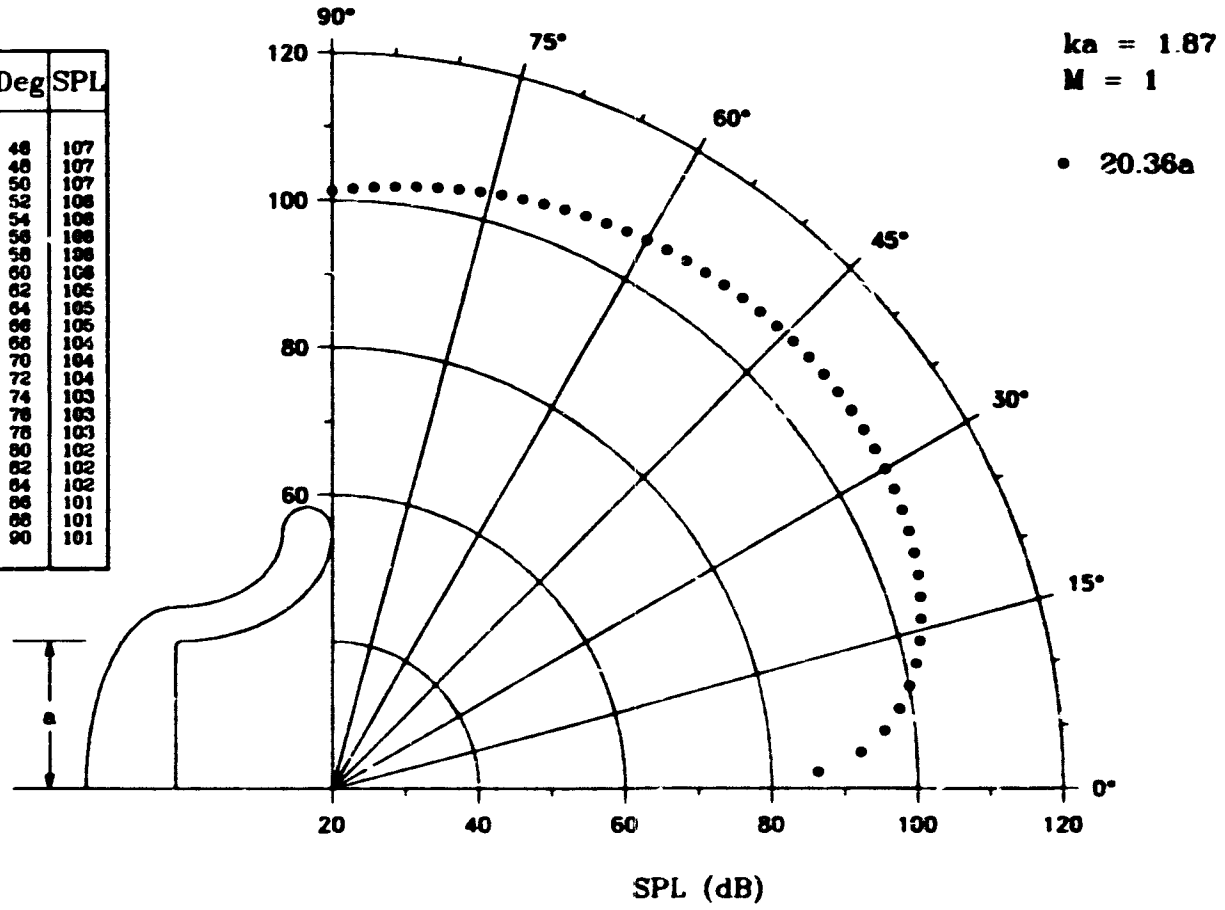

Fig. 5 (M,N) = (1,1)

LANGLEY BELLMOUTH

Deg	SPL	Deg	SPL
0	0	46	109
2	88	48	109
4	94	50	108
6	97	52	108
8	100	54	108
10	102	56	108
12	103	58	107
14	104	60	107
16	105	62	107
18	106	64	106
20	107	66	106
22	107	68	106
24	108	70	105
26	108	72	105
28	108	74	105
30	109	76	104
32	109	78	104
34	109	80	104
36	109	82	103
38	109	84	103
40	109	86	103
42	109	88	102
44	109	90	102

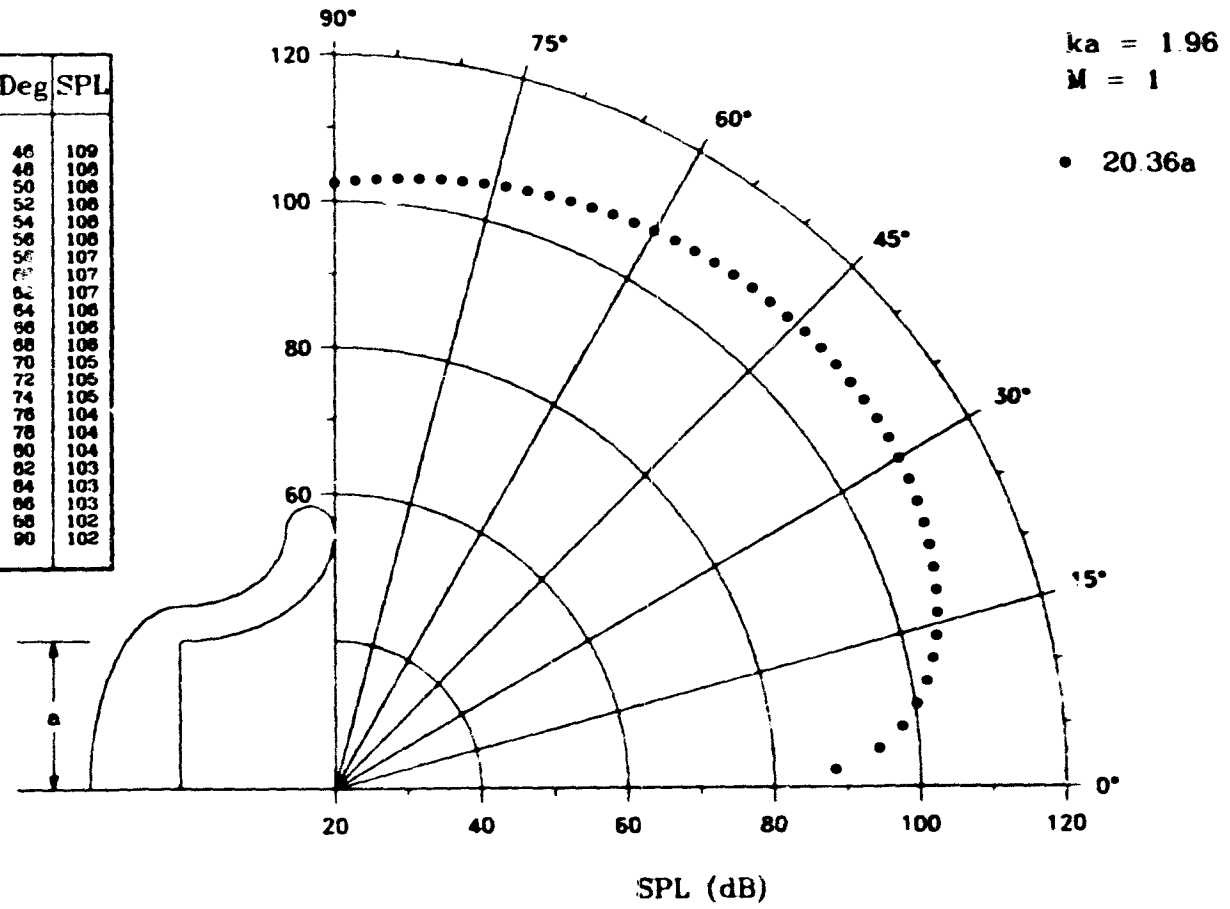

Fig. 6 (M,N) = (1,1)

LANGLEY BELLMOUTH

Deg	SPL	Deg	SPL
0	0	46	111
2	91	48	111
4	97	50	111
6	101	52	110
8	103	54	110
10	105	56	110
12	106	58	110
14	107	60	109
16	108	62	109
18	109	64	108
20	110	66	108
22	110	68	108
24	111	70	107
26	111	72	107
28	111	74	106
30	111	76	106
32	112	78	106
34	112	80	105
36	112	82	105
38	112	84	105
40	112	86	104
42	111	88	104
44	111	90	104

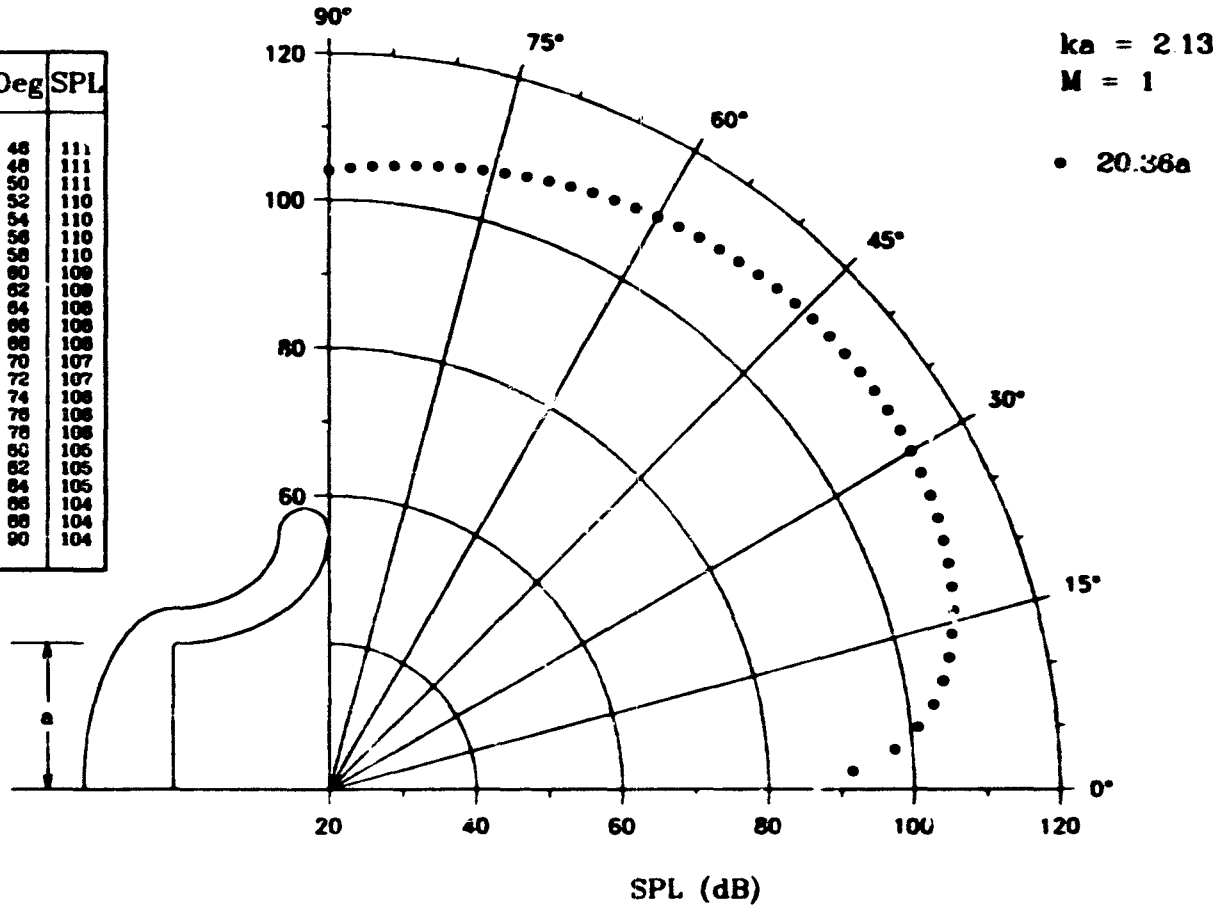

Fig. 7 (M,N) = (1,1)

LANGLEY BELLMOUTH

Deg	SPL	Deg	SPL
0	0	46	114
2	95	48	114
4	101	50	114
6	104	52	113
8	107	54	113
10	108	56	112
12	110	58	112
14	111	60	112
16	112	62	111
18	113	64	111
20	113	66	110
22	114	68	110
24	114	70	109
26	114	72	109
28	115	74	108
30	115	76	108
32	115	78	107
34	115	80	107
36	115	82	106
38	115	84	106
40	115	86	105
42	115	88	105
44	114	90	105

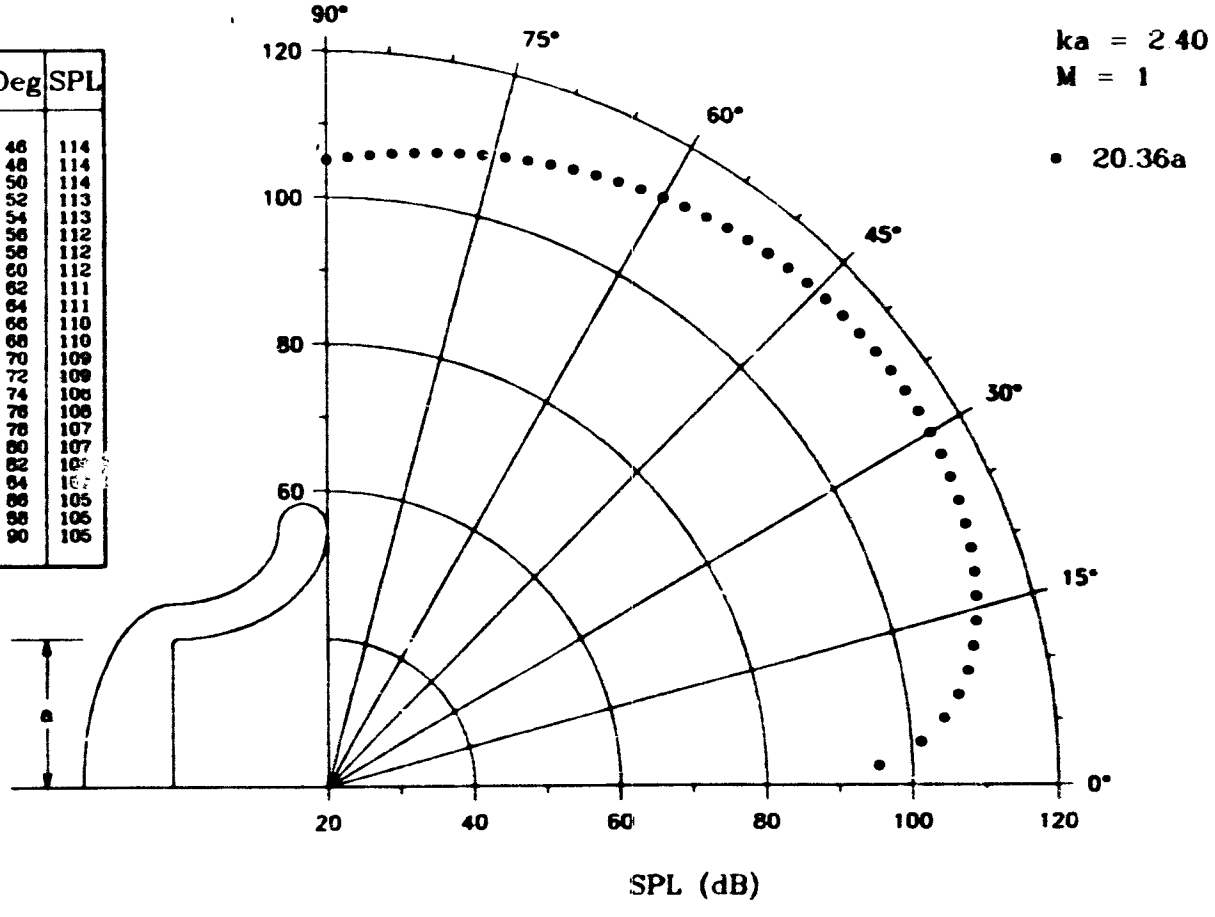

Fig. 8 (M,N) = (1,1)

LANGLEY BELLMOUTH

Deg	SPL	Deg	SPL
0	0	46	117
2	99	48	117
4	105	50	116
6	109	52	116
8	111	54	115
10	113	56	115
12	114	58	114
14	115	60	114
16	116	62	113
18	117	64	113
20	117	66	112
22	118	68	112
24	118	70	111
26	118	72	111
28	118	74	110
30	119	76	110
32	119	78	109
34	118	80	109
36	118	82	108
38	118	84	108
40	118	86	107
42	118	88	107
44	117	90	106

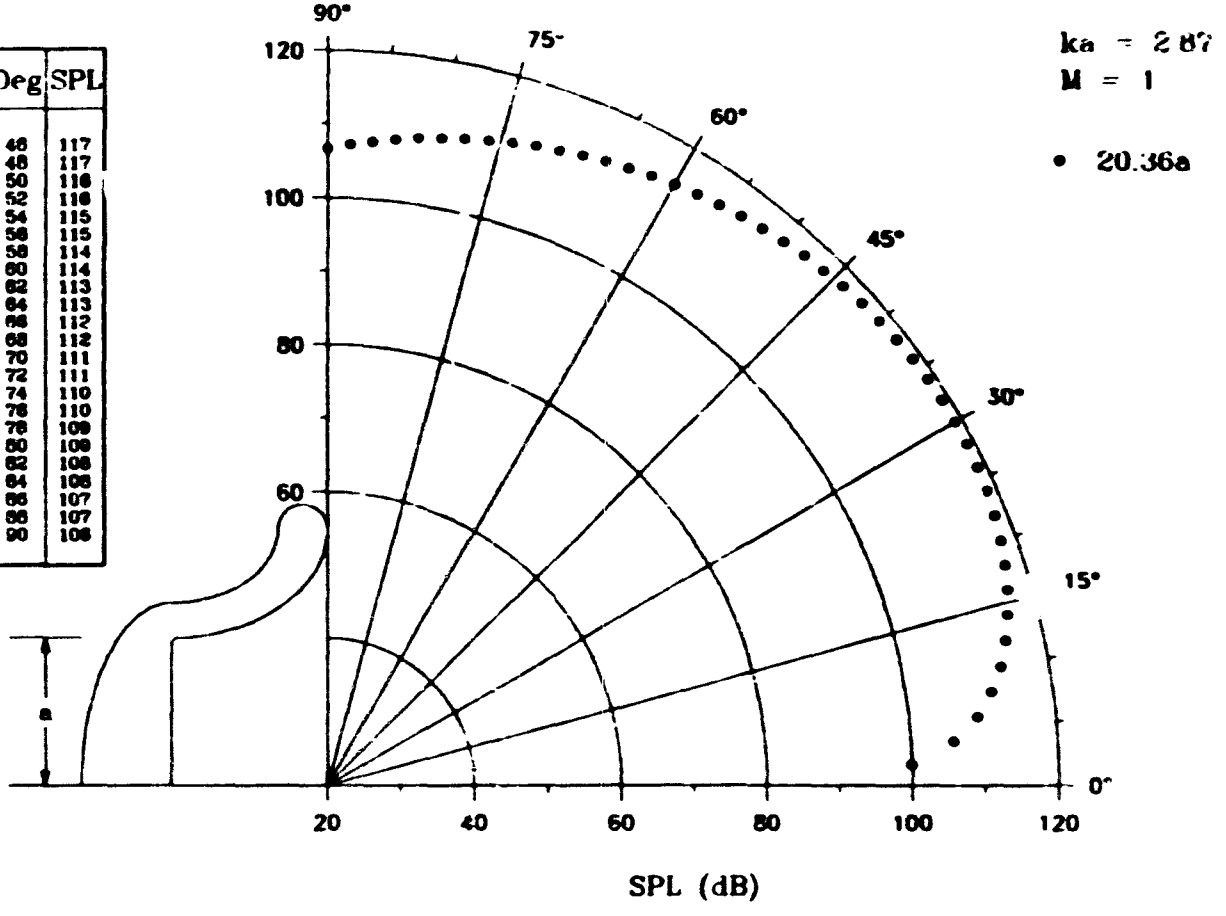

Fig. 9 (M,N) = (1,1)

LANGLEY BELLMOUTH

Deg	SPL	Deg	SPL
0	0	46	120
2	106	48	119
4	112	50	119
6	115	52	118
8	117	54	117
10	119	56	117
12	120	58	116
14	121	60	116
16	122	62	115
18	122	64	114
20	123	66	114
22	123	68	113
24	123	70	113
26	123	72	112
28	123	74	112
30	123	76	111
32	123	78	110
34	123	80	110
36	122	82	110
38	122	84	109
40	121	86	109
42	121	88	108
44	120	90	108

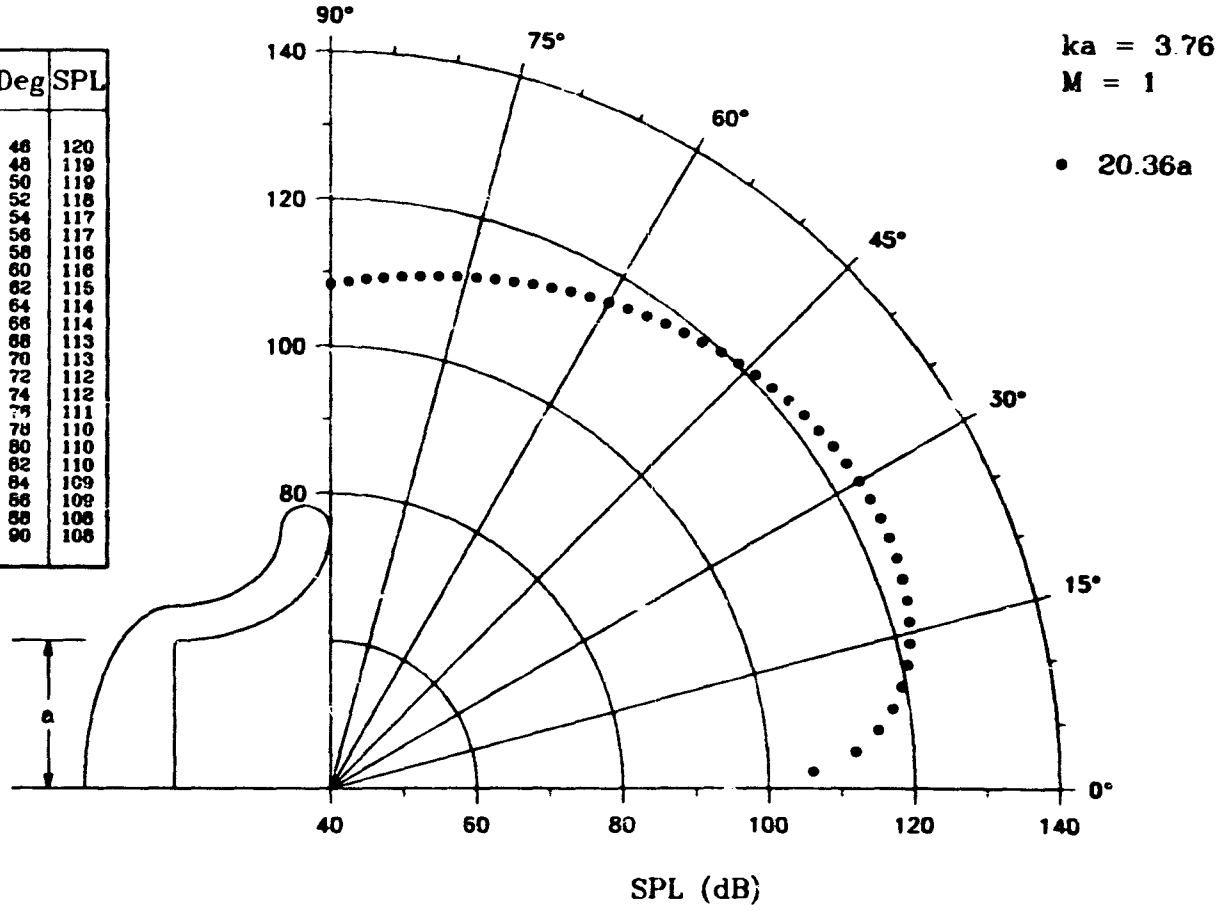

Fig. 10 (M,N) = (1,1)

LANGLEY BELLMOUTH

Deg	SPL	Deg	SPL
0	0	46	121
2	109	48	120
4	115	50	120
6	119	52	119
8	121	54	118
10	123	56	117
12	124	58	117
14	125	60	116
16	126	62	115
18	126	64	114
20	126	66	113
22	127	68	113
24	128	70	112
26	128	72	111
28	128	74	111
30	128	76	110
32	125	78	110
34	125	80	109
36	124	82	109
38	124	84	108
40	123	86	108
42	123	88	108
44	122	90	107

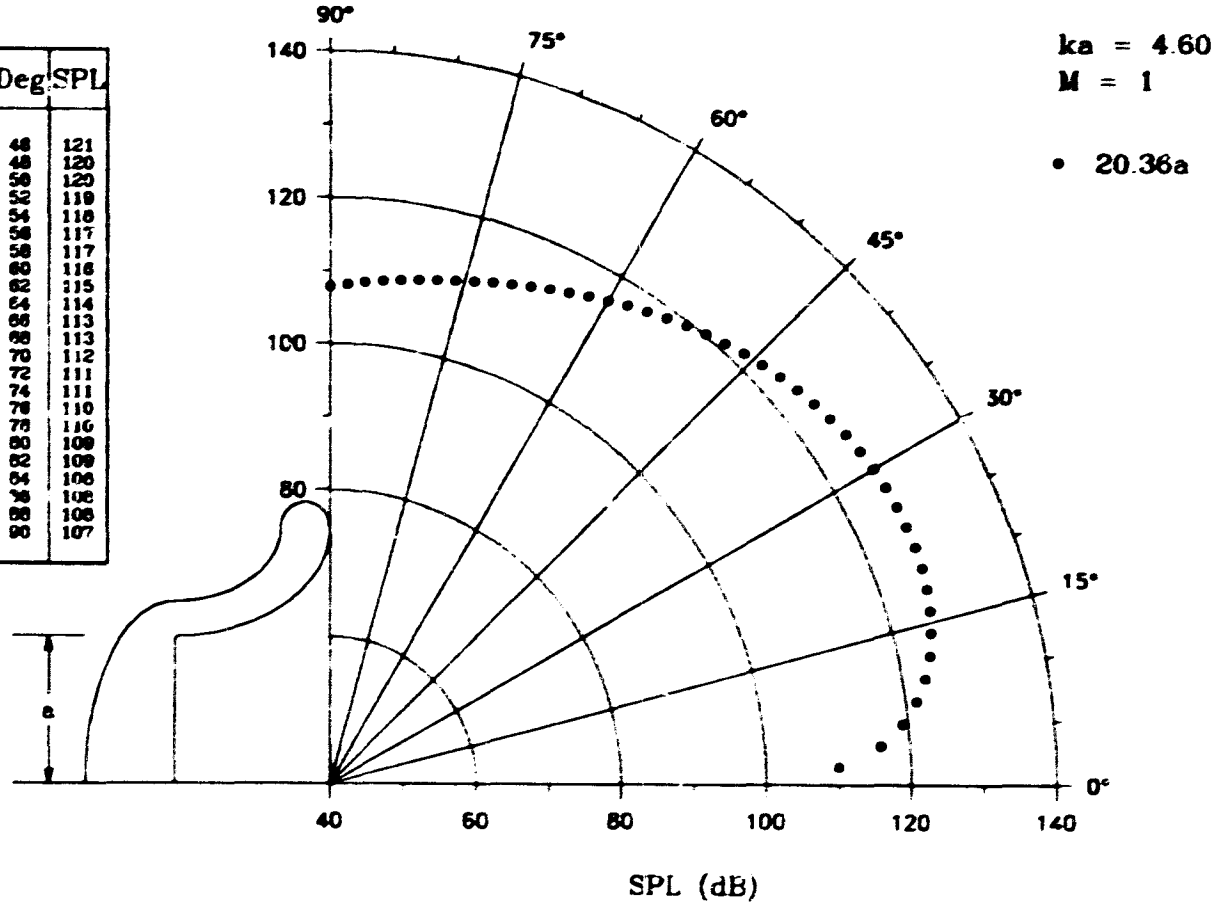

Fig. 11 (M,N) = (1,1)

LANGLEY BELLMOUTH

Deg	SPL	Deg	SPL
0	0	46	122
2	112	48	121
4	116	50	120
6	121	52	119
8	124	54	118
10	125	56	117
12	126	58	116
14	127	60	115
16	128	62	114
18	128	64	114
20	128	66	113
22	128	68	112
24	128	70	112
26	128	72	111
28	128	74	110
30	127	76	110
32	127	78	109
34	126	80	109
36	126	82	108
38	125	84	108
40	124	86	107
42	123	88	107
44	122	90	106

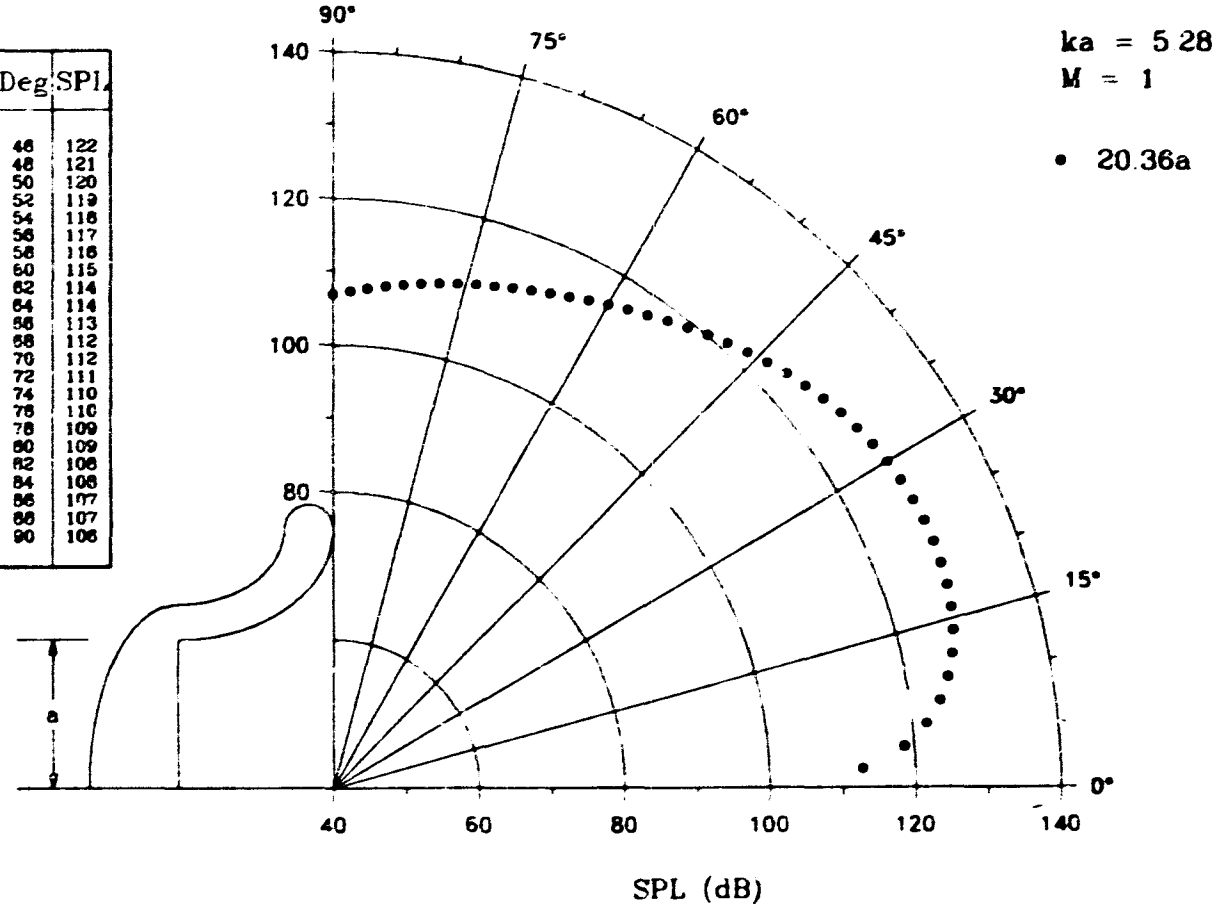

Fig. 12 (M,N) = (1,1)

LANGLEY BELLMOUTH

Deg	SPL	Deg	SPL
0	0	46	109
2	65	48	109
4	77	50	109
6	84	52	109
8	89	54	109
10	93	56	109
12	95	58	108
14	98	60	108
16	100	62	108
18	102	64	107
20	103	66	107
22	104	68	107
24	105	70	106
26	106	72	106
28	107	74	105
30	108	76	105
32	108	78	104
34	108	80	104
36	109	82	103
38	109	84	103
40	109	86	102
42	109	88	102
44	109	90	102

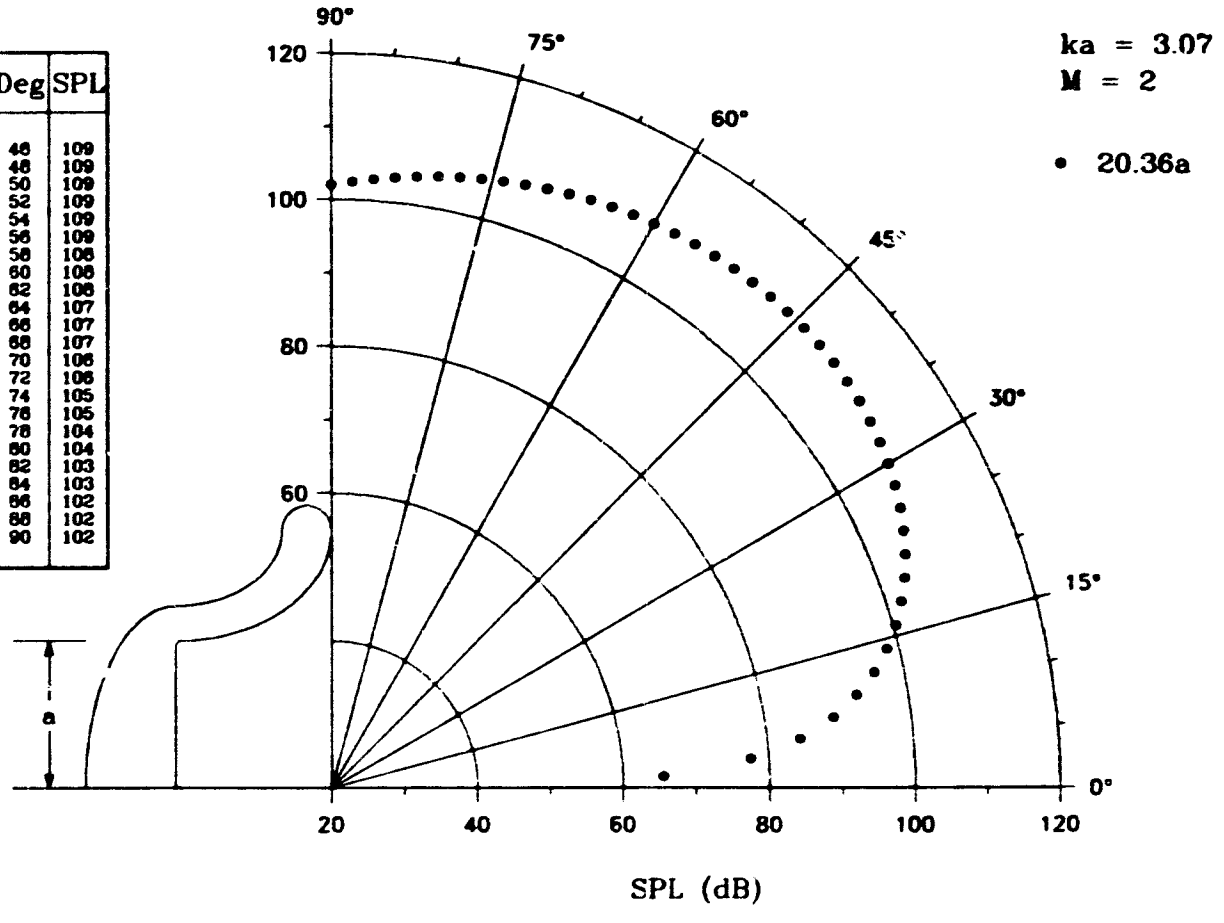

Fig. 13 (M,N) = (2,1)

LANGLEY BELLMOUTH

Deg	SPL	Deg	SPL
0	0	46	110
2	66	48	110
4	78	50	110
6	84	52	109
8	89	54	109
10	93	56	109
12	96	58	109
14	98	60	108
16	100	62	108
18	102	64	108
20	103	66	107
22	105	68	107
24	106	70	106
26	107	72	106
28	107	74	106
30	108	76	105
32	109	78	105
34	109	80	104
36	109	82	104
38	110	84	103
40	110	86	103
42	110	88	102
44	110	90	102

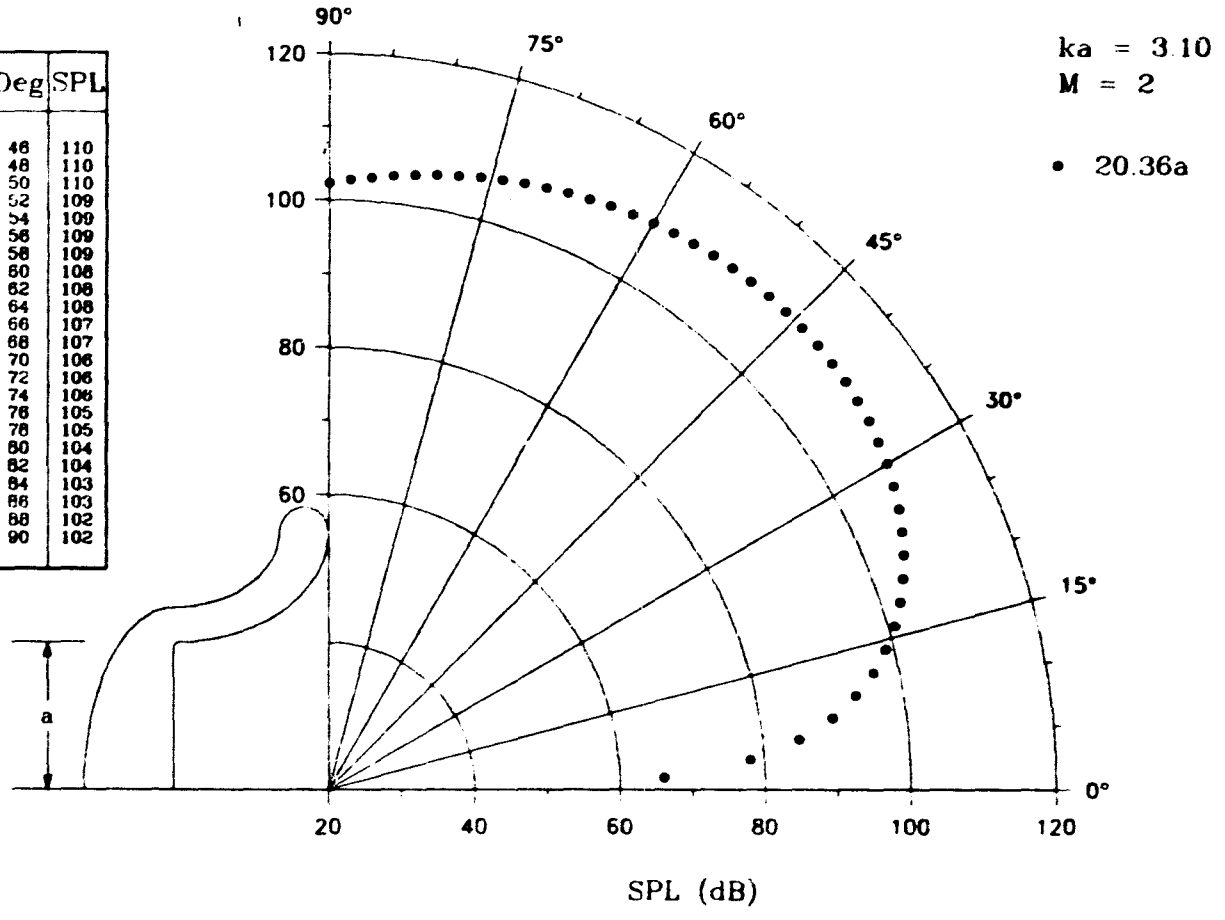

Fig. 14 (M,N) = (2,1)

LANGLEY BELLMOUTH

Deg	SPL	Deg	SPL
0	0	46	112
2	68	48	111
4	80	50	111
6	87	52	111
8	92	54	111
10	95	56	111
12	98	58	110
14	101	60	110
16	103	62	110
18	104	64	109
20	106	66	109
22	107	68	108
24	108	70	108
26	109	72	108
28	110	74	107
30	110	76	107
32	111	78	106
34	111	80	106
36	111	82	105
38	111	84	105
40	112	86	104
42	112	88	104
44	112	90	103

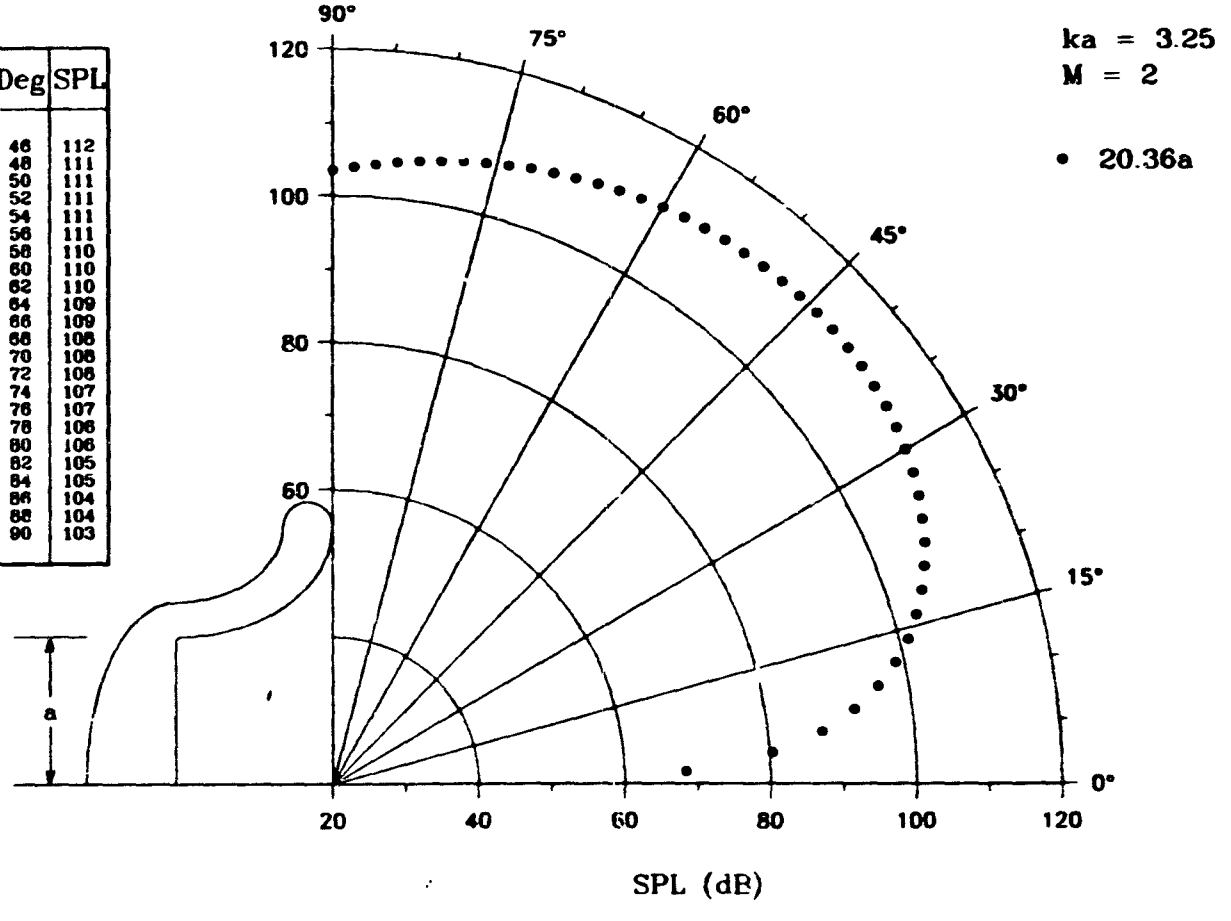

Fig. 15 (M,N) = (2,1)

LANGLEY BELLMOUTH

Deg	SPL	Deg	SPL
0	0	46	114
2	72	48	114
4	84	50	114
6	91	52	114
8	96	54	113
10	99	56	113
12	102	58	113
14	104	60	112
16	106	62	112
18	108	64	111
20	109	66	111
22	111	68	110
24	111	70	110
26	112	72	109
28	113	74	109
30	113	76	109
32	114	78	108
34	114	80	108
36	114	82	107
38	114	84	107
40	115	86	106
42	114	88	106
44	114	90	105

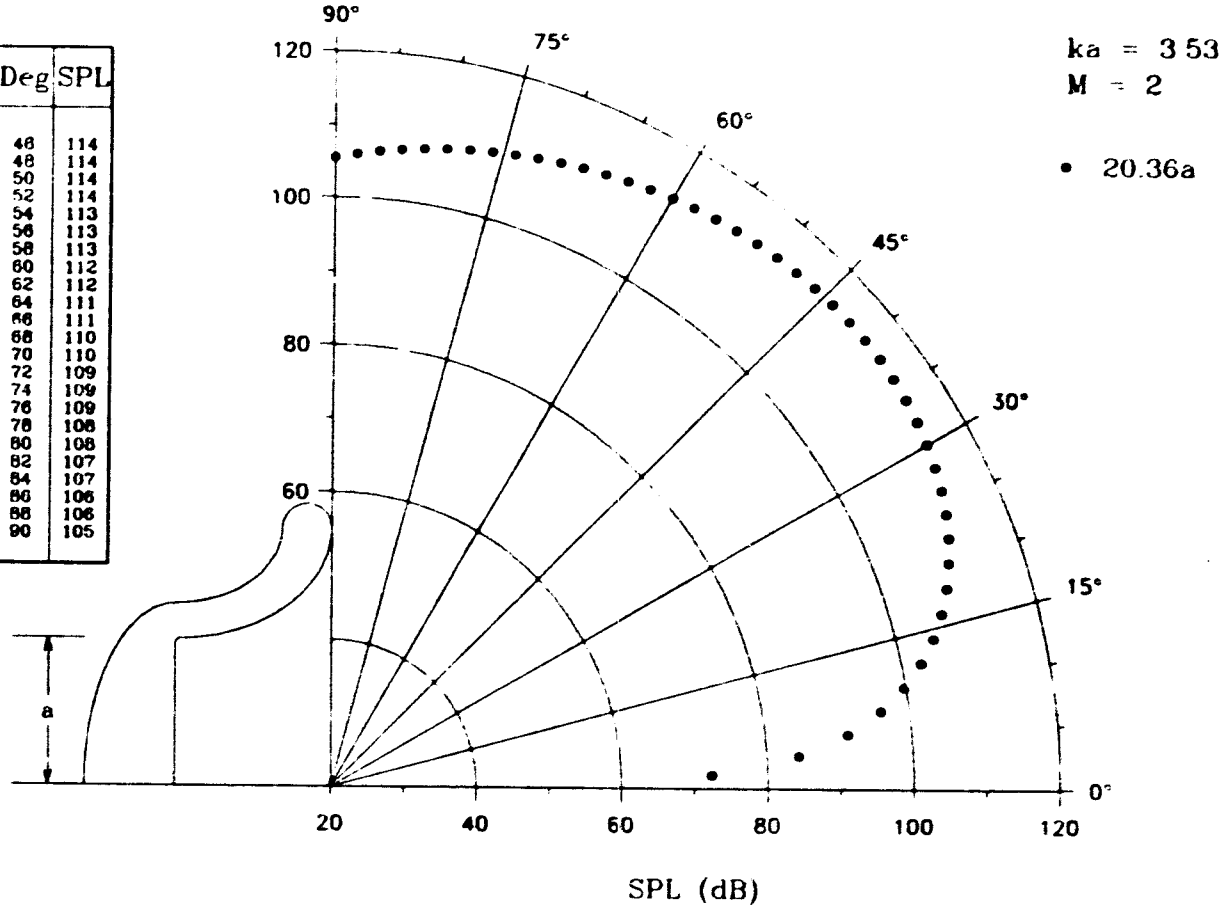

Fig. 16 (M,N) = (2,1)

LANGLEY BELLMOUTH

Deg	SPL	Deg	SPL
0	0	46	117
2	77	48	117
4	89	50	117
6	96	52	116
8	101	54	116
10	104	56	115
12	107	58	115
14	109	60	114
16	111	62	114
18	113	64	113
20	114	66	113
22	115	68	112
24	116	70	112
26	117	72	111
28	117	74	111
30	118	76	110
32	118	78	110
34	118	80	109
36	118	82	109
38	118	84	108
40	118	86	108
42	118	88	108
44	118	90	107

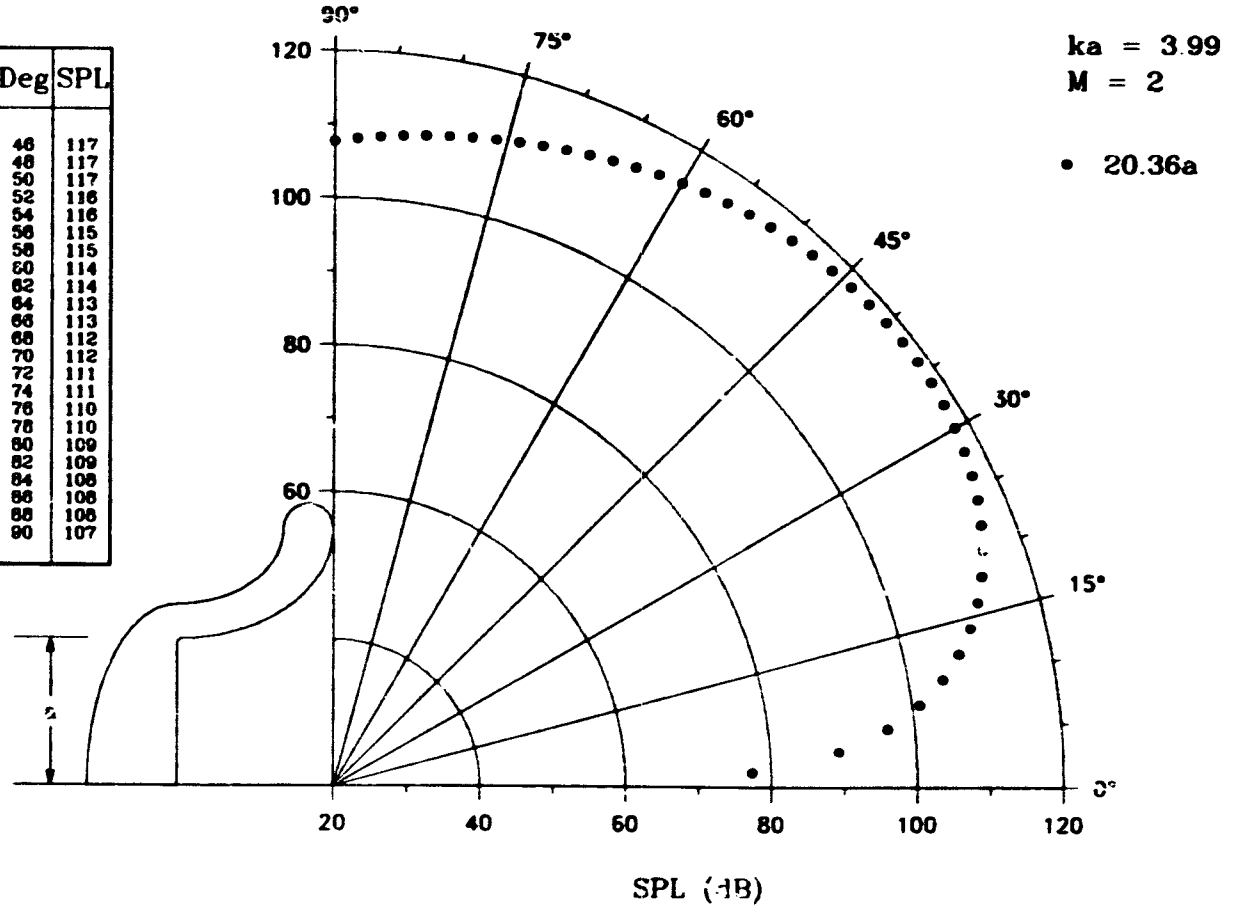

Fig. 17 (M,N) = (2,1)

LANGLEY BELLMOUTH

Deg	SPL	Deg	SPL
0	0	46	120
2	82	48	119
4	94	50	119
6	101	52	118
8	105	54	118
10	109	56	117
12	112	58	117
14	114	60	116
16	116	62	116
18	117	64	115
20	118	66	114
22	119	68	114
24	120	70	113
26	121	72	112
28	121	74	112
30	121	76	111
32	121	78	111
34	121	80	110
36	121	82	109
38	121	84	109
40	121	86	108
42	121	88	108
44	120	90	107

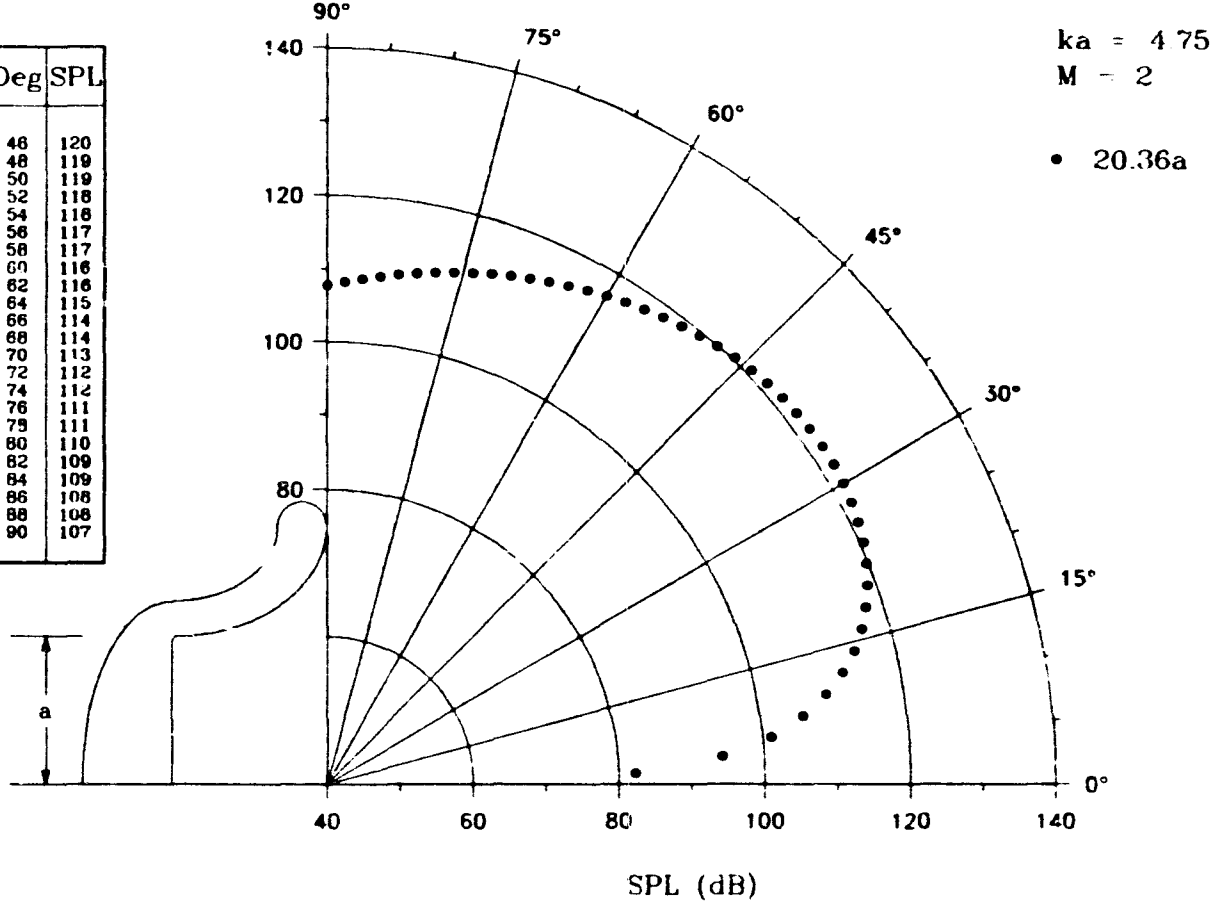

Fig. 18 (M,N) = (2,1)

LANGLEY BELLMOUTH

Deg	SPL	Deg	SPL
0	0	46	121
2	85	48	121
4	97	50	120
6	104	52	119
8	108	54	119
10	112	56	118
12	114	58	117
14	117	60	117
16	118	62	116
18	120	64	115
20	121	66	114
22	122	68	114
24	122	70	113
26	123	72	112
28	123	74	112
30	123	76	111
32	123	78	110
34	123	80	110
36	123	82	109
38	123	84	109
40	123	86	108
42	122	88	108
44	122	90	107

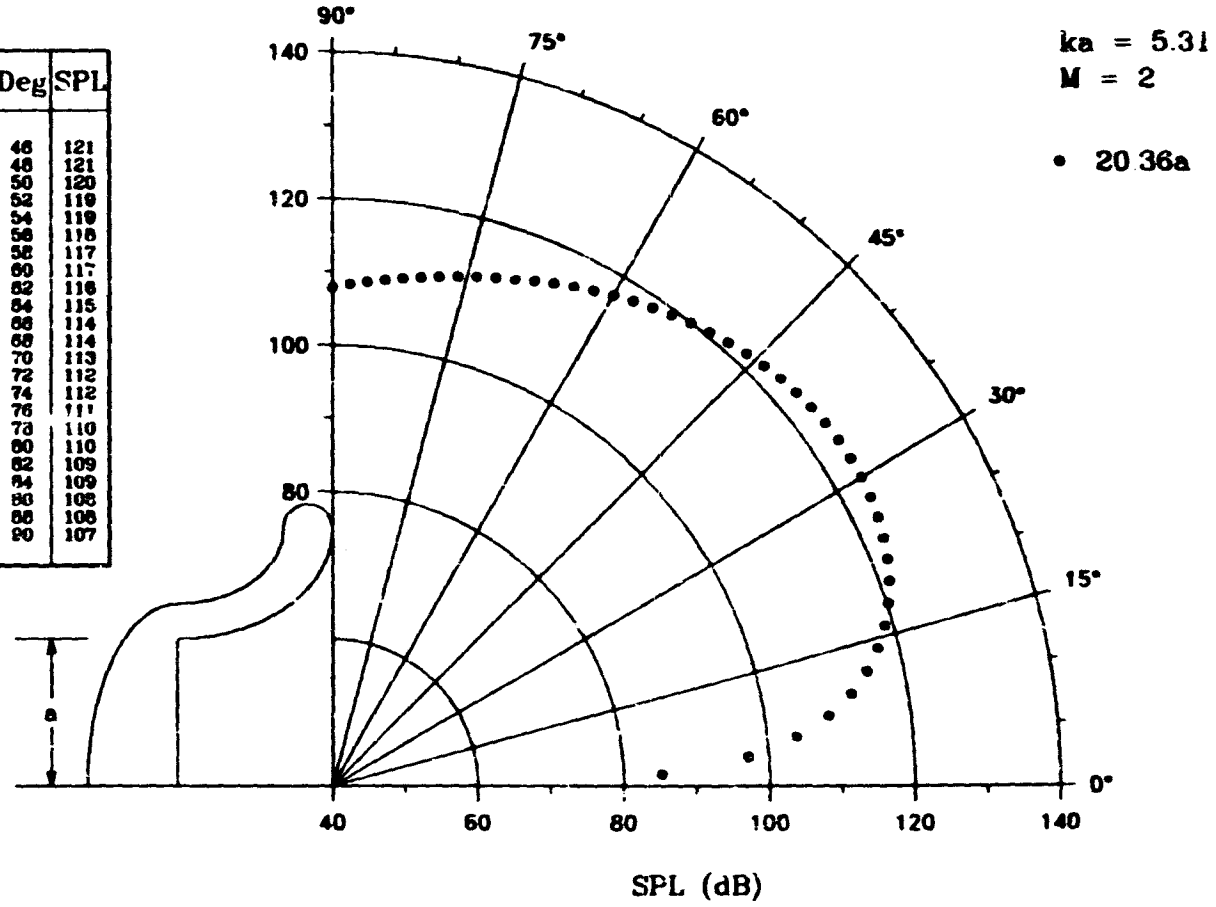

Fig. 19 (M,N) = (2,1)

LANGLEY BELLMOUTH

Deg	SPL	Deg	SPL
0	0	46	122
2	90	48	122
4	101	50	121
6	108	52	120
8	113	54	119
10	116	56	118
12	119	58	117
14	121	60	116
16	123	62	115
18	124	64	115
20	125	66	114
22	126	68	113
24	126	70	112
26	127	72	112
28	127	74	111
30	127	76	110
32	127	78	110
34	128	80	109
36	128	82	109
38	125	84	109
40	125	86	108
42	124	88	108
44	123	90	107

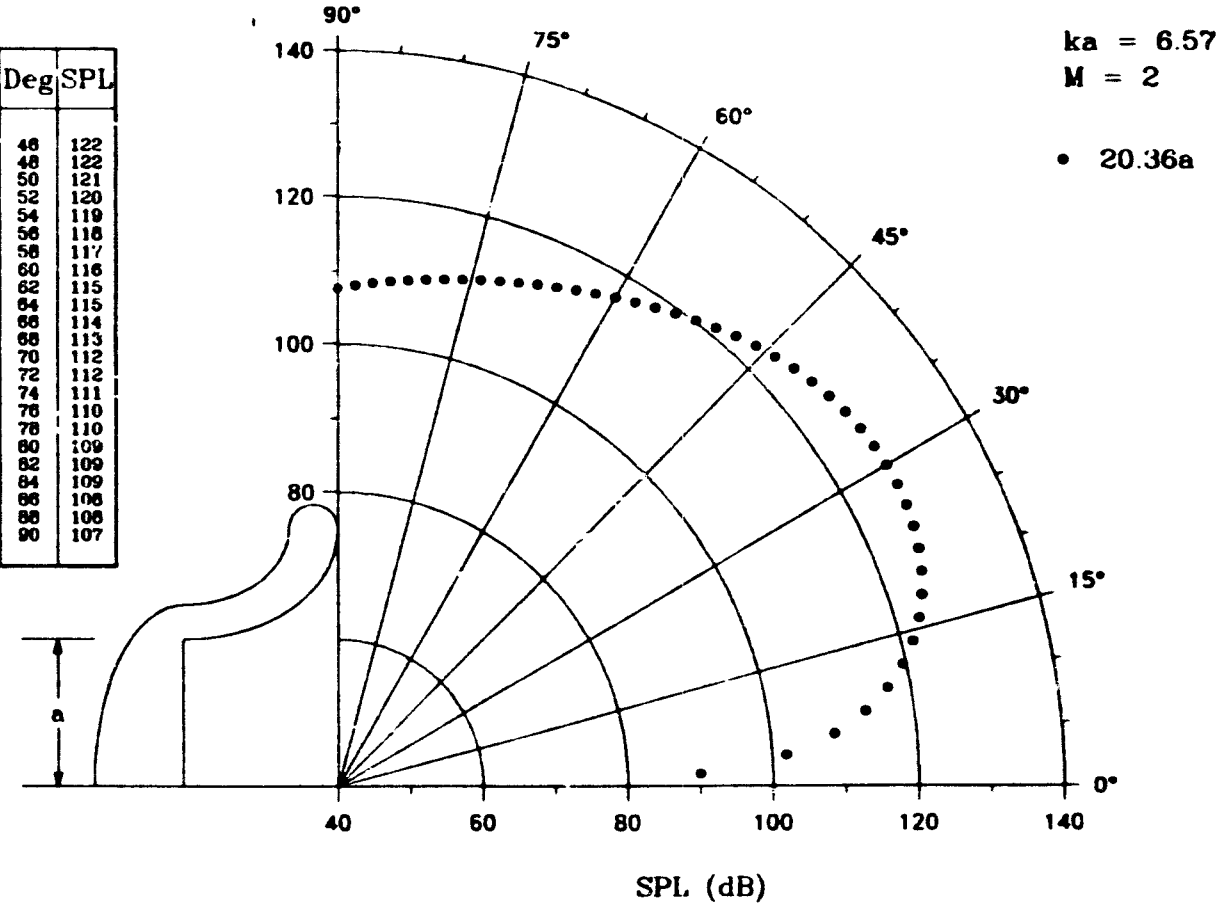

Fig. 20 (M,N) = (2,1)

LANGLEY BELLMOUTH

Deg	SPL	Deg	SPL
0	0	46	111
2	21	48	111
4	45	50	111
6	58	52	111
8	69	54	111
10	78	56	111
12	82	58	110
14	87	60	110
16	91	62	110
18	94	64	109
20	97	66	109
22	100	68	108
24	102	70	108
26	104	72	107
28	105	74	107
30	107	76	106
32	108	78	106
34	109	80	105
36	109	82	104
38	110	84	104
40	111	86	104
42	111	88	103
44	111	90	103

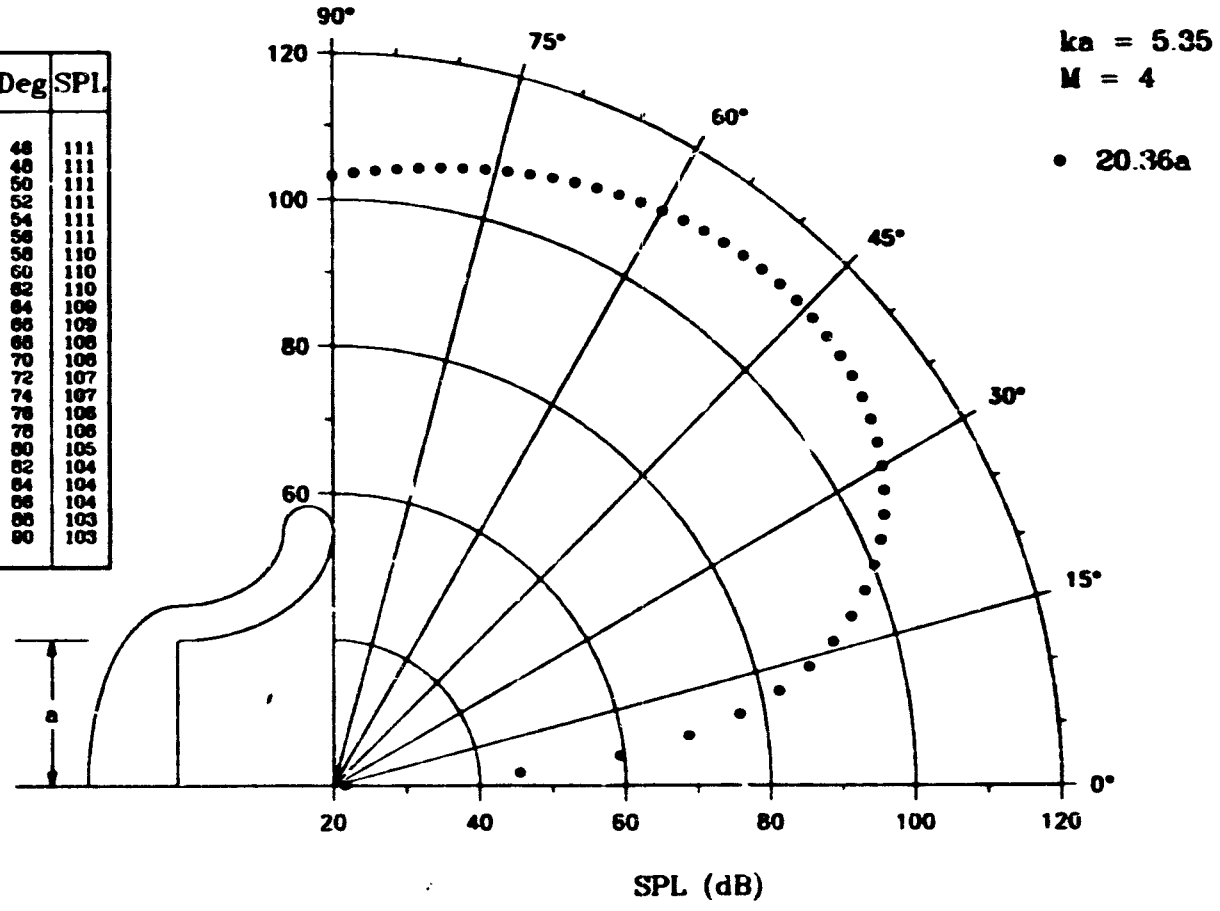

Fig. 21 (M,N) = (4,1)

LANGLEY BELLMOUTH

Deg	SPL	Deg	SPL
0	0	46	112
2	22	48	112
4	46	50	112
6	60	52	112
8	70	54	111
10	77	56	111
12	83	58	111
14	88	60	111
16	92	62	110
18	95	64	110
20	98	66	109
22	101	68	109
24	103	70	108
26	104	72	108
28	106	74	107
30	107	76	107
32	108	78	106
34	109	80	105
36	110	82	105
38	111	84	104
40	111	86	104
42	112	88	104
44	112	90	103

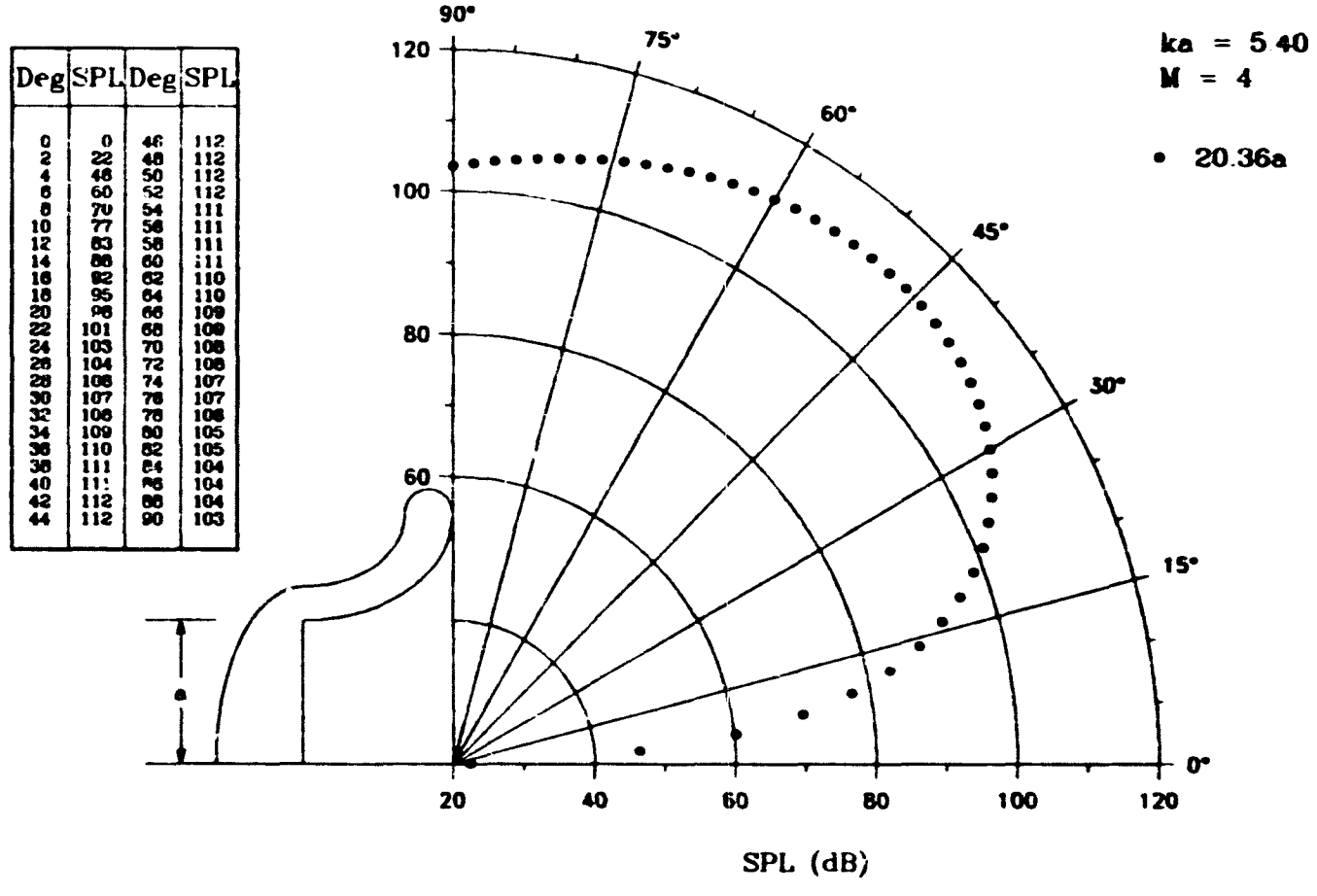

Fig. 22 (M,N) = (4,1)

LANGLEY BELLMOUTH

Deg	SPL	Deg	SPL
0	0	46	114
2	28	48	114
4	55	50	114
6	73	52	114
8	83	54	114
10	90	56	114
12	96	58	113
14	91	60	113
16	95	62	112
18	98	64	112
20	101	66	111
22	104	68	111
24	106	70	110
26	108	72	110
28	109	74	109
30	110	76	109
32	111	78	108
34	112	80	108
36	113	82	107
38	114	84	106
40	114	86	106
42	114	88	105
44	114	90	105

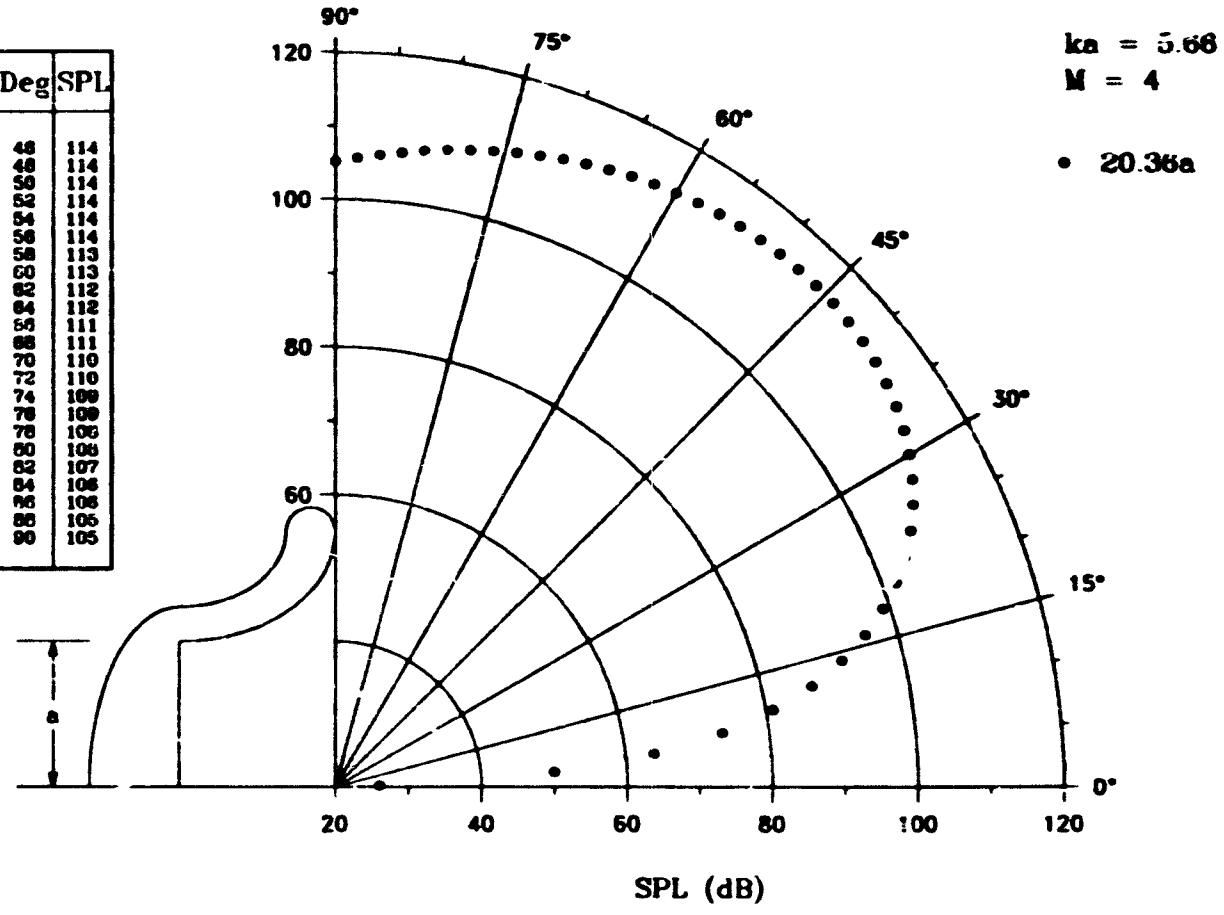

Fig. 23 (M,N) = (4,1)

LANGLEY BELLMOUTH

Deg	SPL	Deg	SPL
0	0	46	118
2	30	48	117
4	54	50	117
6	68	52	117
8	78	54	117
10	85	56	116
12	91	58	116
14	96	60	115
16	100	62	115
18	103	64	114
20	106	66	114
22	108	68	113
24	110	70	113
26	112	72	112
28	113	74	111
30	114	76	111
32	115	78	110
34	116	80	110
36	117	82	109
38	117	84	108
40	117	86	108
42	116	88	107
44	116	90	107

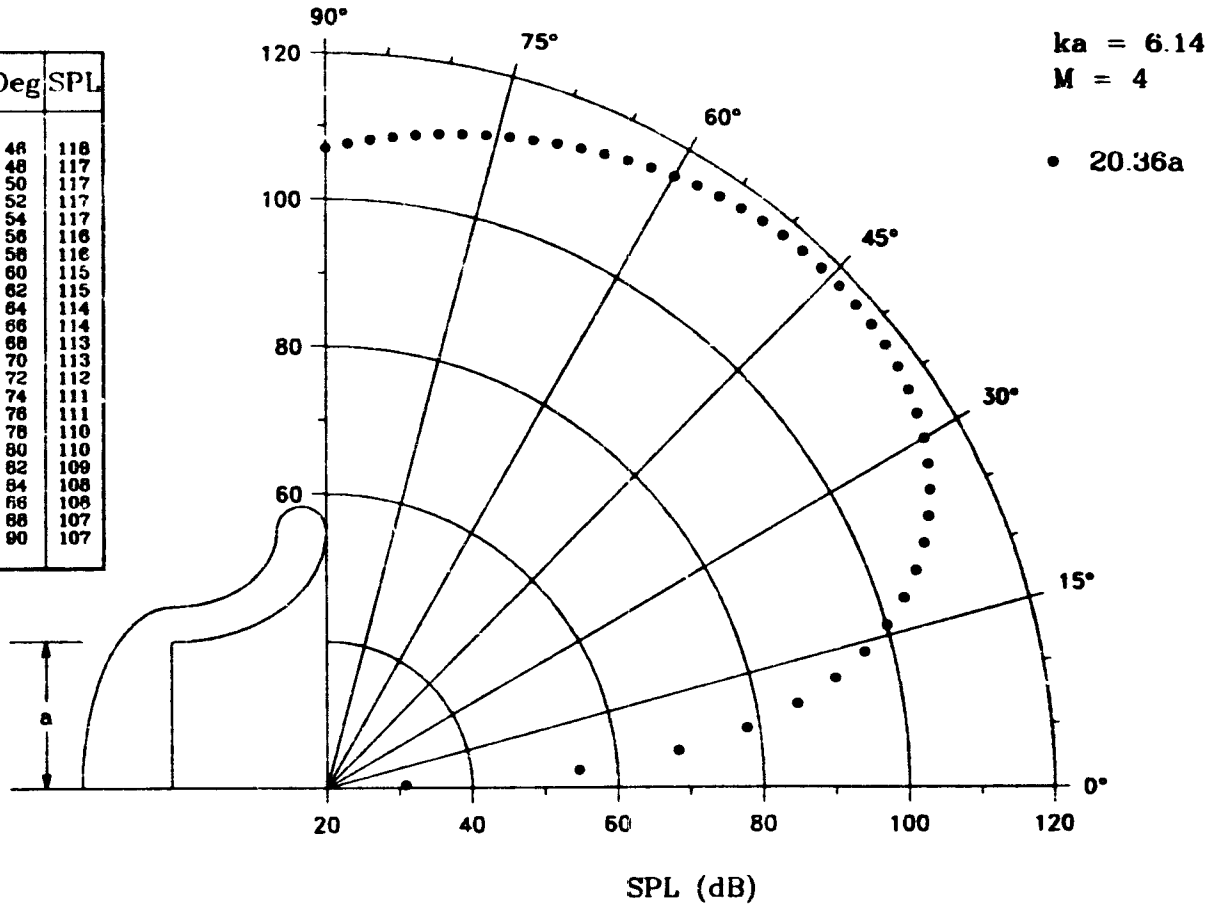

Fig. 24 (M,N) = (4,1)

LANGLEY BELLMOUTH

Deg	SPL	Deg	SPL
0	0	46	121
2	36	48	121
4	59	50	120
6	73	52	120
8	83	54	119
10	90	56	119
12	96	58	118
14	101	60	117
16	104	62	117
18	108	64	116
20	110	66	115
22	113	68	114
24	114	70	114
26	116	72	113
28	117	74	112
30	118	76	112
32	119	78	111
34	120	80	110
36	120	82	110
38	121	84	109
40	121	86	109
42	121	88	108
44	121	90	108

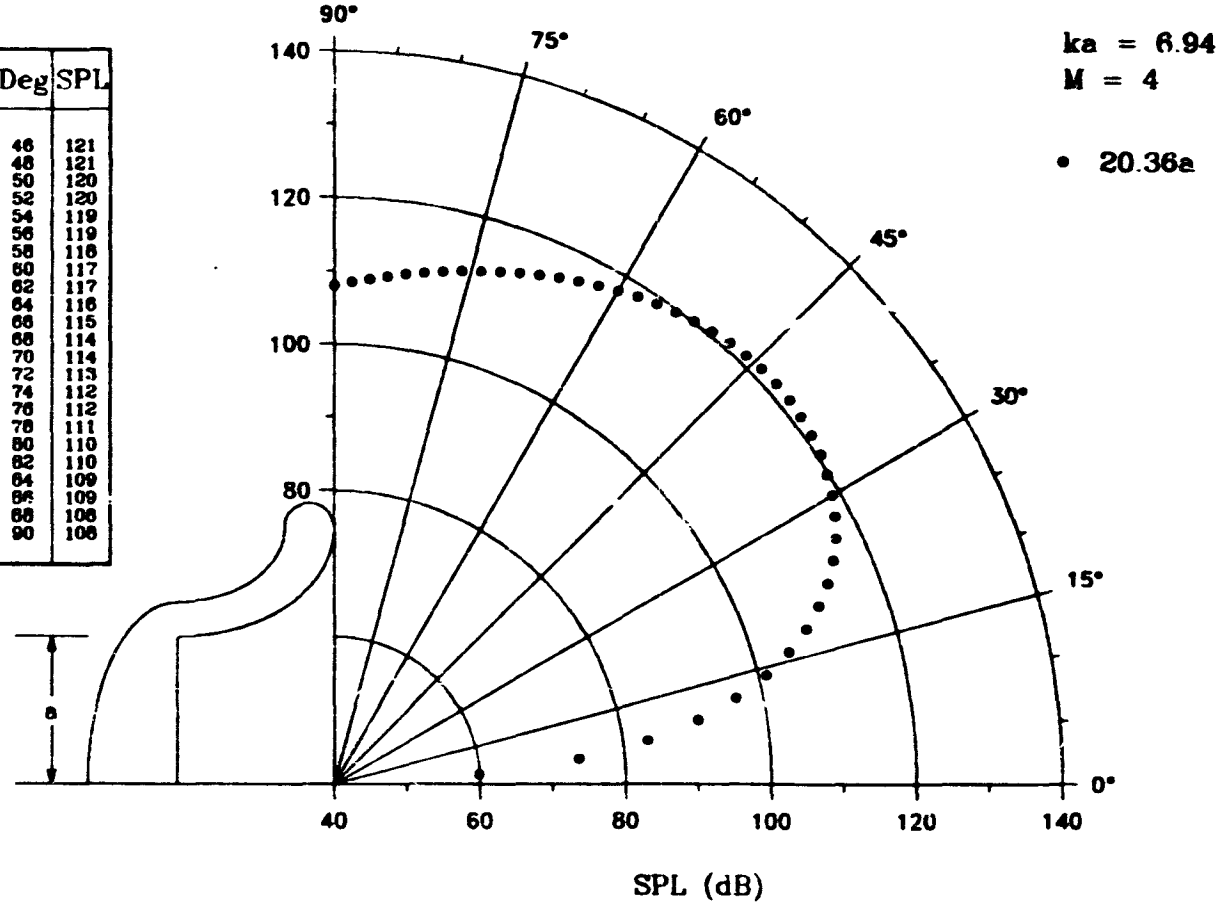

Fig. 25 (M,N) = (4,1)

LANGLEY BELLMOUTH

Deg	SPL	Deg	SPL
0	0	46	123
2	41	48	122
4	65	50	122
6	79	52	121
8	88	54	120
10	96	56	119
12	101	58	119
14	106	60	118
16	110	62	117
18	113	64	116
20	116	66	115
22	118	68	115
24	120	70	114
26	121	72	113
28	122	74	112
30	123	76	112
32	124	78	111
34	124	80	110
36	124	82	110
38	124	84	109
40	124	86	108
42	124	88	108
44	124	90	106

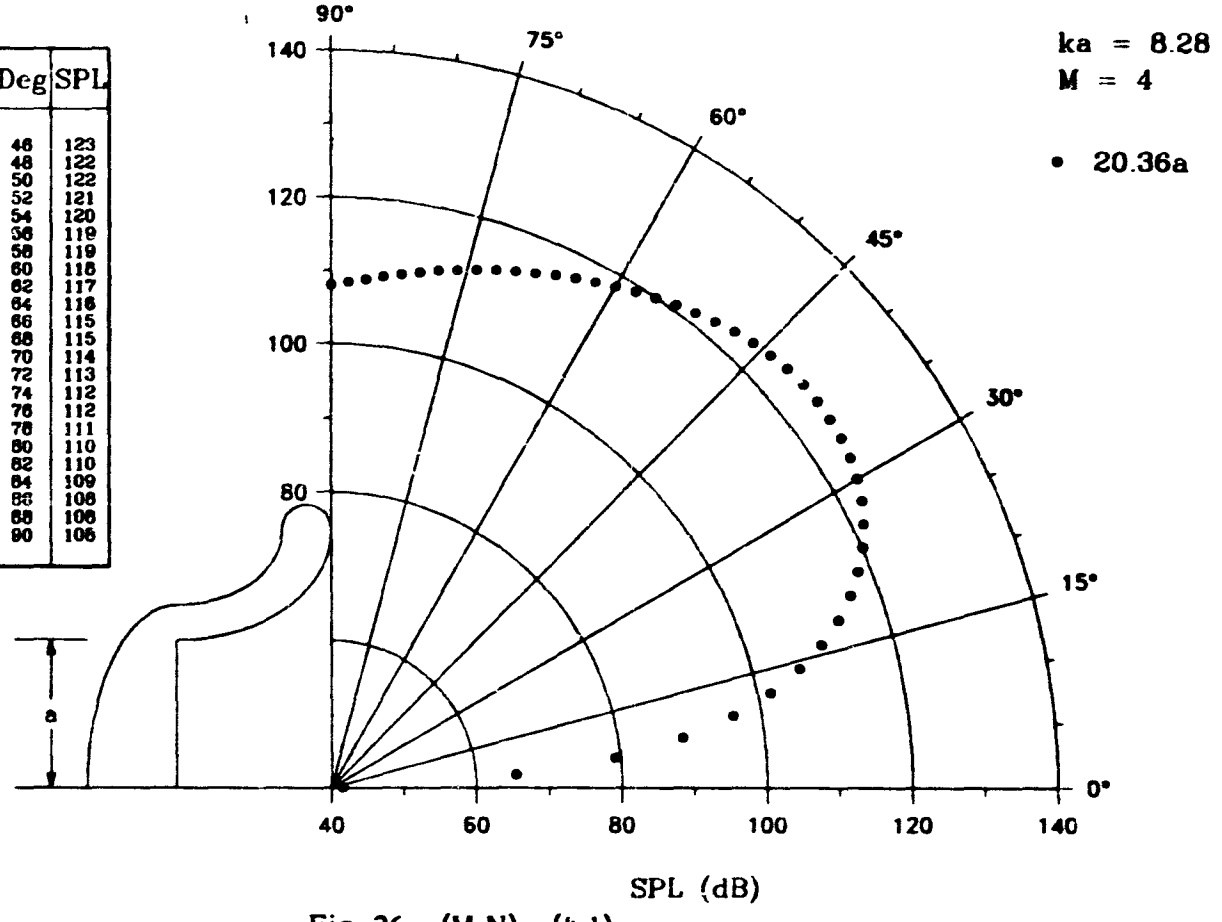

Fig. 26 (M,N) = (4,1)

LANGLEY BELLMOUTH

Deg	SPL	Deg	SPL
0	0	46	112
2	-70	48	113
4	-22	50	113
6	5	52	113
8	24	54	113
10	39	56	113
12	51	58	113
14	60	60	112
16	68	62	112
18	75	64	111
20	81	66	111
22	86	68	110
24	91	70	110
26	94	72	109
28	98	74	108
30	101	76	108
32	103	78	107
34	105	80	106
36	107	82	106
38	109	84	105
40	110	86	104
42	111	88	103
44	112	90	103

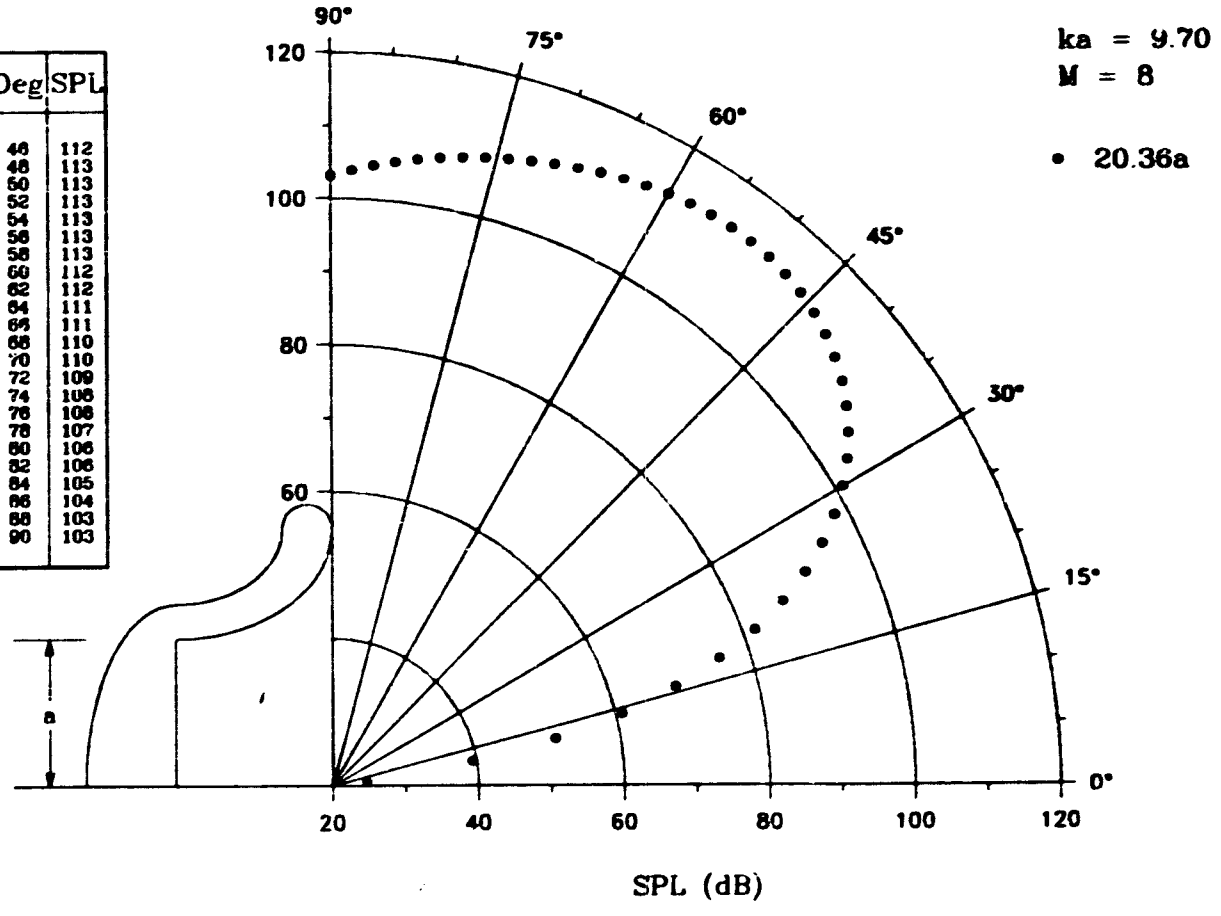

Fig. 27 (M,N) = (8,1)

LANGLEY BELLMOUTH

Deg	SPL	Deg	SPL
0	0	48	113
2	-69	48	114
4	-21	50	114
6	6	52	113
8	25	54	114
10	40	56	114
12	52	58	114
14	62	60	113
16	70	62	113
18	77	64	112
20	82	66	112
22	87	68	111
24	92	70	110
26	96	72	110
28	99	74	109
30	102	76	108
32	104	78	108
34	106	80	107
36	108	82	106
38	110	84	106
40	111	86	105
42	112	88	104
44	113	90	103

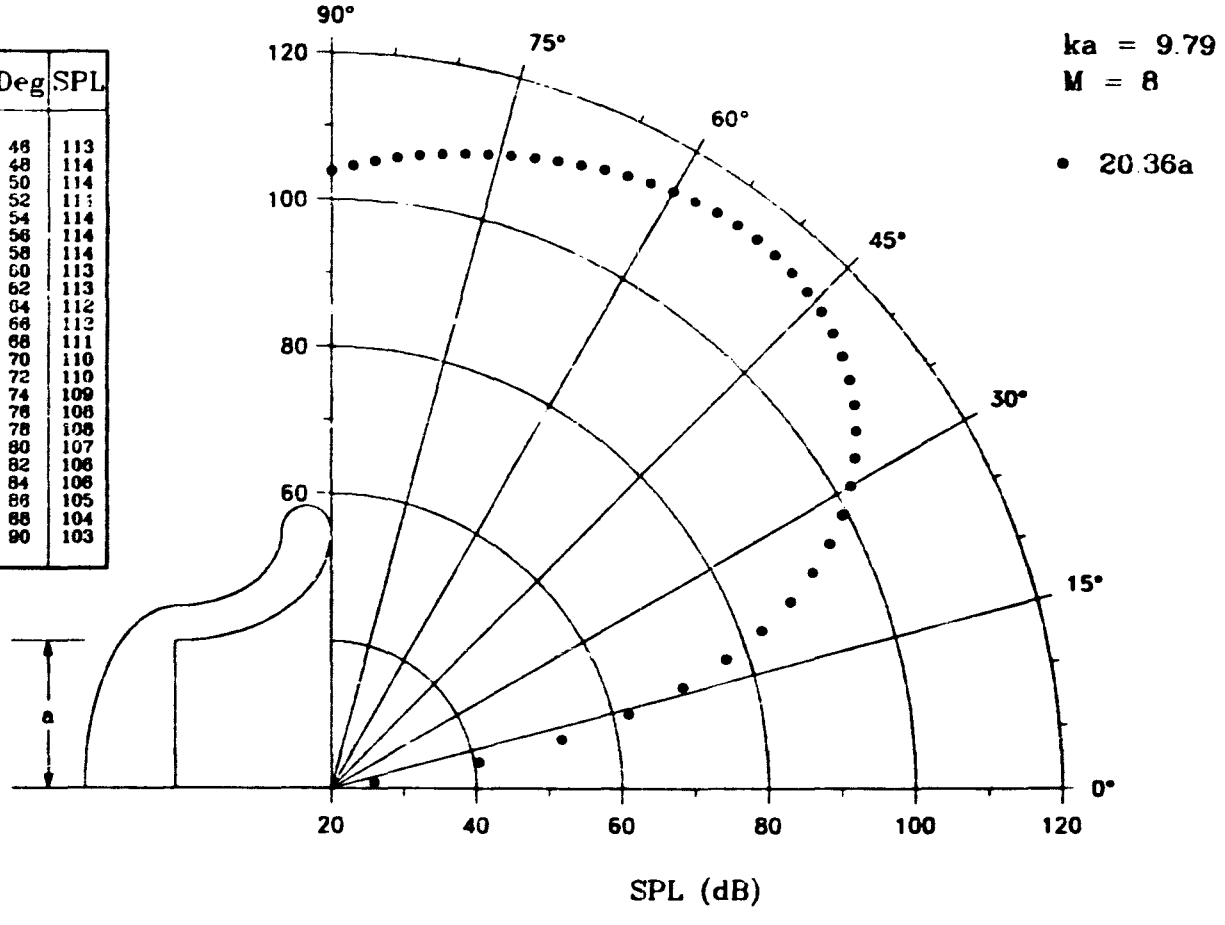

Fig. 28 (M,N) = (8,1)

LANGLEY BELLMOUTH

Deg	SPL	Deg	SPL
0	0	46	117
2	-64	48	116
4	-16	50	116
6	11	52	116
8	30	54	117
10	45	56	117
12	56	58	117
14	66	60	116
16	74	62	116
18	81	64	115
20	87	66	114
22	92	68	114
24	96	70	113
26	100	72	112
28	103	74	111
30	106	76	111
32	108	78	110
34	110	80	109
36	112	82	109
38	114	84	108
40	115	86	107
42	116	88	107
44	117	90	106

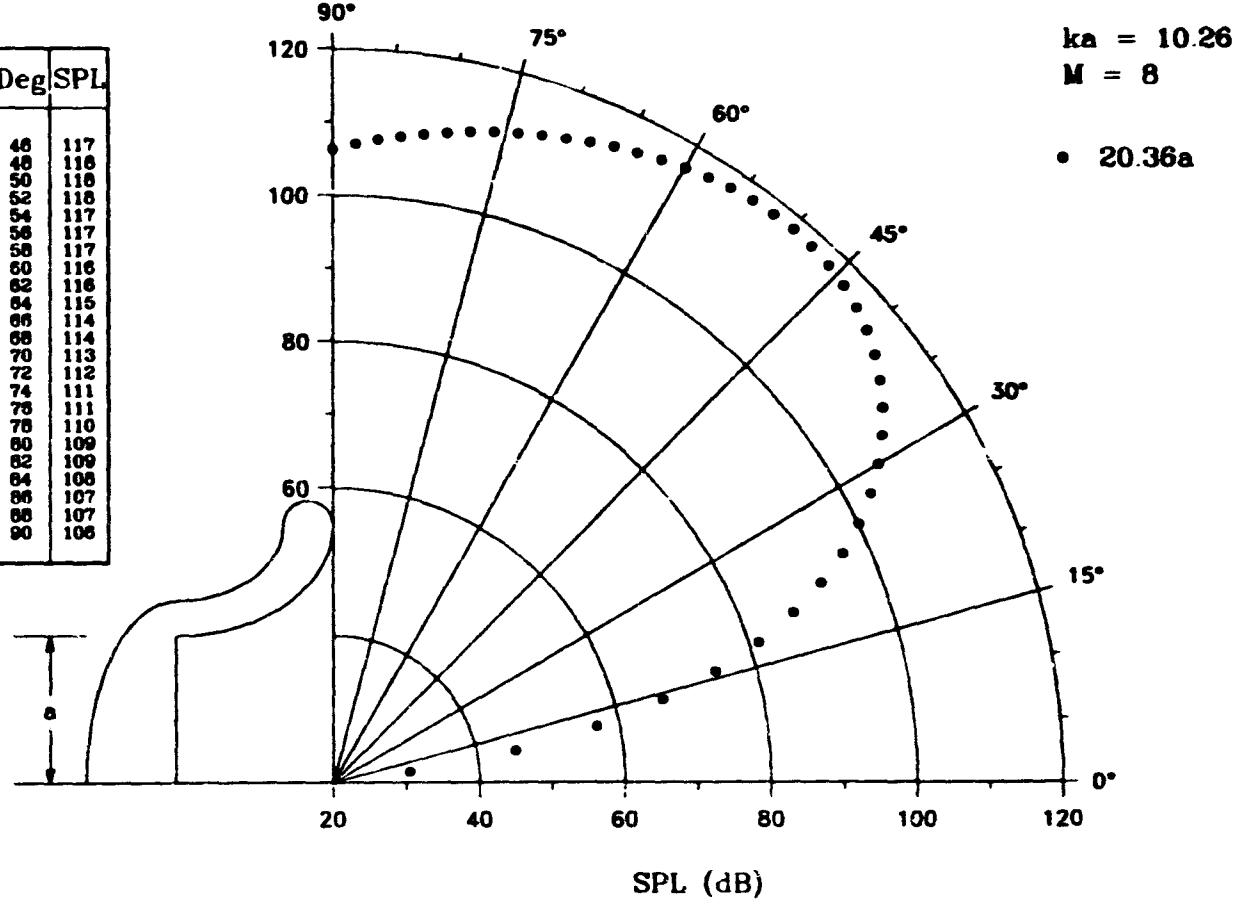

Fig. 29 (M,N) = (8,1)

LANGLEY BELLMOUTH

Deg	SPL	Deg	SPL
0	0	46	121
2	-59	48	121
4	-11	50	121
6	15	52	121
8	35	54	120
10	49	56	120
12	61	58	119
14	70	60	119
16	78	62	118
18	85	64	117
20	91	66	116
22	96	68	116
24	101	70	115
26	104	72	114
28	108	74	113
30	111	76	113
32	113	78	112
34	115	80	111
36	117	82	110
38	118	84	110
40	119	86	109
42	120	88	108
44	121	90	107

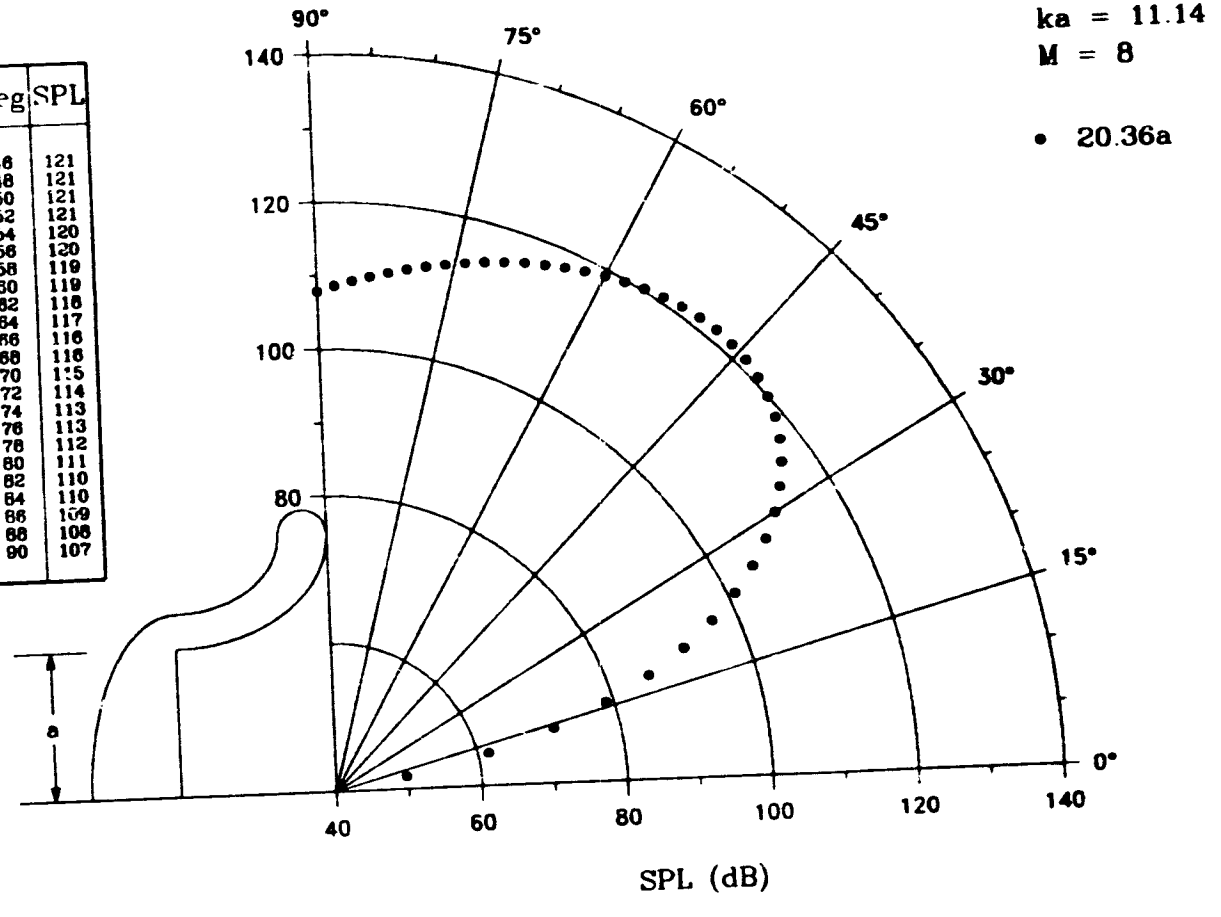

Fig. 30 (M,N) = (8,1)

LANGLEY BELLMOUTH

Deg	SPL	Deg	SPL
0	0	46	124
2	−60	48	124
4	−12	50	123
6	15	52	123
8	35	54	122
10	51	56	121
12	63	58	120
14	74	60	120
16	82	62	119
18	90	64	118
20	97	66	117
22	102	68	116
24	107	70	115
26	111	72	114
28	114	74	113
30	117	76	113
32	119	78	112
34	121	80	111
36	122	82	110
38	123	84	110
40	124	86	109
42	124	88	109
44	124	90	108

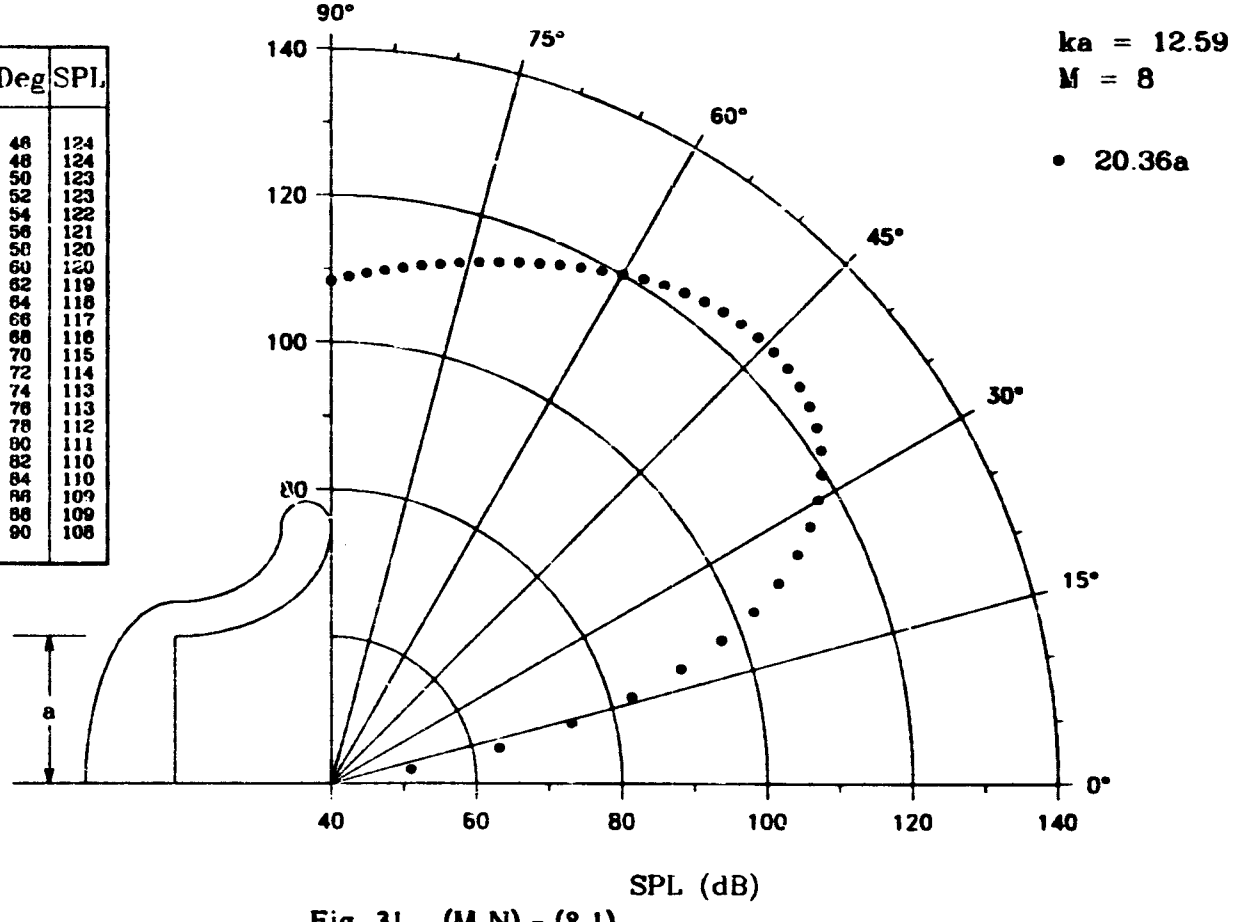

Fig. 31 (M,N) = (8,1)

LANGLEY BELLMOUTH

Deg	SPL	Deg	SPL
0	0	46	126
2	-41	48	126
4	6	50	125
6	33	52	124
8	53	54	123
10	67	56	122
12	79	58	120
14	88	60	119
16	96	62	118
18	103	64	117
20	108	66	116
22	112	68	115
24	116	70	114
26	119	72	113
28	121	74	112
30	123	76	112
32	125	78	111
34	126	80	110
36	127	82	110
38	127	84	109
40	127	86	108
42	127	88	108
44	127	90	107

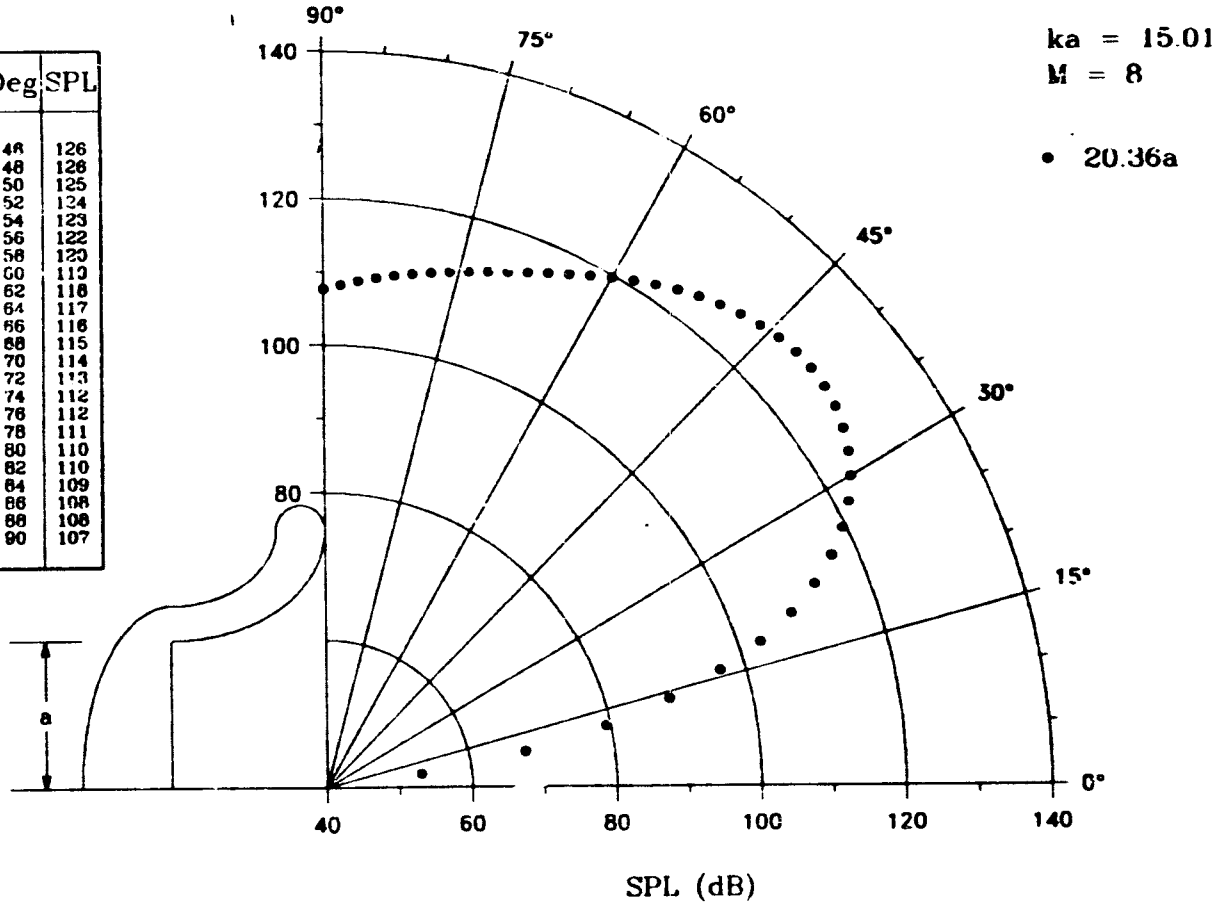

Fig. 32 (M,N) = (8,1)

LANGLEY BELLMOUTH

Deg	SPL	Deg	SPL
0	0	46	111
2	54	48	112
4	77	50	113
6	91	52	114
8	100	54	115
10	106	56	115
12	111	58	115
14	115	60	115
16	117	62	115
18	119	64	114
20	120	66	114
22	120	68	113
24	118	70	112
26	116	72	111
28	113	74	111
30	110	76	110
32	112	78	109
34	115	80	108
36	116	82	107
38	116	84	107
40	116	86	106
42	114	88	105
44	113	90	104

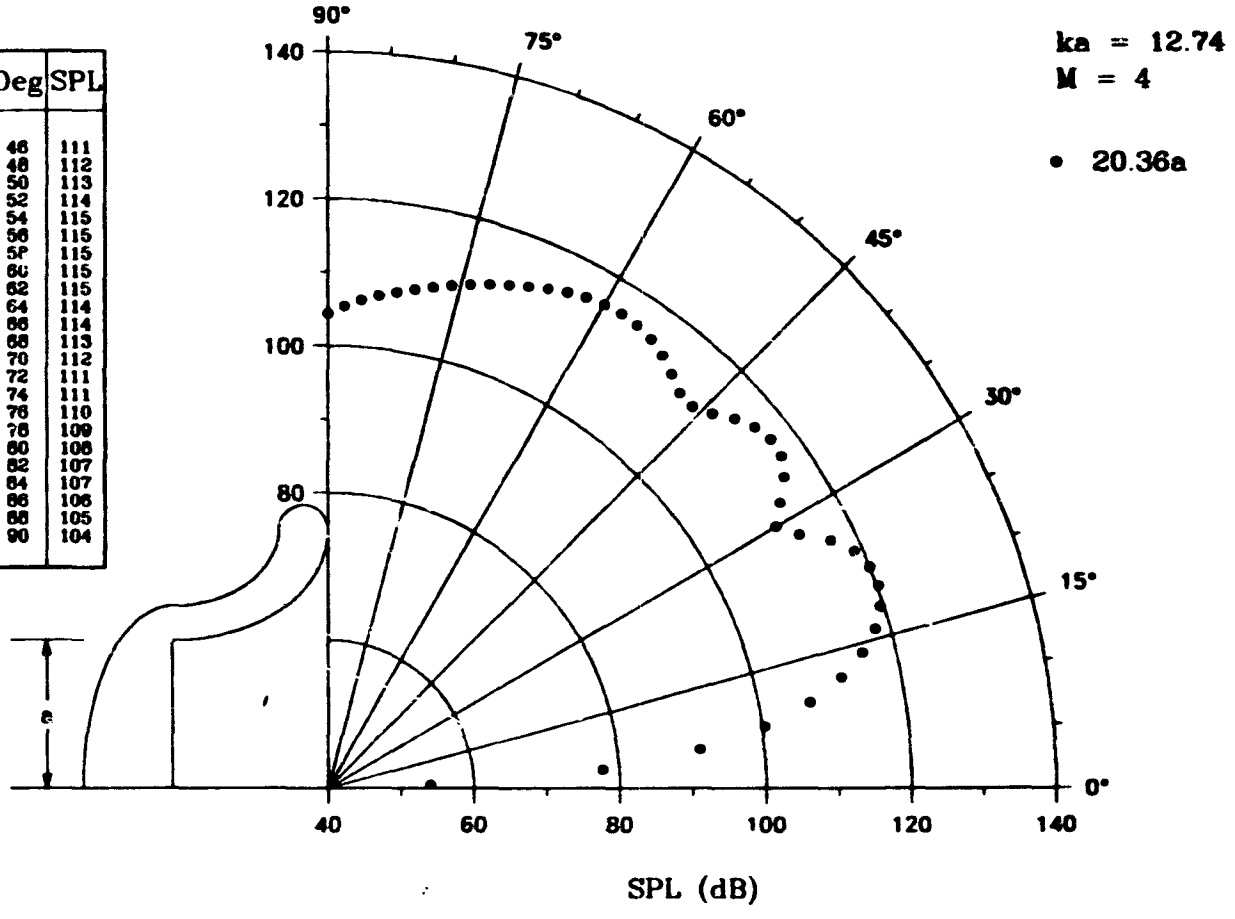

Fig. 33 (M,N) = (4,3)

LANGLEY BELLMOUTH

Deg	SPL	Deg	SPL
0	0	46	113
2	55	48	113
4	79	50	114
6	92	52	115
8	101	54	116
10	108	56	117
12	113	58	117
14	116	60	116
16	119	62	116
18	120	64	115
20	121	66	115
22	121	68	114
24	119	70	113
26	117	72	112
28	113	74	112
30	111	76	111
32	114	78	110
34	116	80	109
36	117	82	108
38	117	84	108
40	117	86	107
42	115	88	106
44	113	90	105

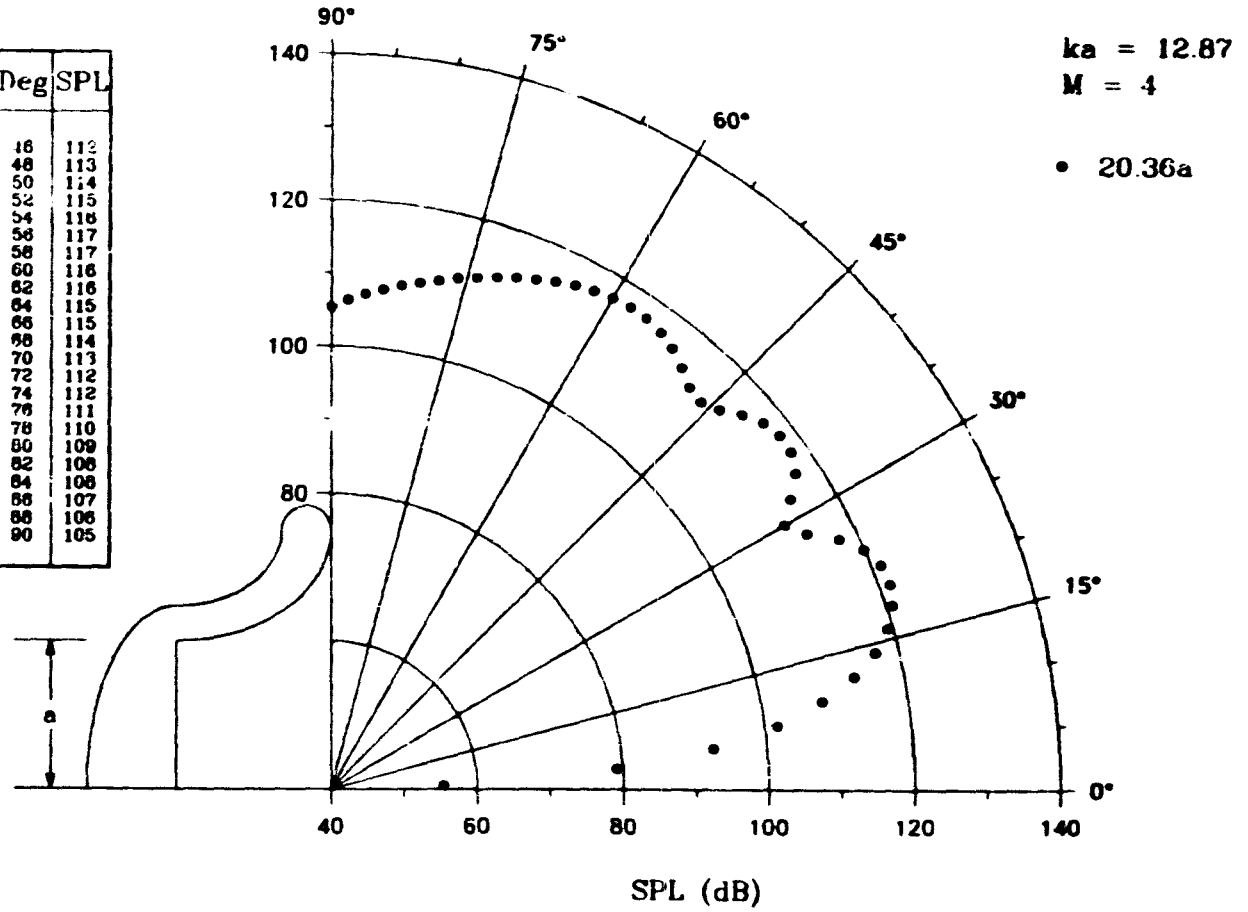

Fig. 34 (M,N) = (4,3)

LANGLEY BELLMOUTH

Deg	SPL	Deg	SPL
0	0	46	116
2	80	48	117
4	83	50	119
6	97	52	120
8	106	54	120
10	112	56	121
12	117	58	120
14	121	60	120
16	123	62	119
18	124	64	119
20	125	66	118
22	124	68	117
24	122	70	116
26	119	72	116
28	114	74	115
30	115	76	114
32	116	78	113
34	120	80	112
36	121	82	111
38	120	84	110
40	119	86	109
42	117	88	108
44	115	90	108

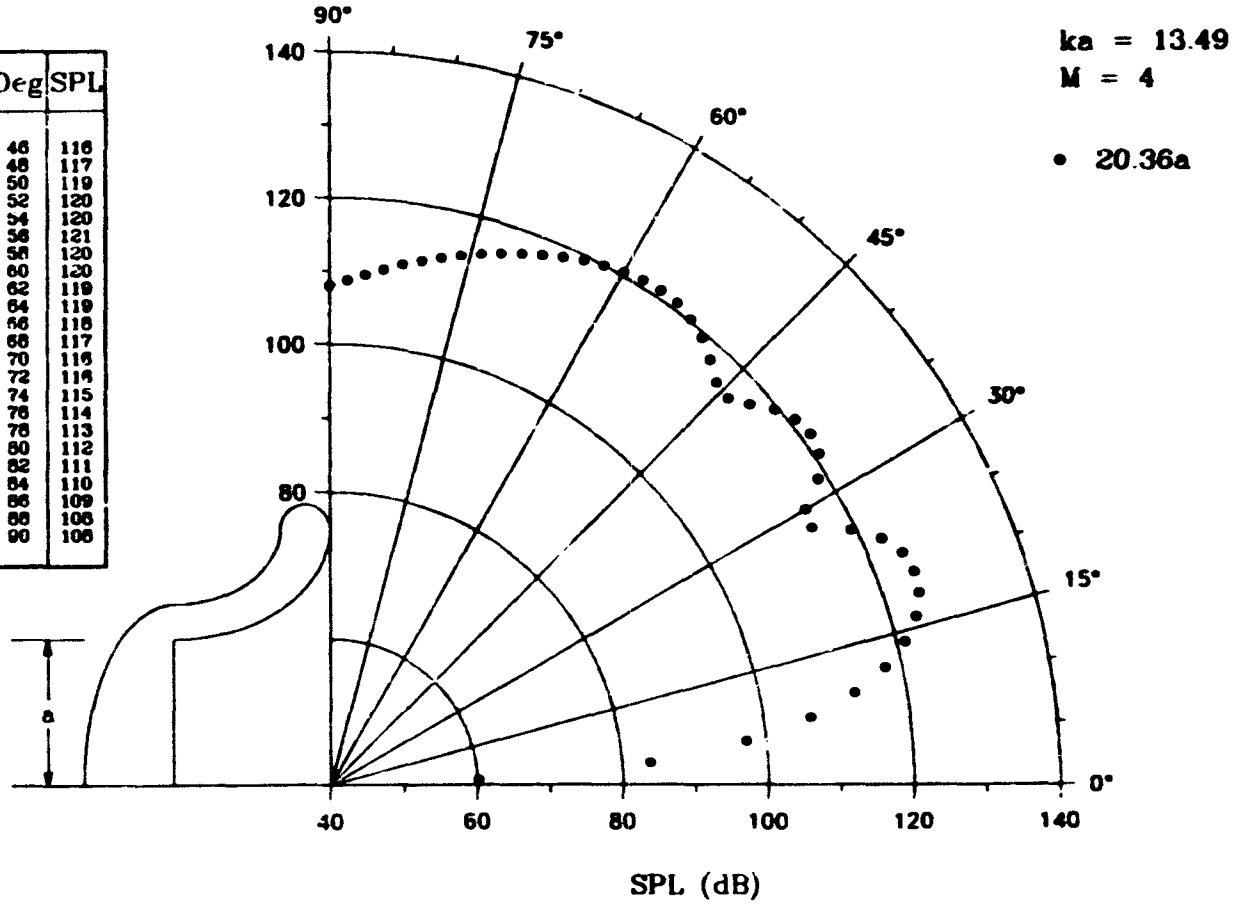

Fig. 35 (M,N) = (4,3)

LANGLEY BELLMOUTH

Deg	SPL	Deg	SPL
0	0	46	122
2	65	48	123
4	89	50	124
6	102	52	124
8	111	54	124
10	117	56	124
12	121	58	123
14	125	60	123
16	126	62	122
18	127	64	121
20	127	66	120
22	125	68	119
24	122	70	118
26	116	72	117
28	116	74	116
30	120	76	115
32	123	78	114
34	123	80	113
36	122	82	112
38	120	84	111
40	116	86	110
42	117	88	110
44	119	90	109

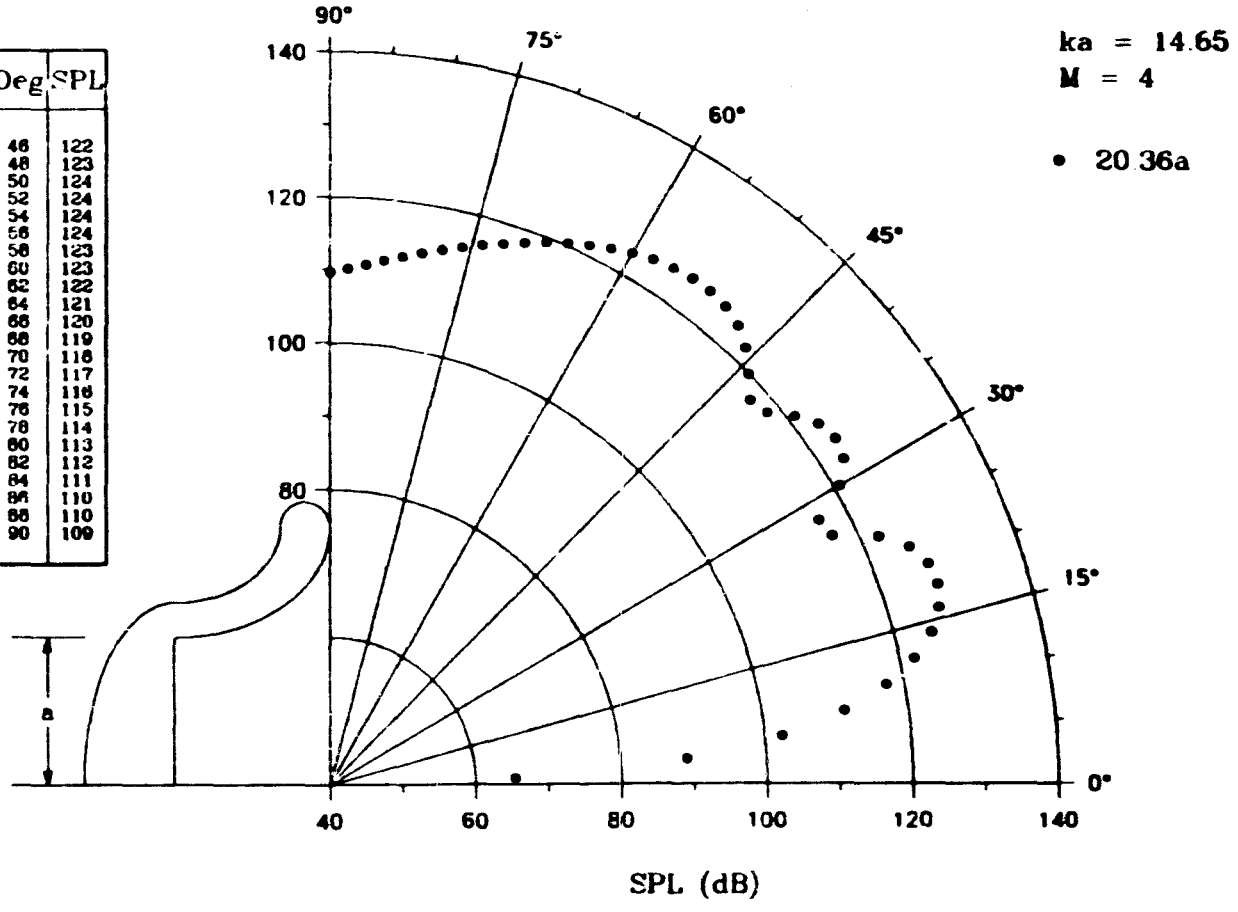

Fig. 36 (M,N) = (4,3)

LANGLEY BELLMOUTH

Deg	SPL	Deg	SPL
0	0	46	128
2	70	48	128
4	93	50	128
6	106	52	128
8	115	54	127
10	121	56	126
12	124	58	125
14	127	60	123
16	128	62	122
18	128	64	121
20	126	66	120
22	122	68	118
24	115	70	117
26	116	72	116
28	122	74	115
30	124	76	114
32	124	78	113
34	122	80	112
36	119	82	112
38	120	84	111
40	123	86	111
42	128	88	110
44	127	90	109

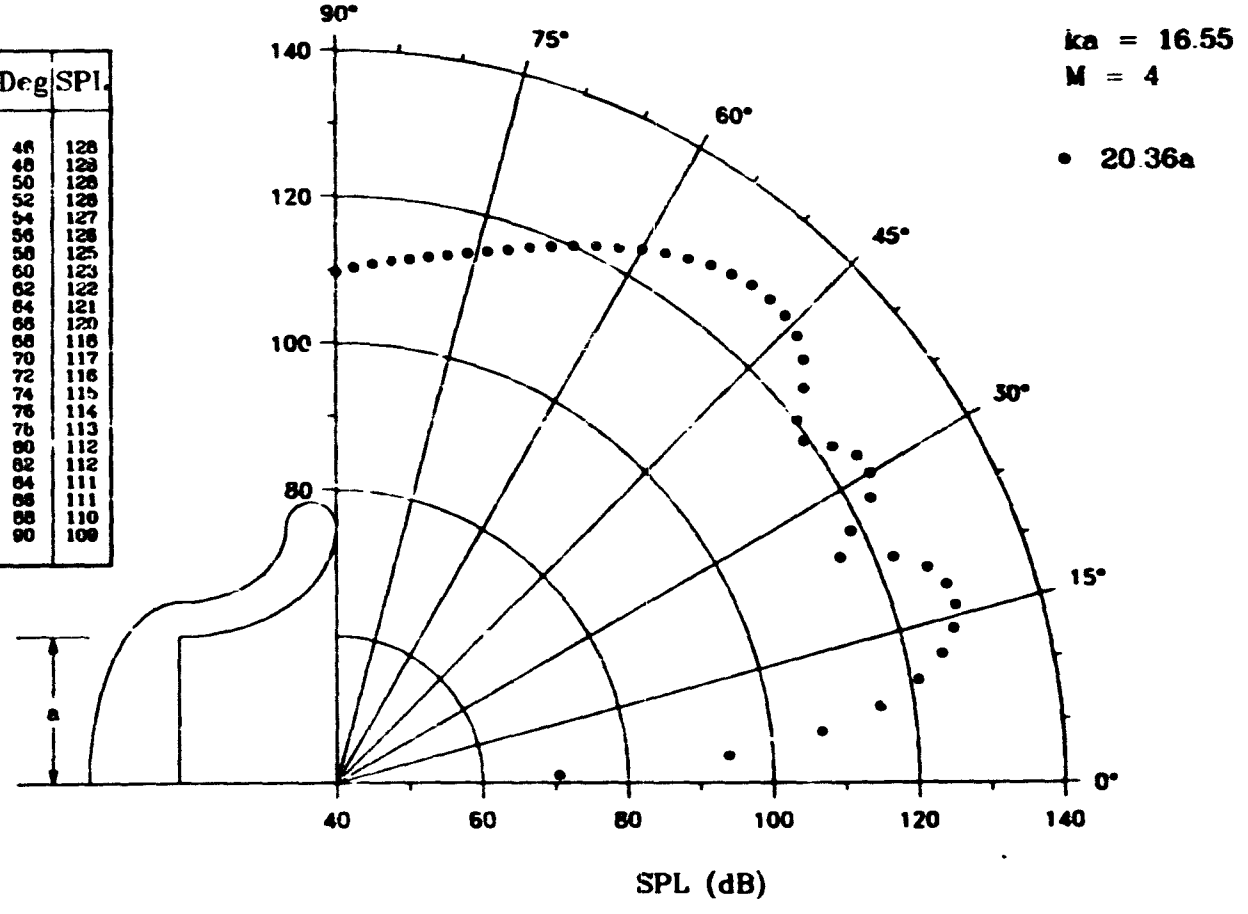

Fig. 37 (M,N) = (4,3)

LANGLEY BELLMOUTH

Deg	SPL	Deg	SPL
0	0	46	131
2	76	48	129
4	99	50	128
6	112	52	124
8	120	54	121
10	125	56	119
12	126	58	116
14	129	60	114
16	126	62	113
18	125	64	112
20	119	66	112
22	121	68	112
24	125	70	111
26	126	72	111
28	125	74	110
30	122	76	110
32	125	78	109
34	129	80	109
36	132	82	108
38	135	84	107
40	133	86	107
42	133	88	106
44	132	90	106

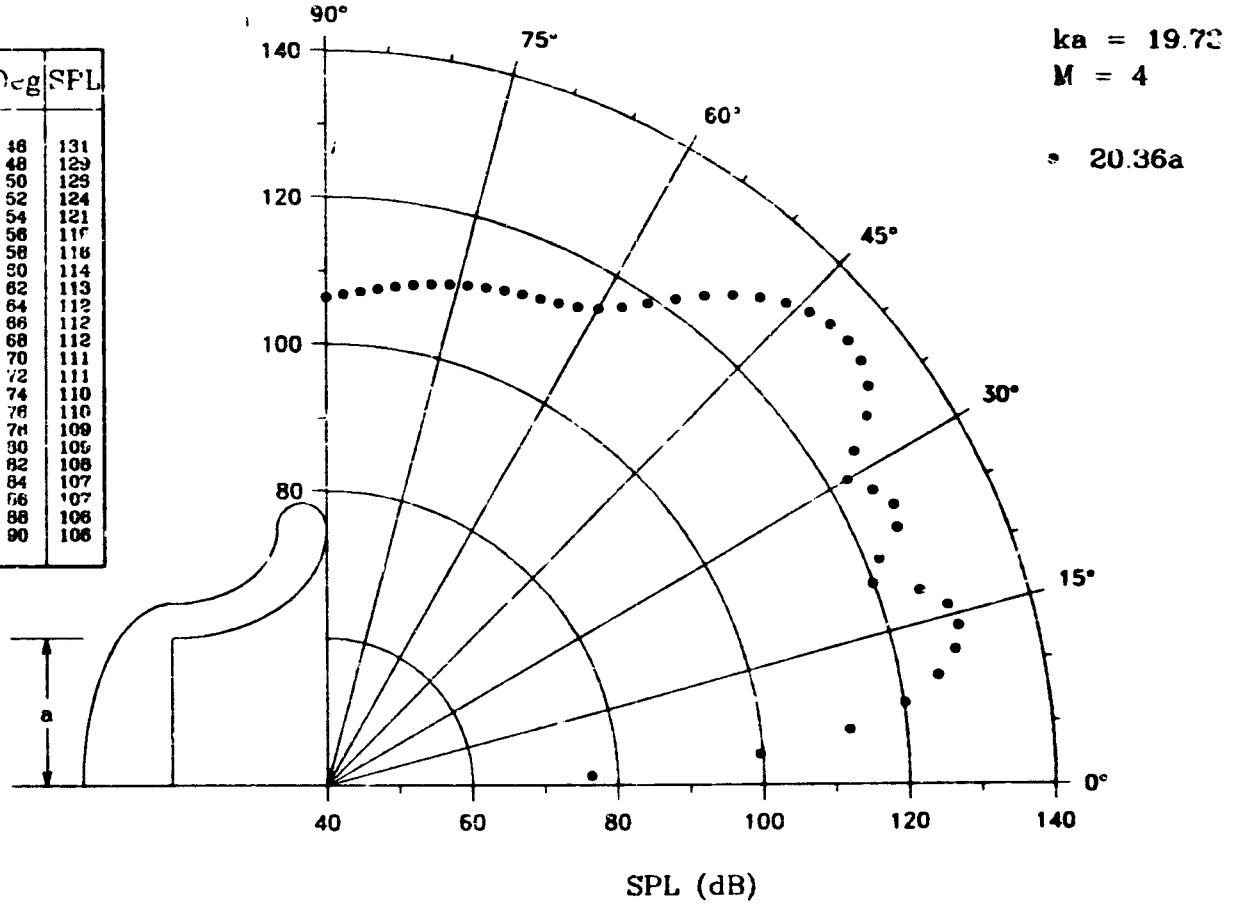

Fig. 38 (M,N) = (4,3)

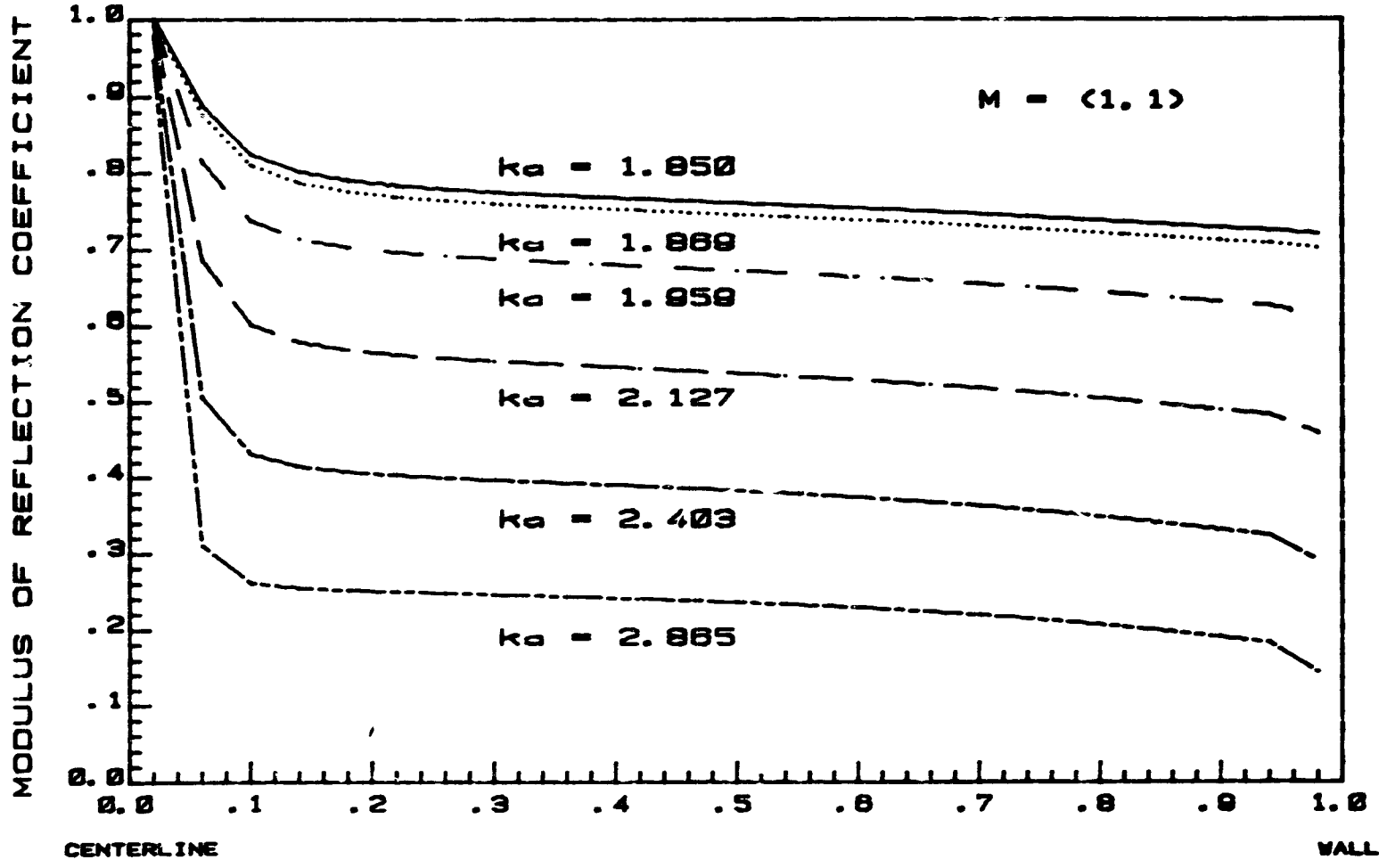

LANGLEY BELLMOUTH (Exit Plane)

Fig. 39a

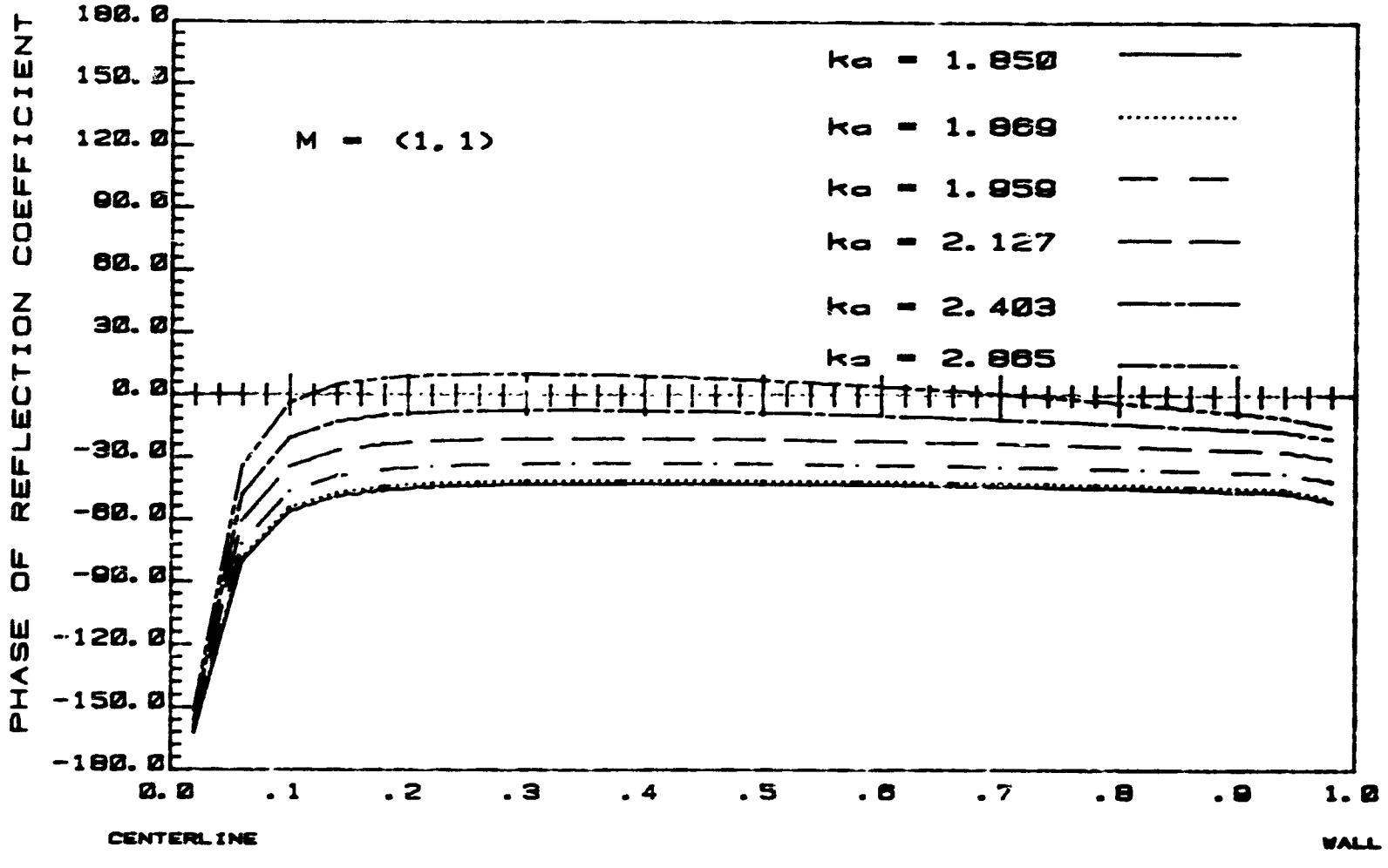

LANGLEY BELLMOUTH (Exit Plane)

Fig. 39b

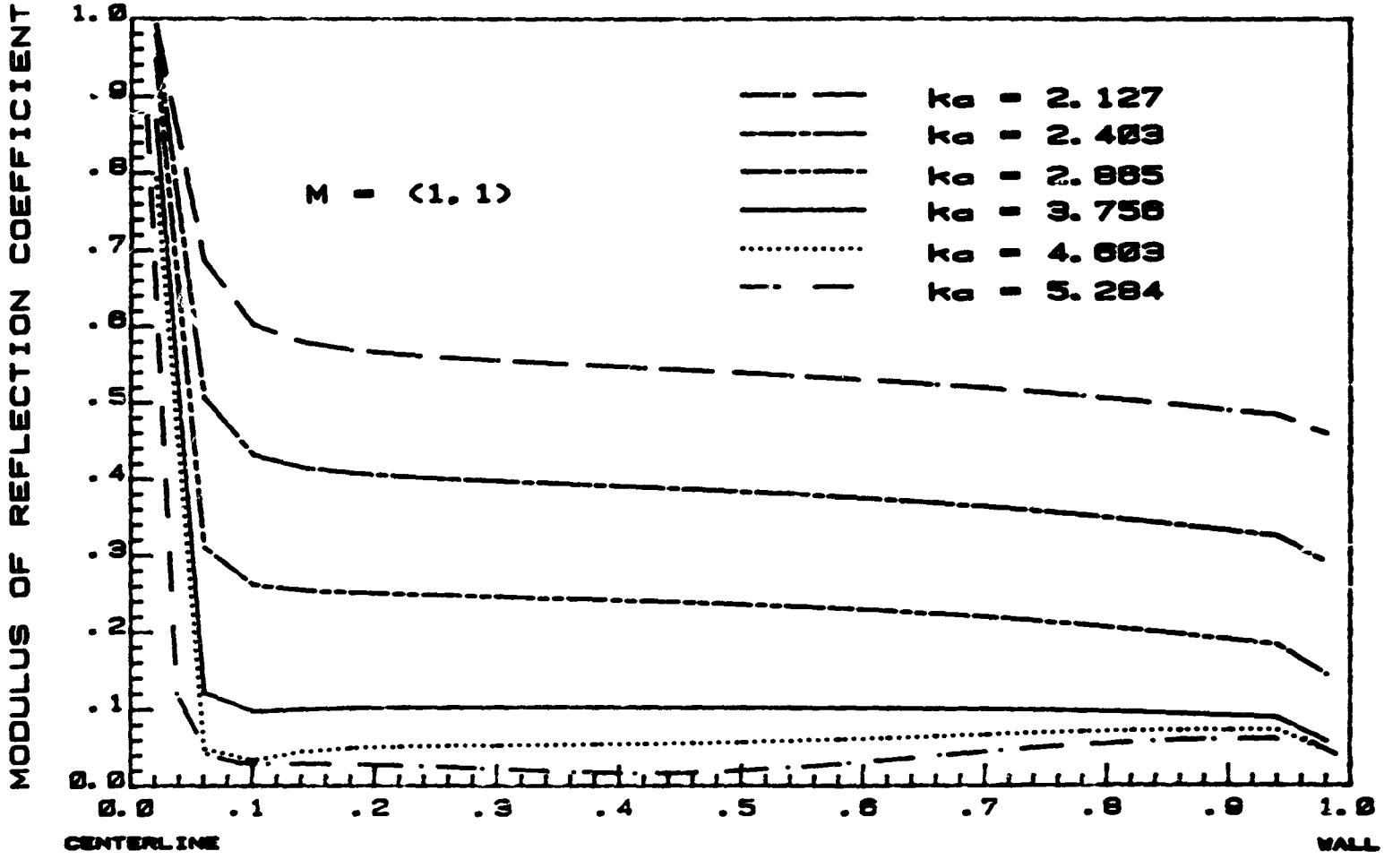

LANGLEY BELLMOUTH (Exit Plane)

Fig. 40a

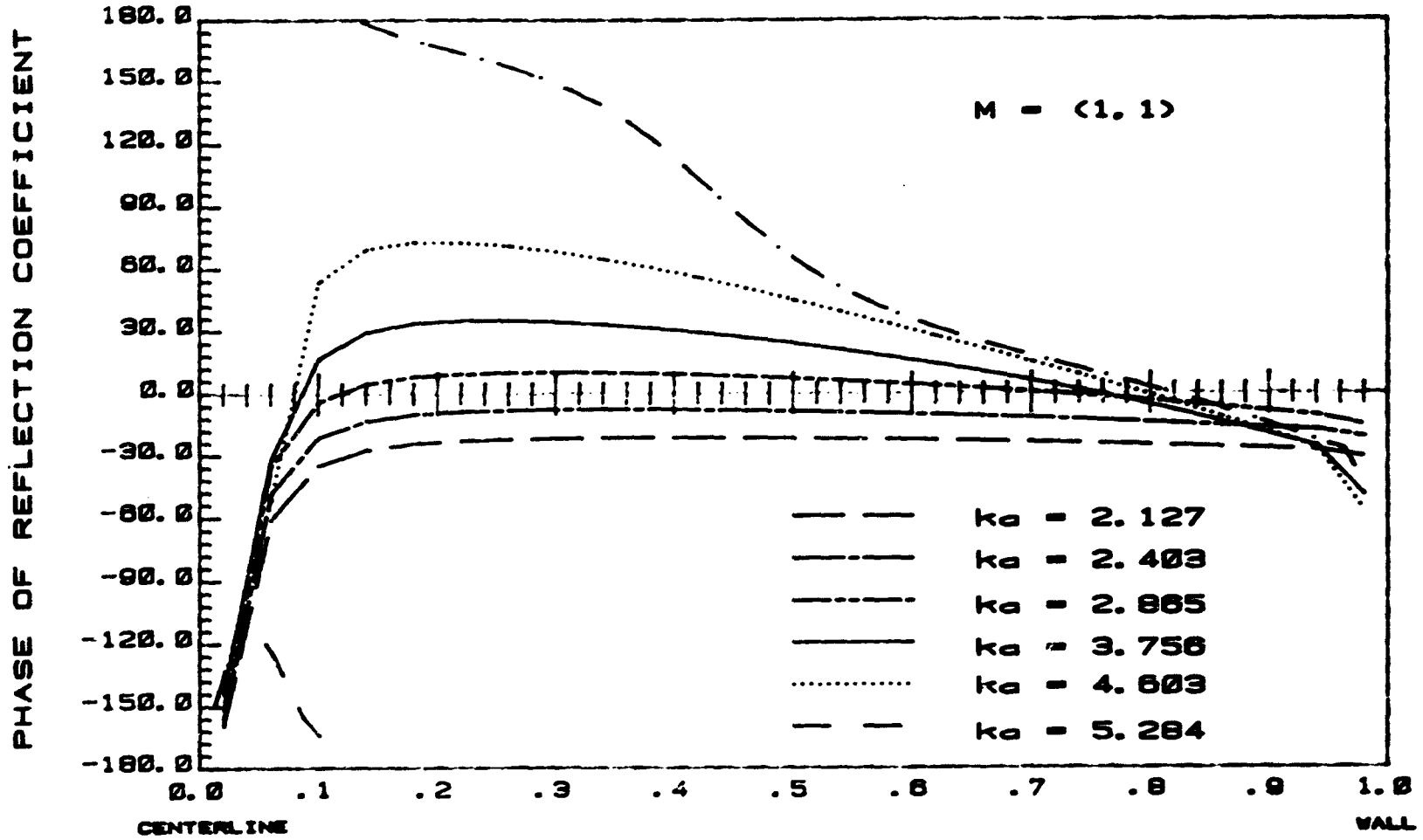

LANGLEY BELLMOUTH (Exit Plane)

Fig. 40b

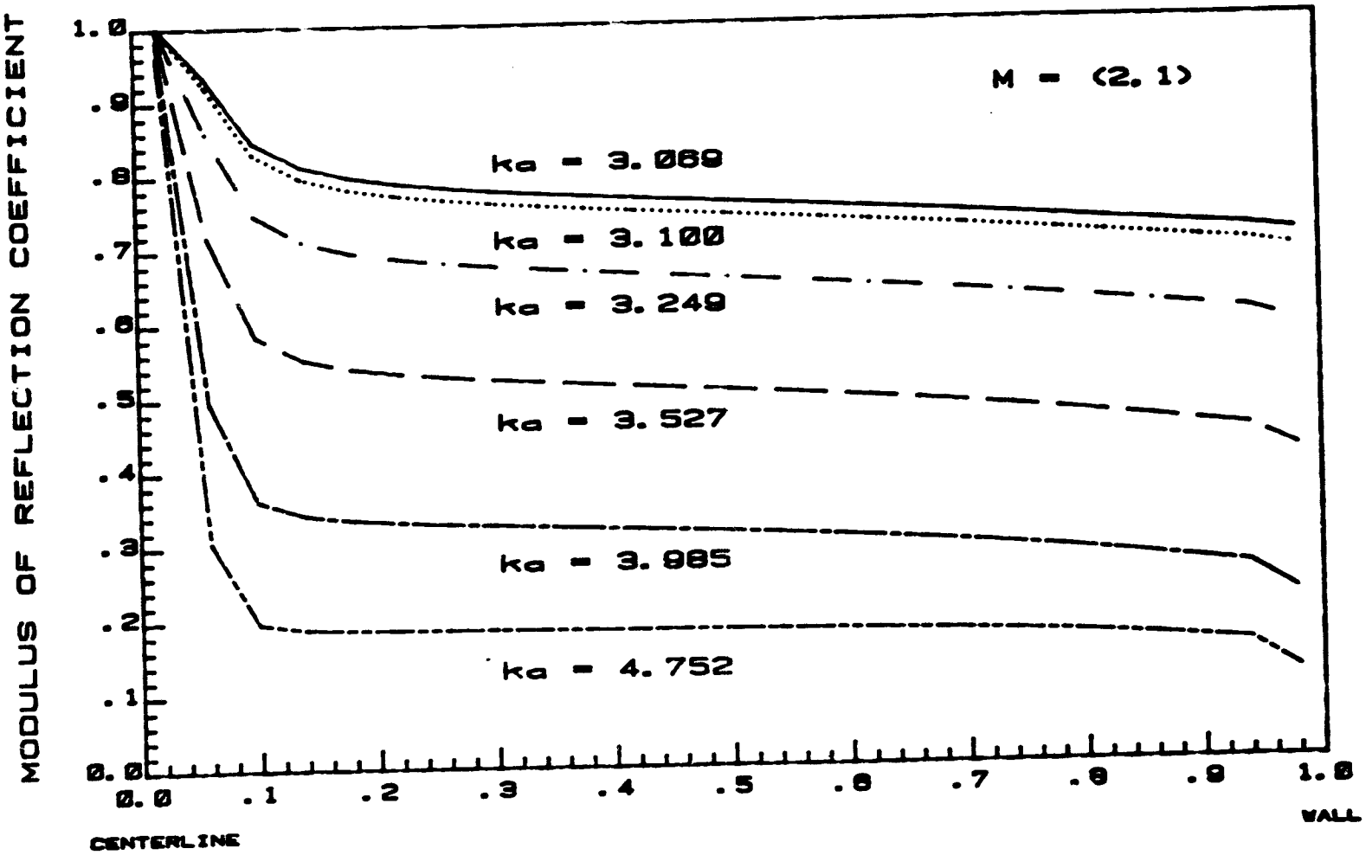

LANGLEY BELLMOUTH (Exit Plane)

Fig. 41a

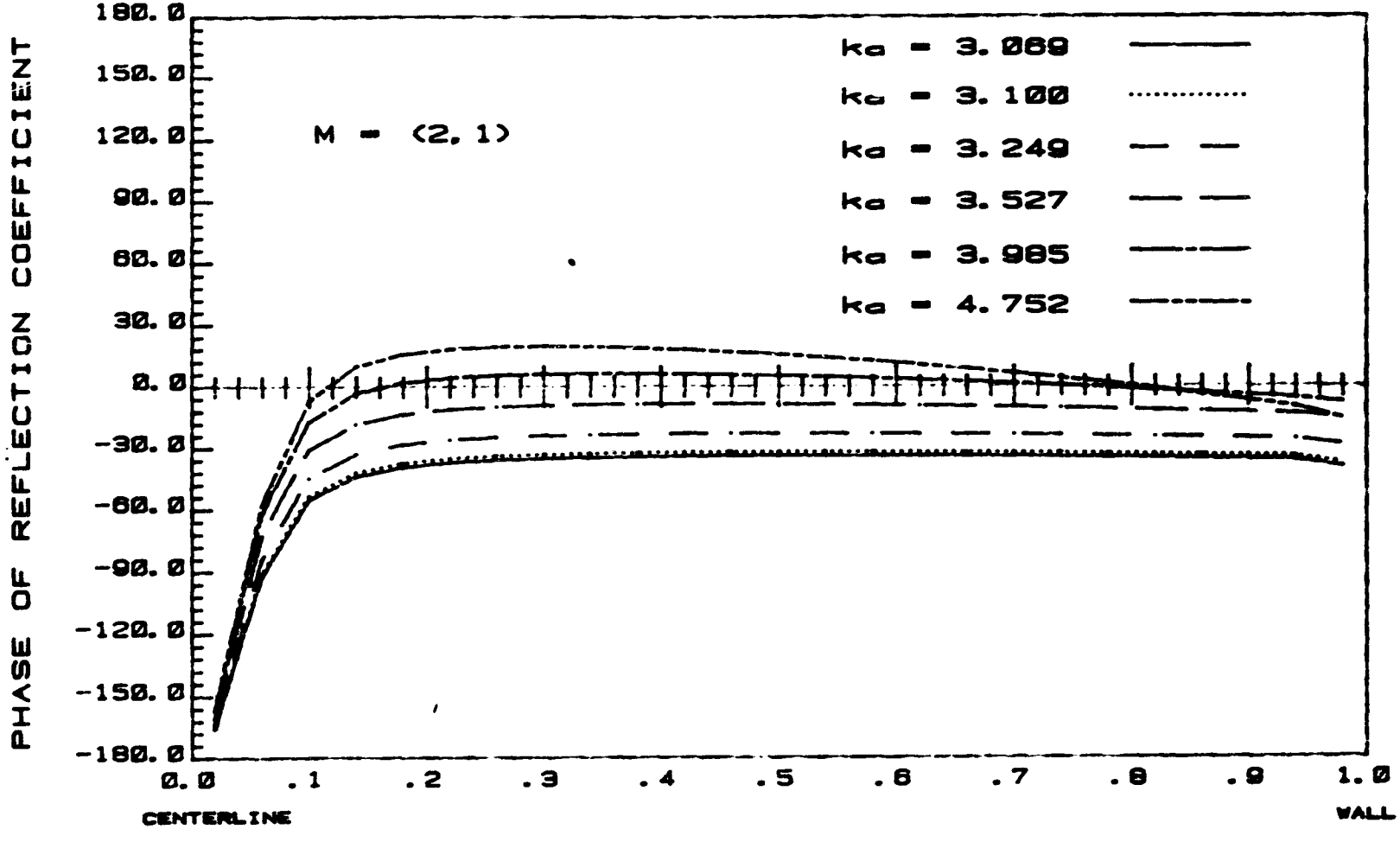

LANGLEY BELLMOUTH (Exit Plane)

Fig. 41b

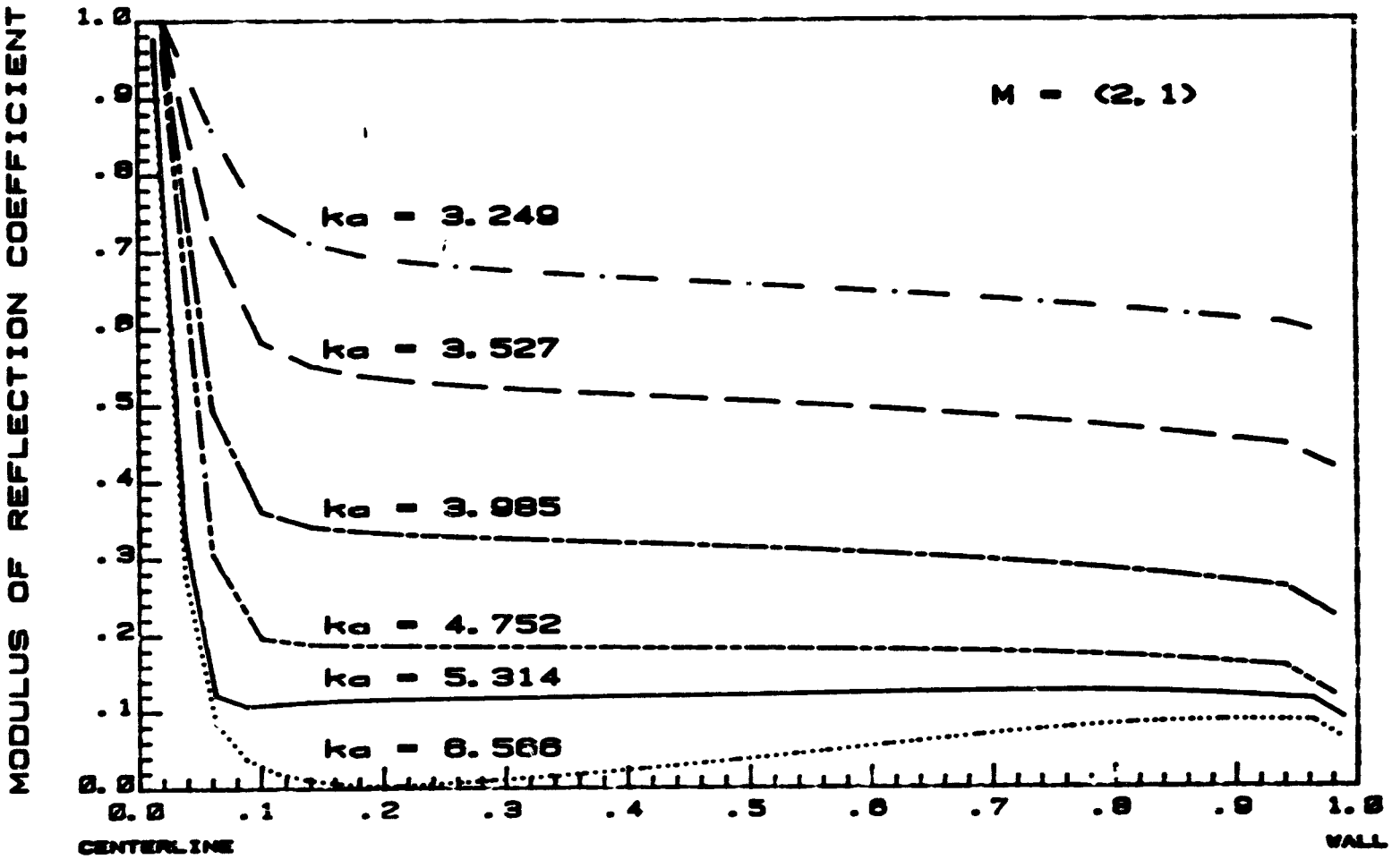

LANGLEY BELLMOUTH (Exit Plane)

Fig. 42a

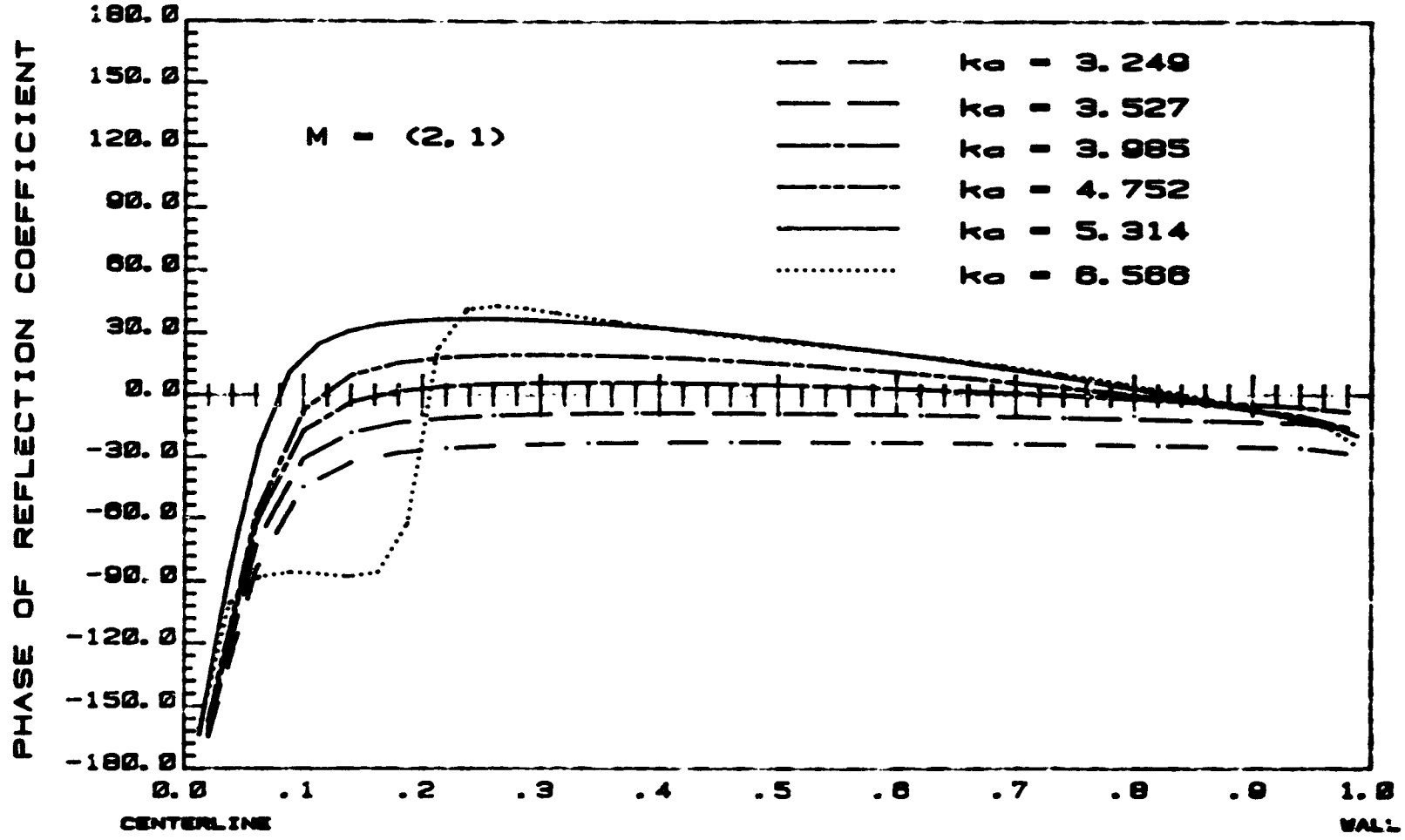

LANGLEY BELLMOUTH (Exit Plane)

Fig. 42b

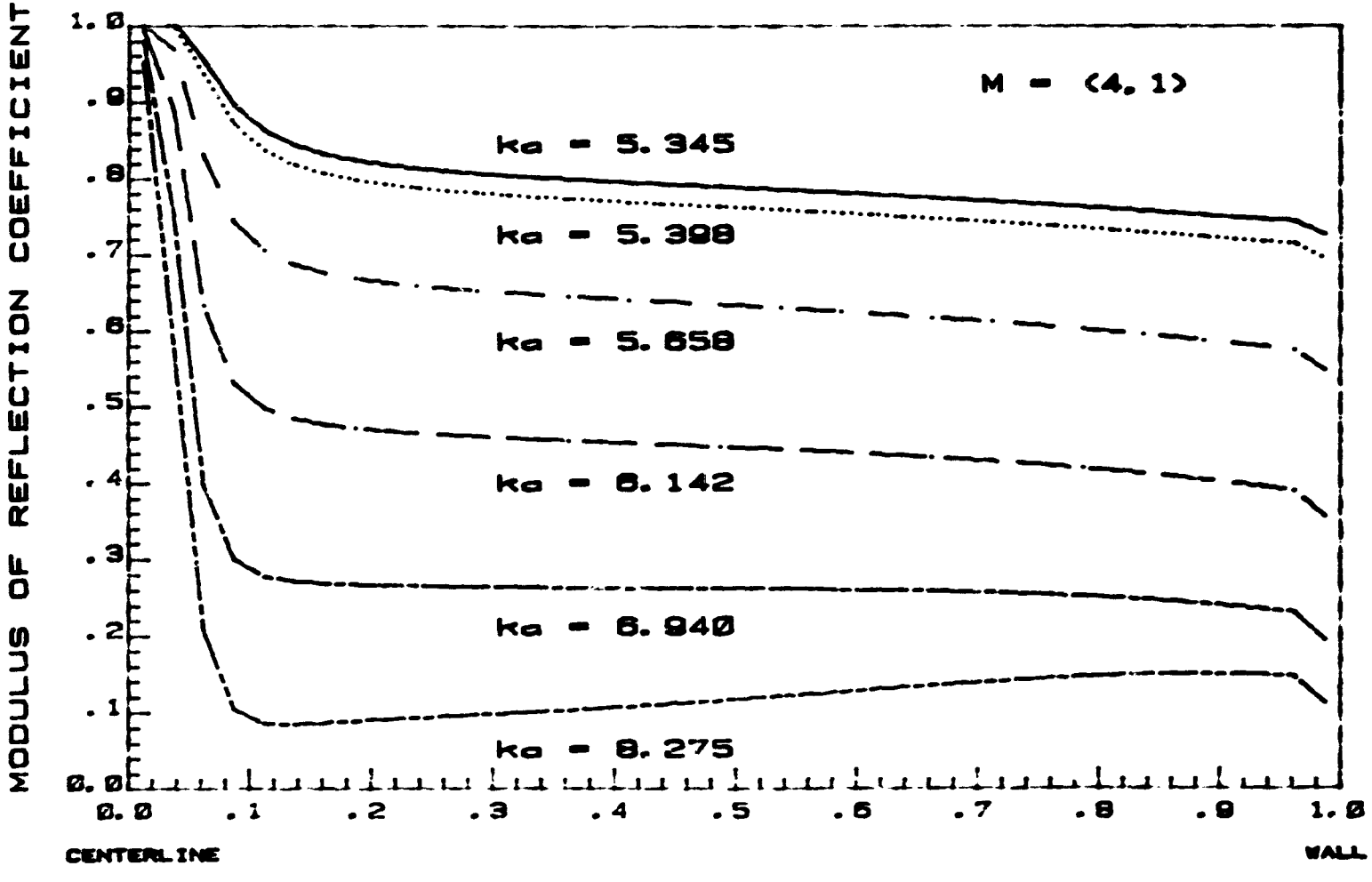

LANGLEY BELLMOUTH (Exit Plane)

Fig. 43a

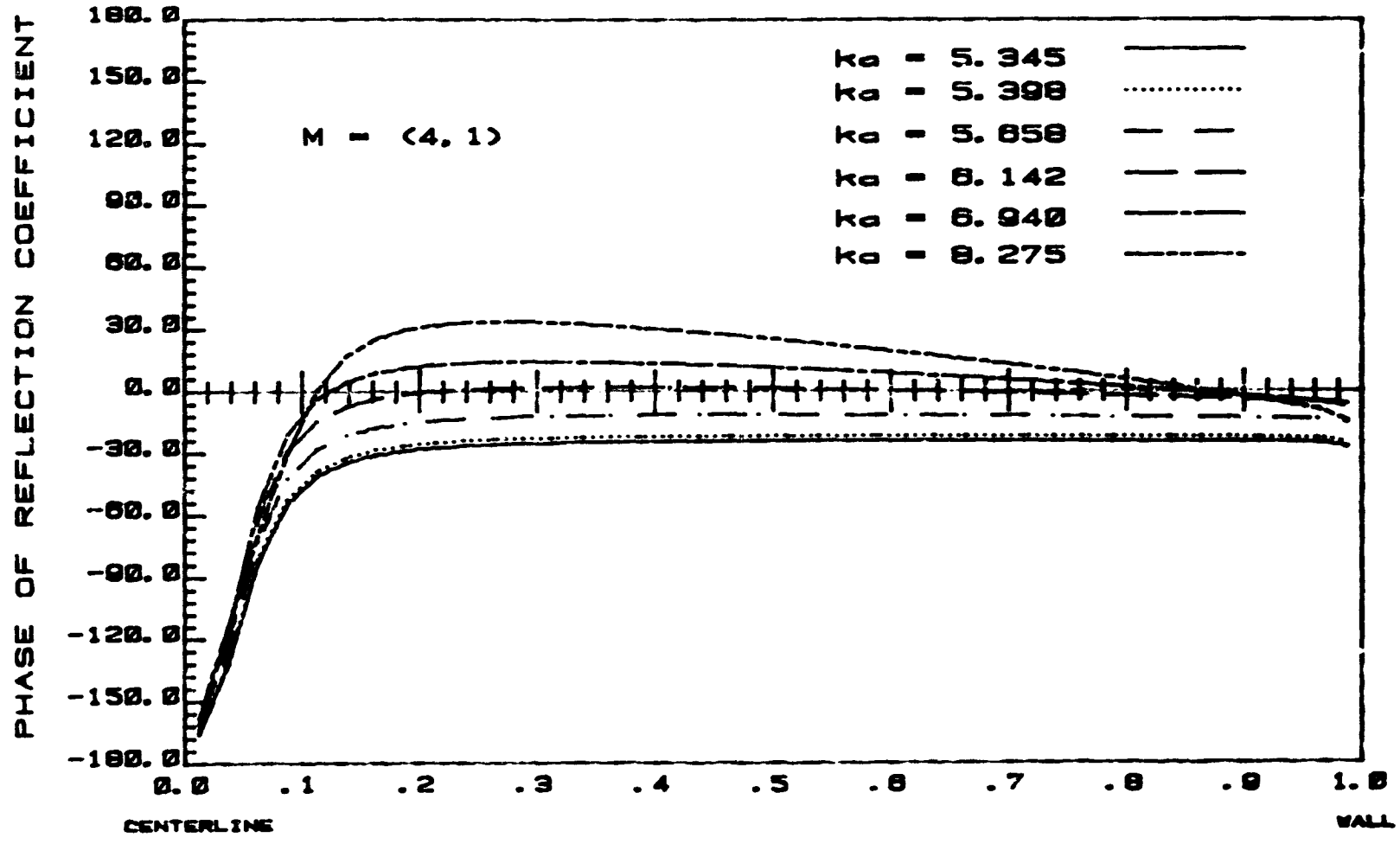

LANGLEY BELLMOUTH (Exit Plane)

Fig. 43b

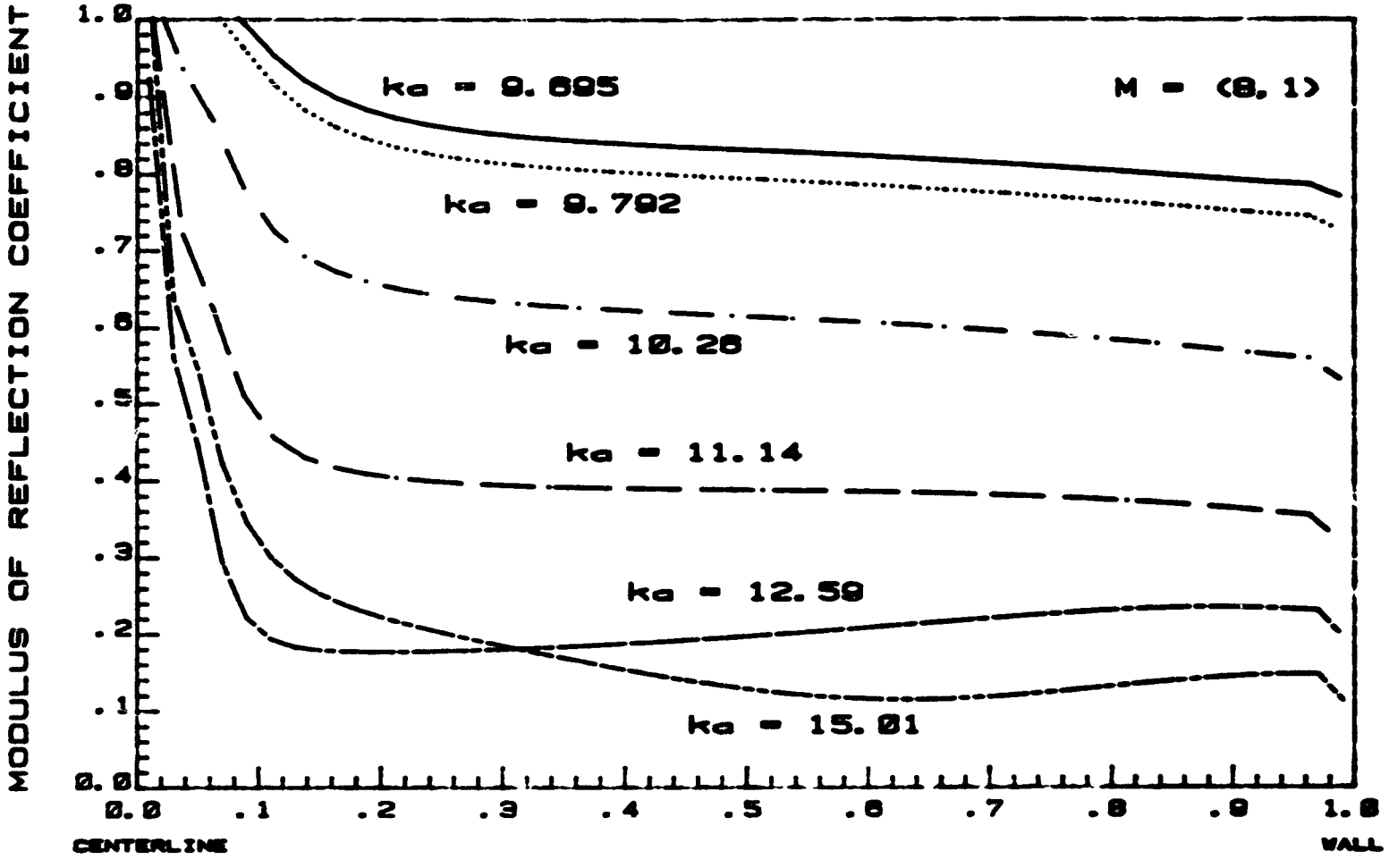

LANGLEY BELLMOUTH (Exit Plane)

Fig. 44a

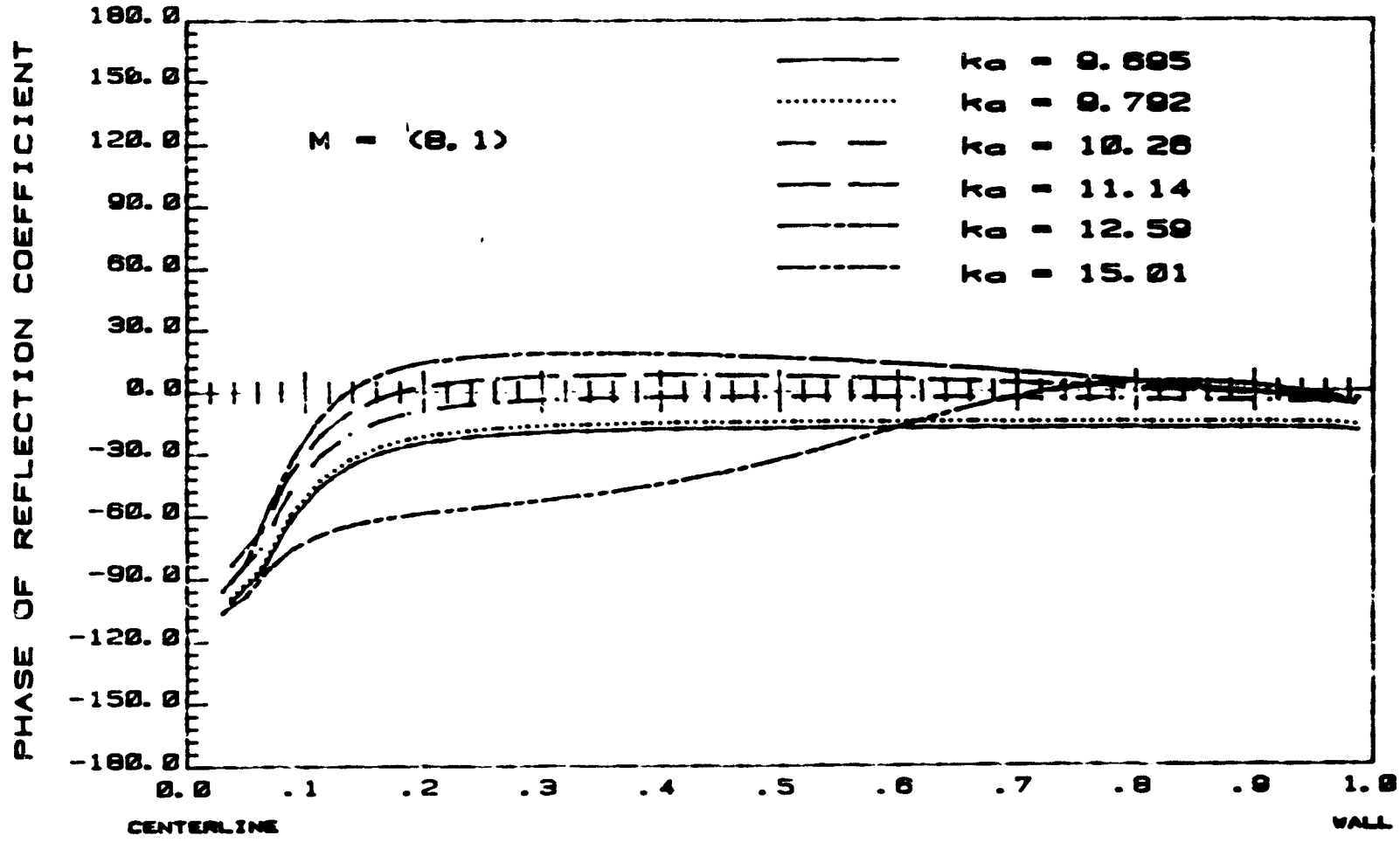

LANGLEY BELLMOUTH (Exit Plane)

Fig. 44b

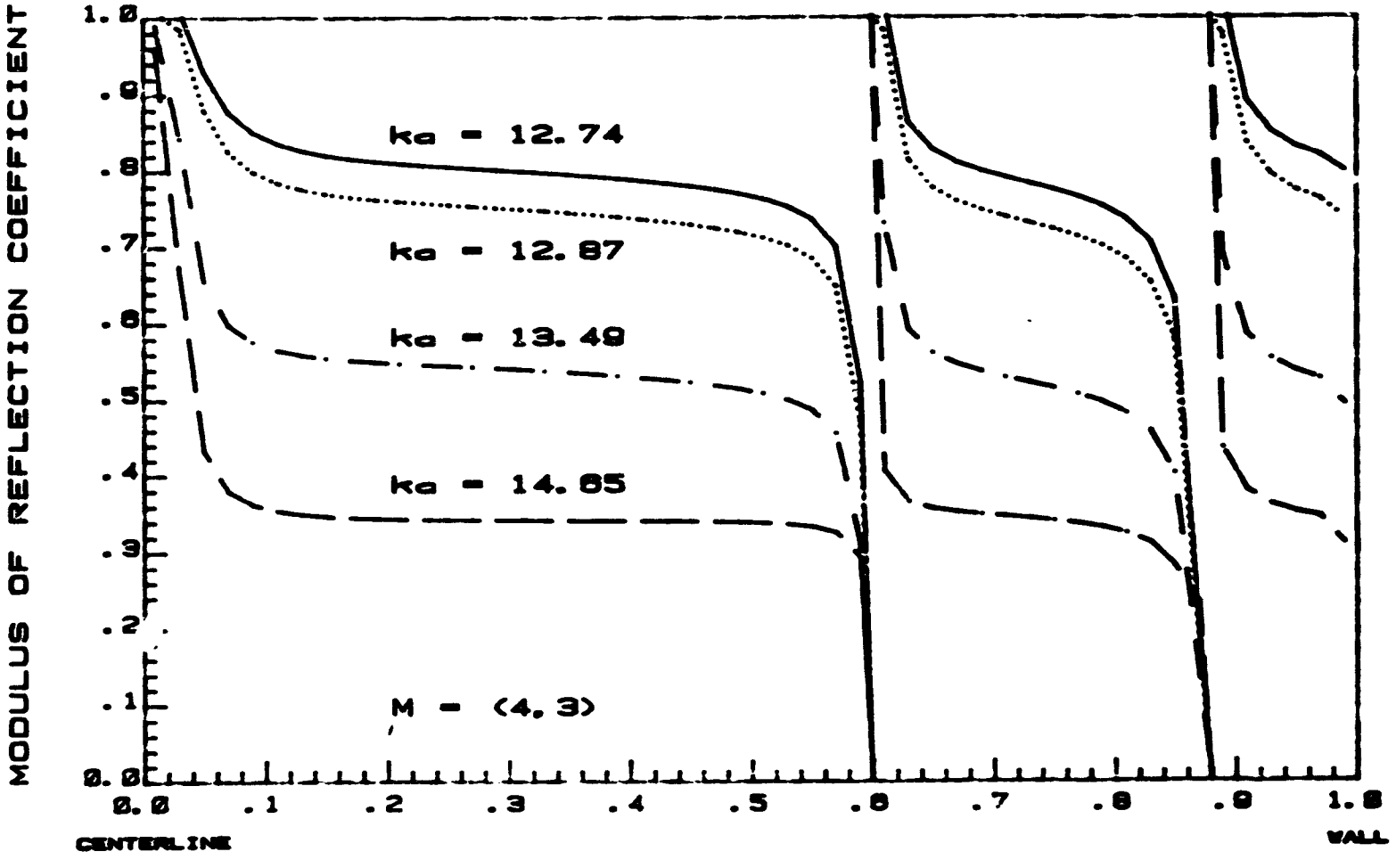

LANGLEY BELLMOUTH (Exit Plane)

Fig. 45a

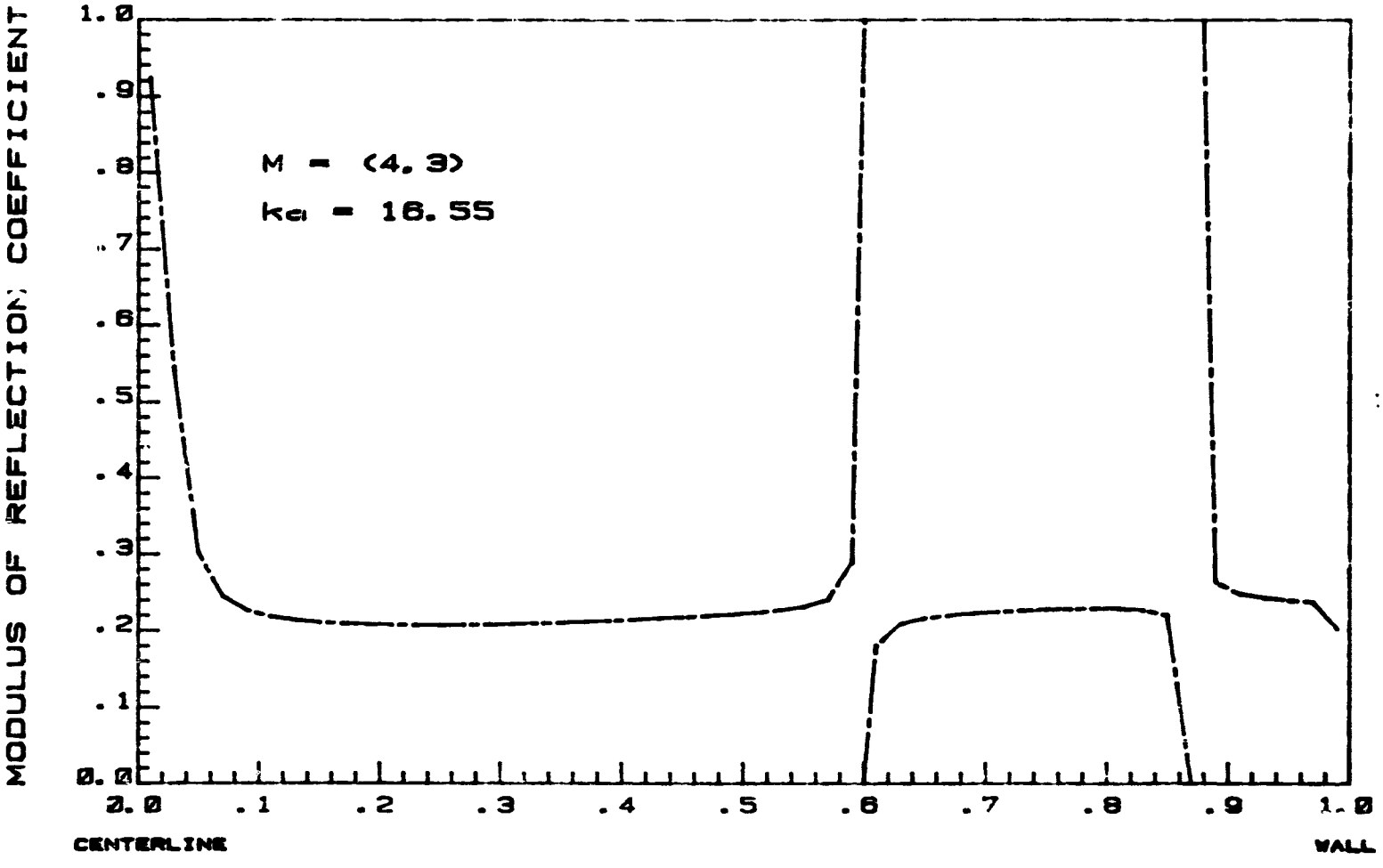

LANGLEY BELLMOUTH (Exit Plane)

Fig. 45b

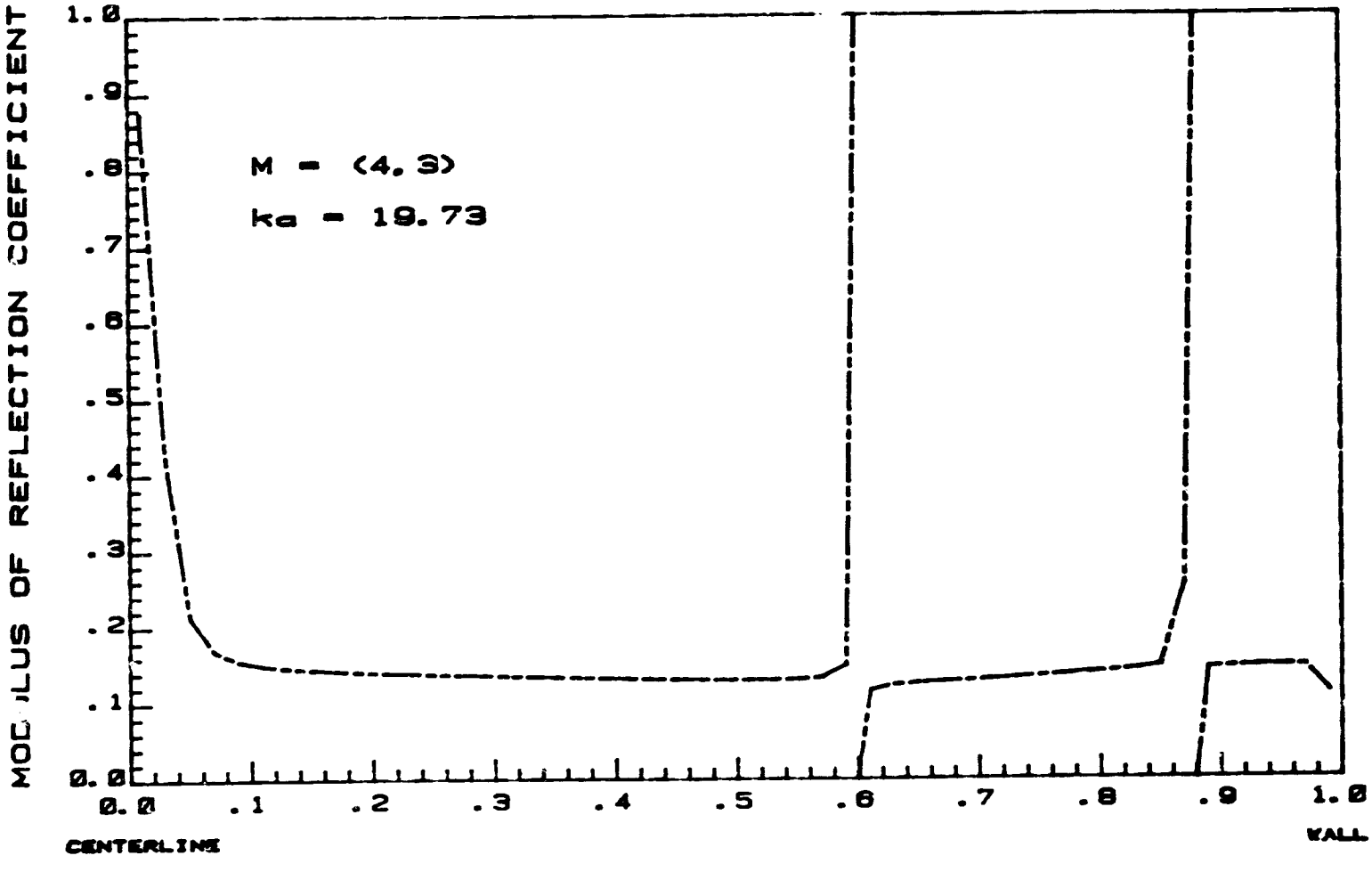

LANGLEY BELLMOUTH (Exit Plane)

Fig. 45c

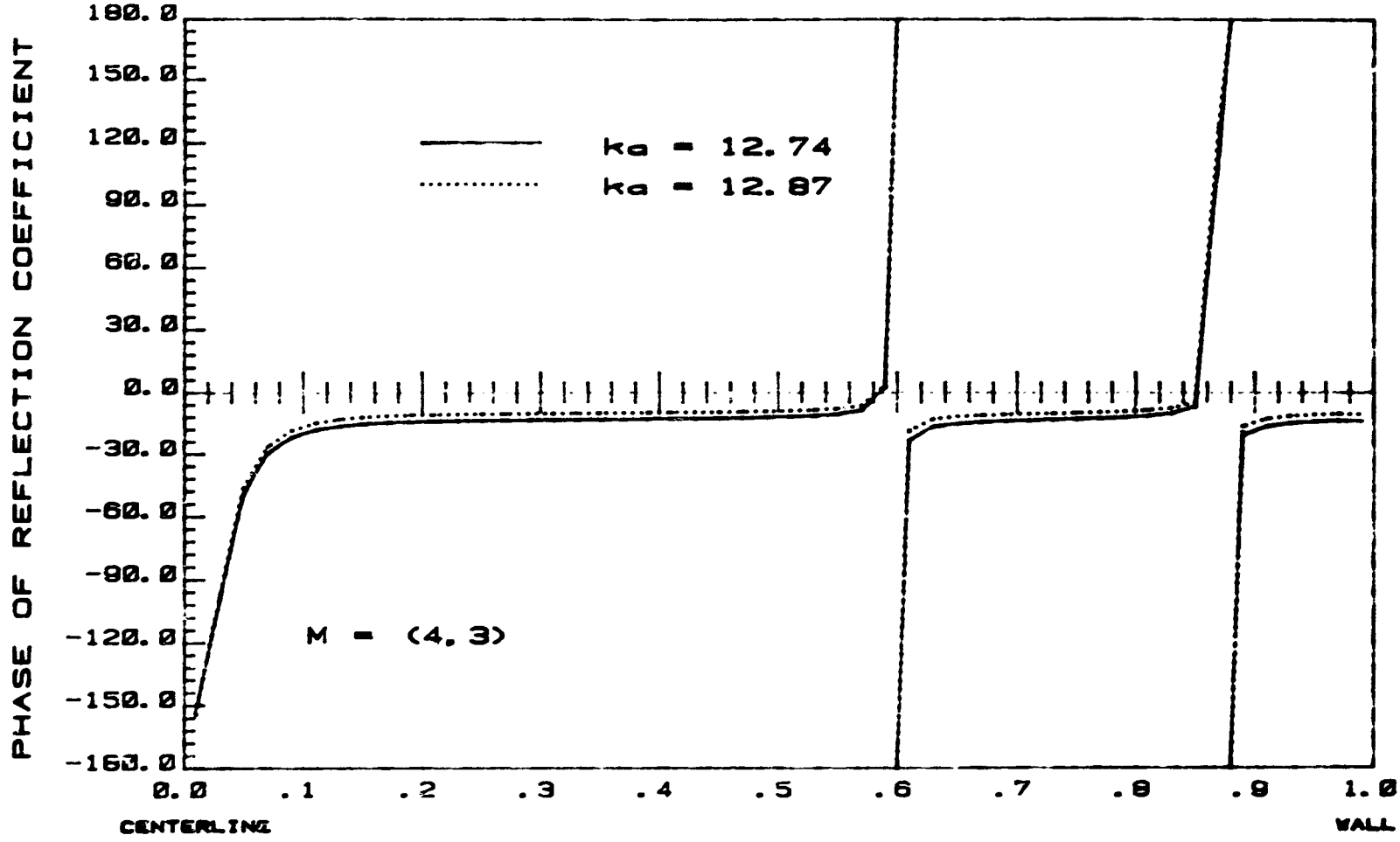

LANGLEY BELLMOUTH (Exit Plane)

Fig. 45d

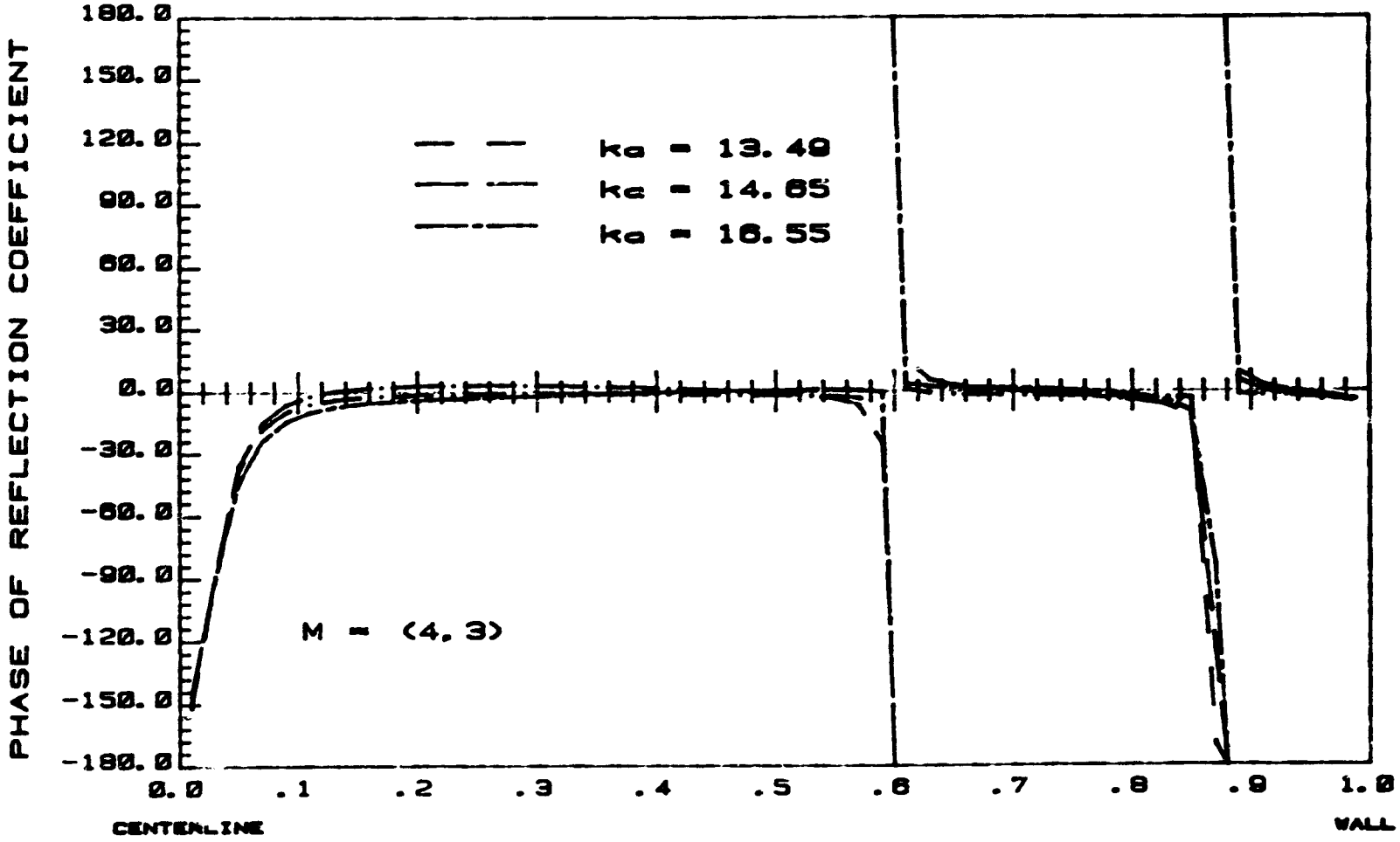

LANGLEY BELLMOUTH (Exit Plane)

Fig. 45e

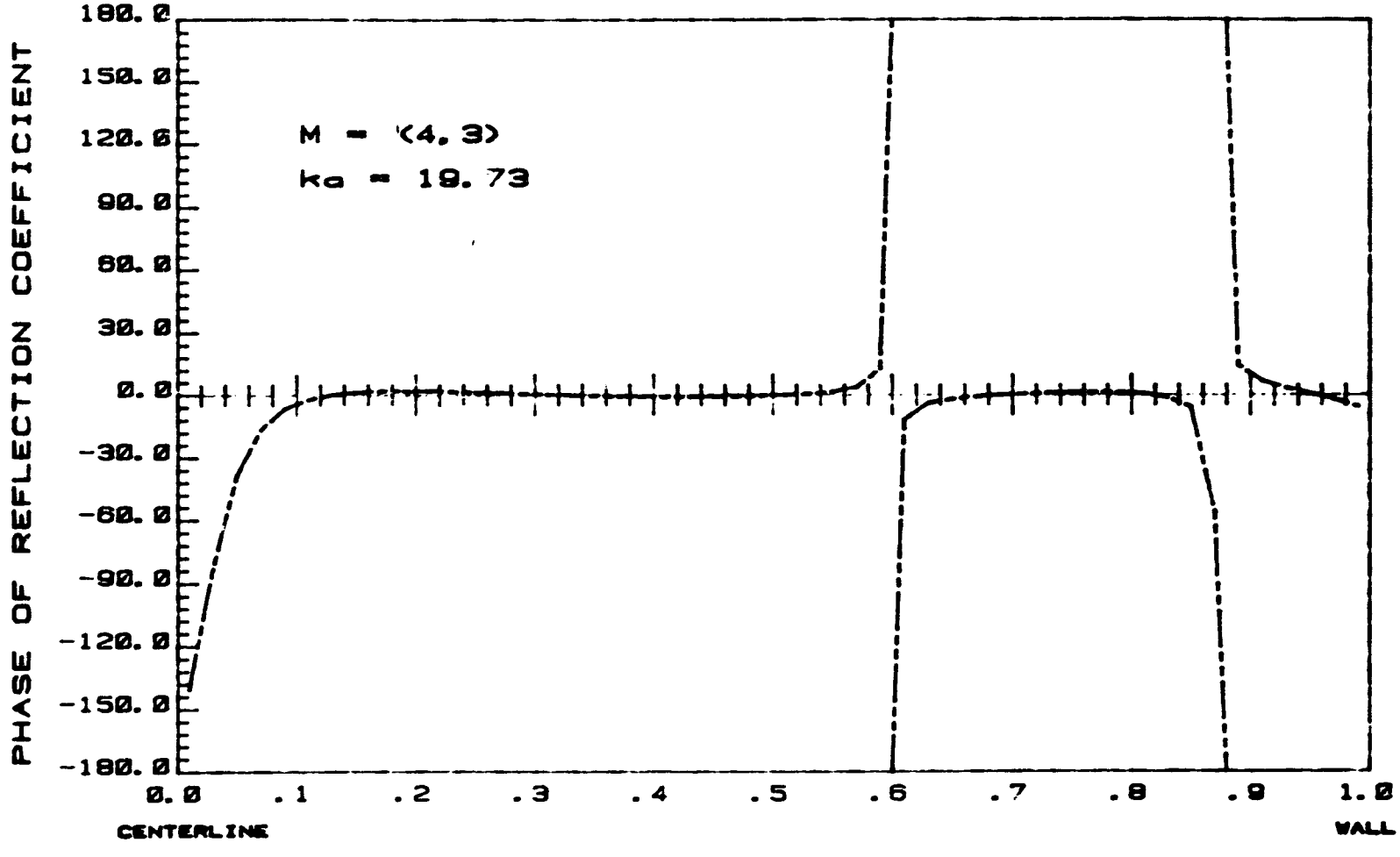

LANGLEY BELLMOUTH (Exit Plane)

Fig. 45f

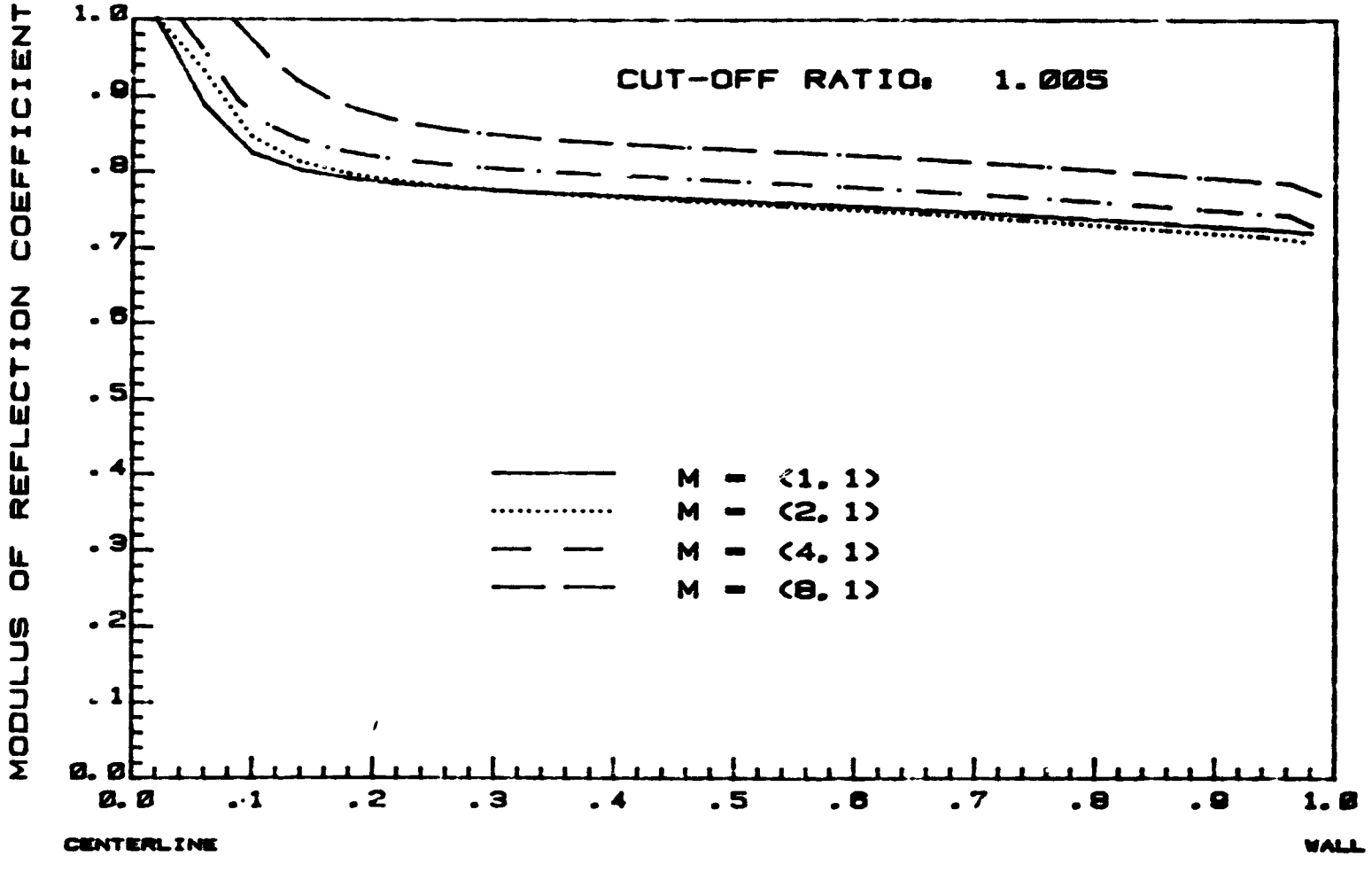

LANGLEY BELLMOUTH (Exit Plane)

Fig. 46a

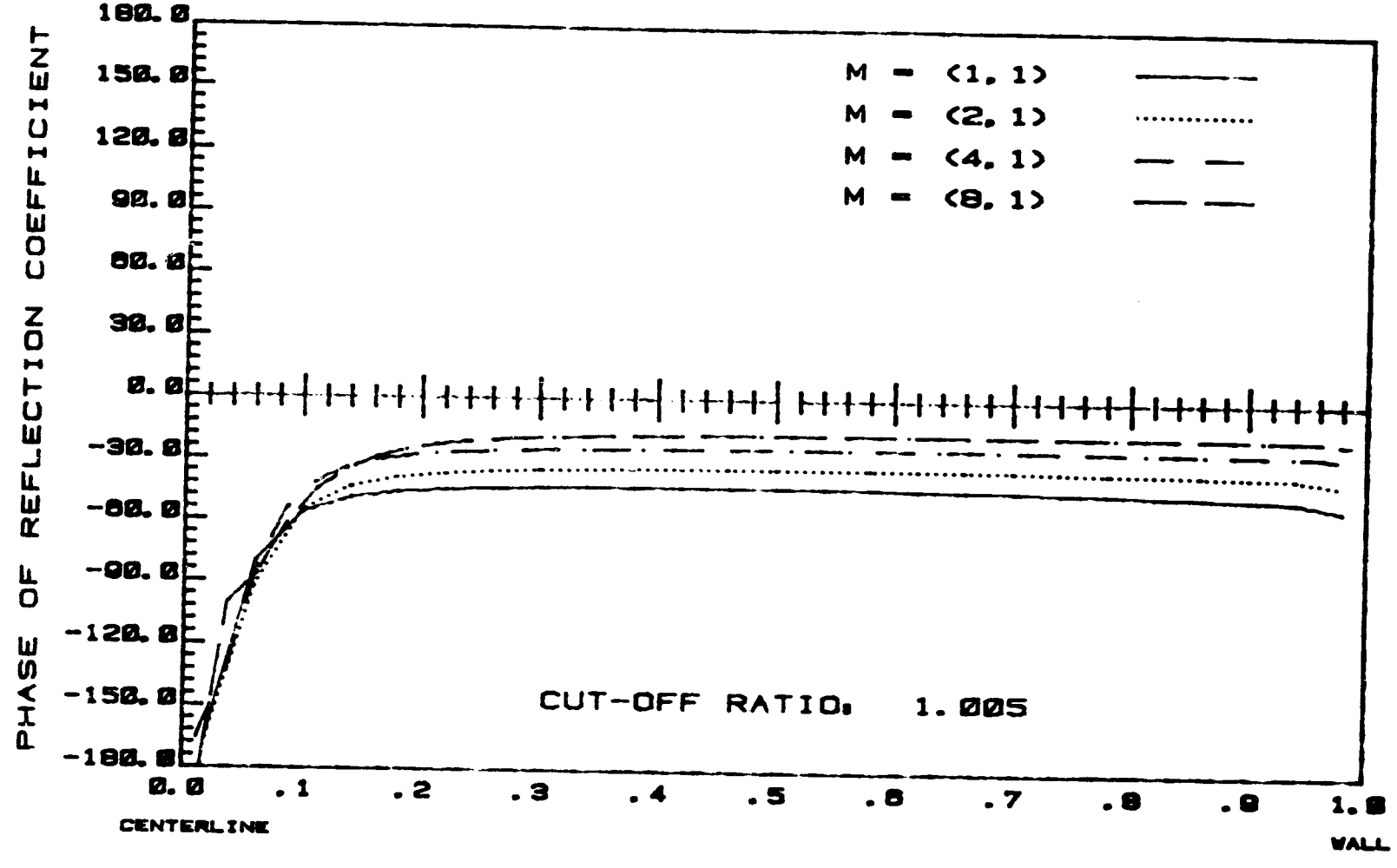

LANGLEY BELLMOUTH (Exit Plane)

Fig. 46b

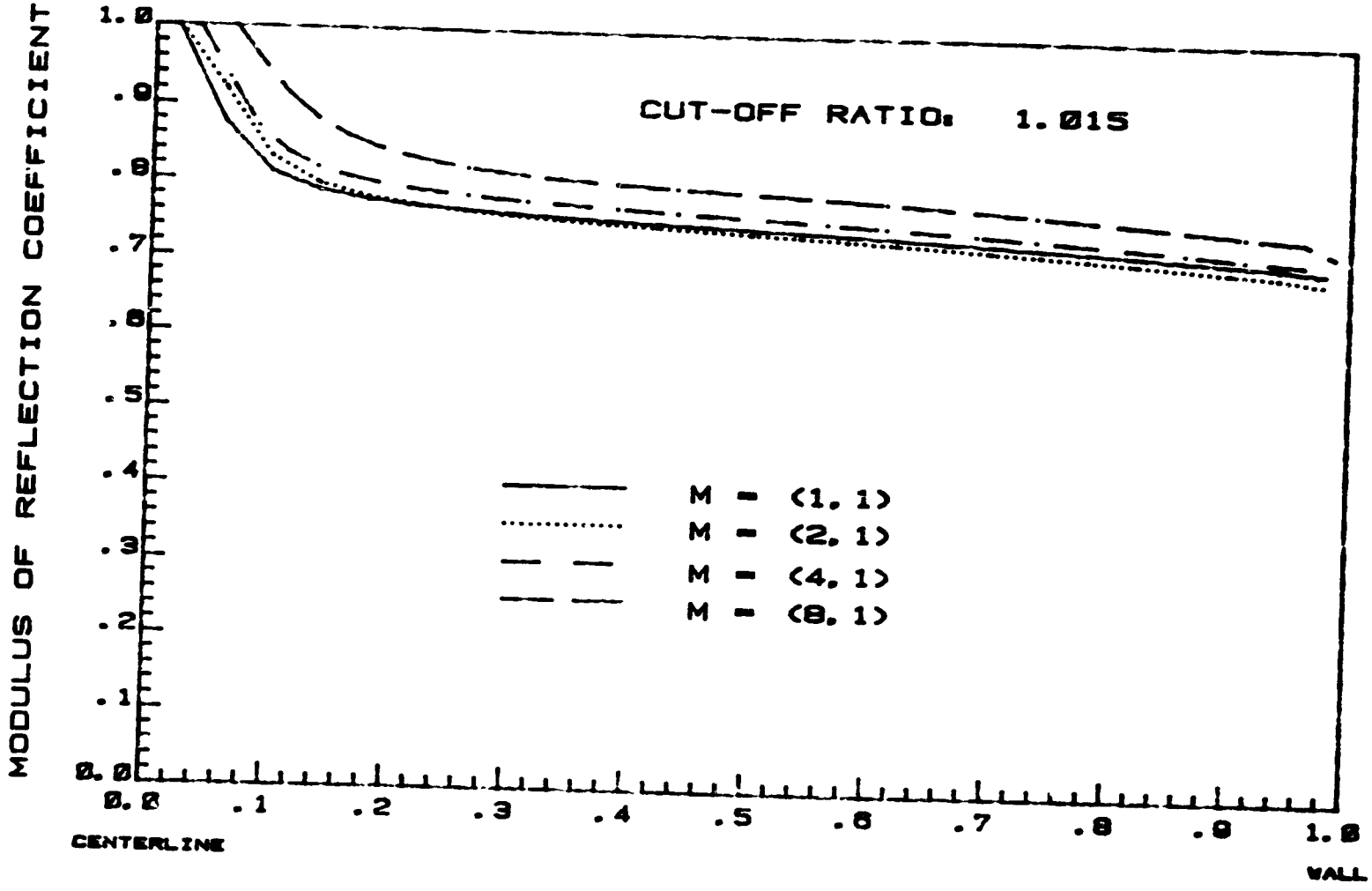

LANGLEY BELLMOUTH (Exit Plane)

Fig. 47a

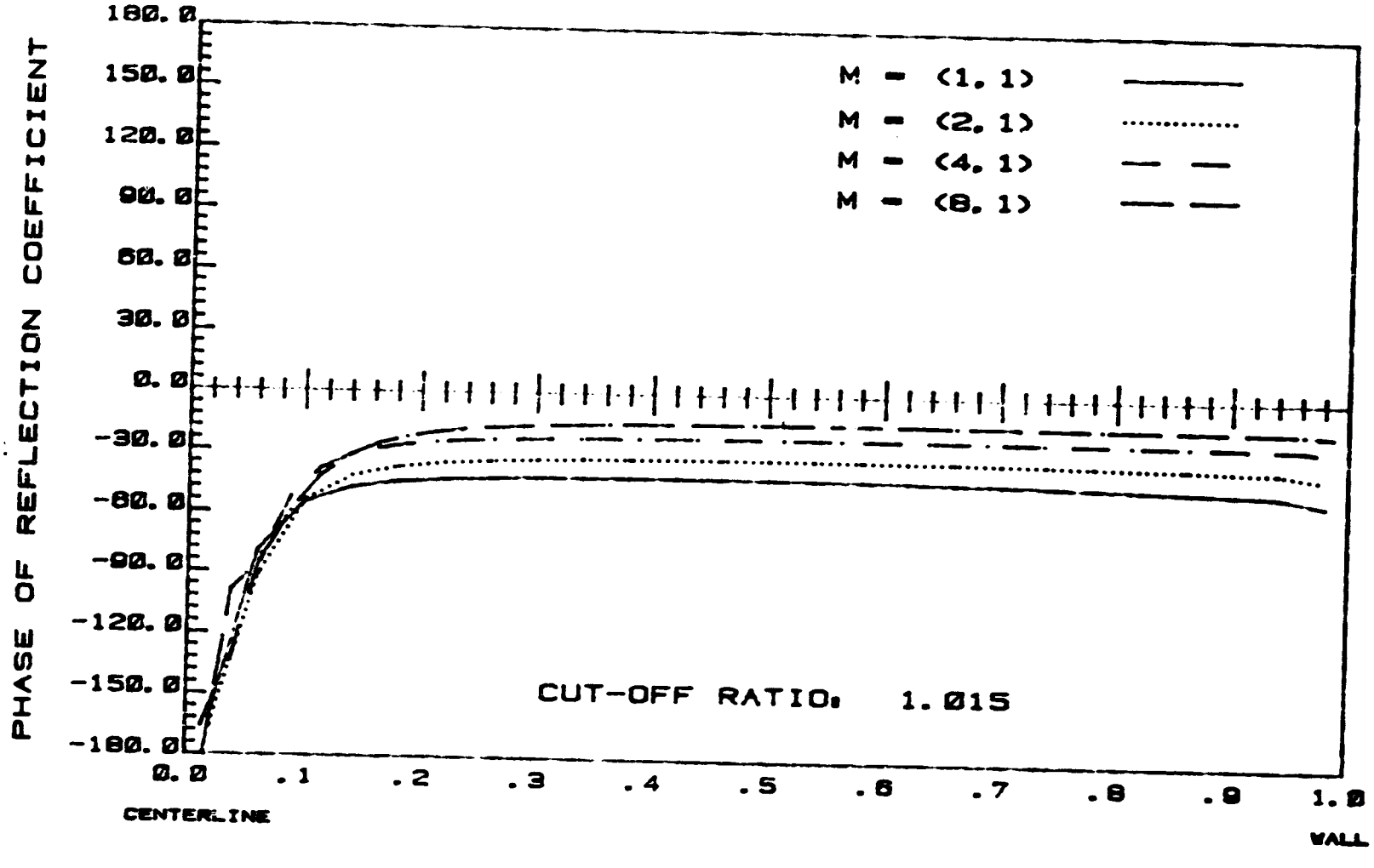

LANGLEY BELLMOUTH (Exit Plane)

Fig. 47b

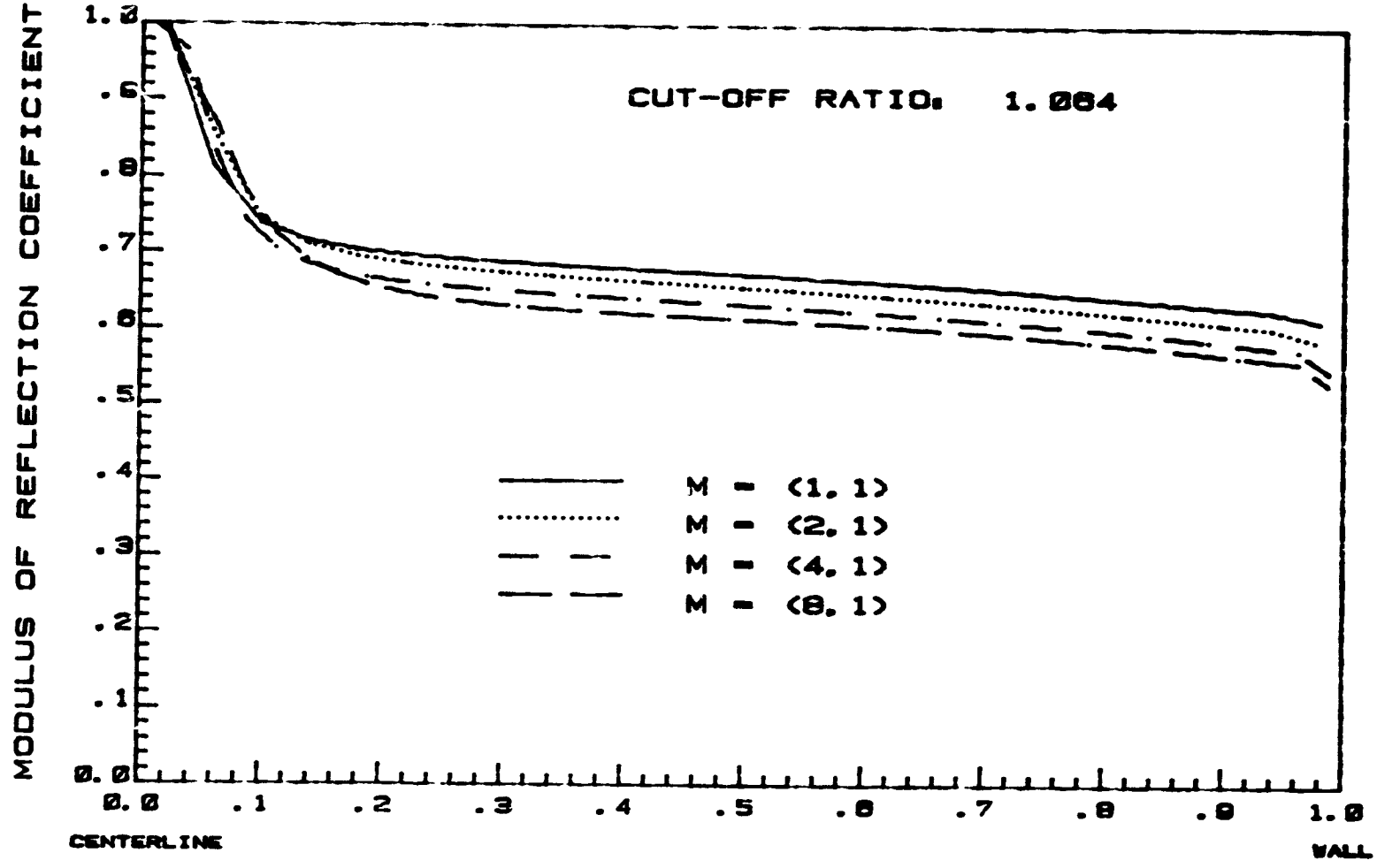

LANGLEY BELLMOUTH (Exit Plane)

Fig. 48a

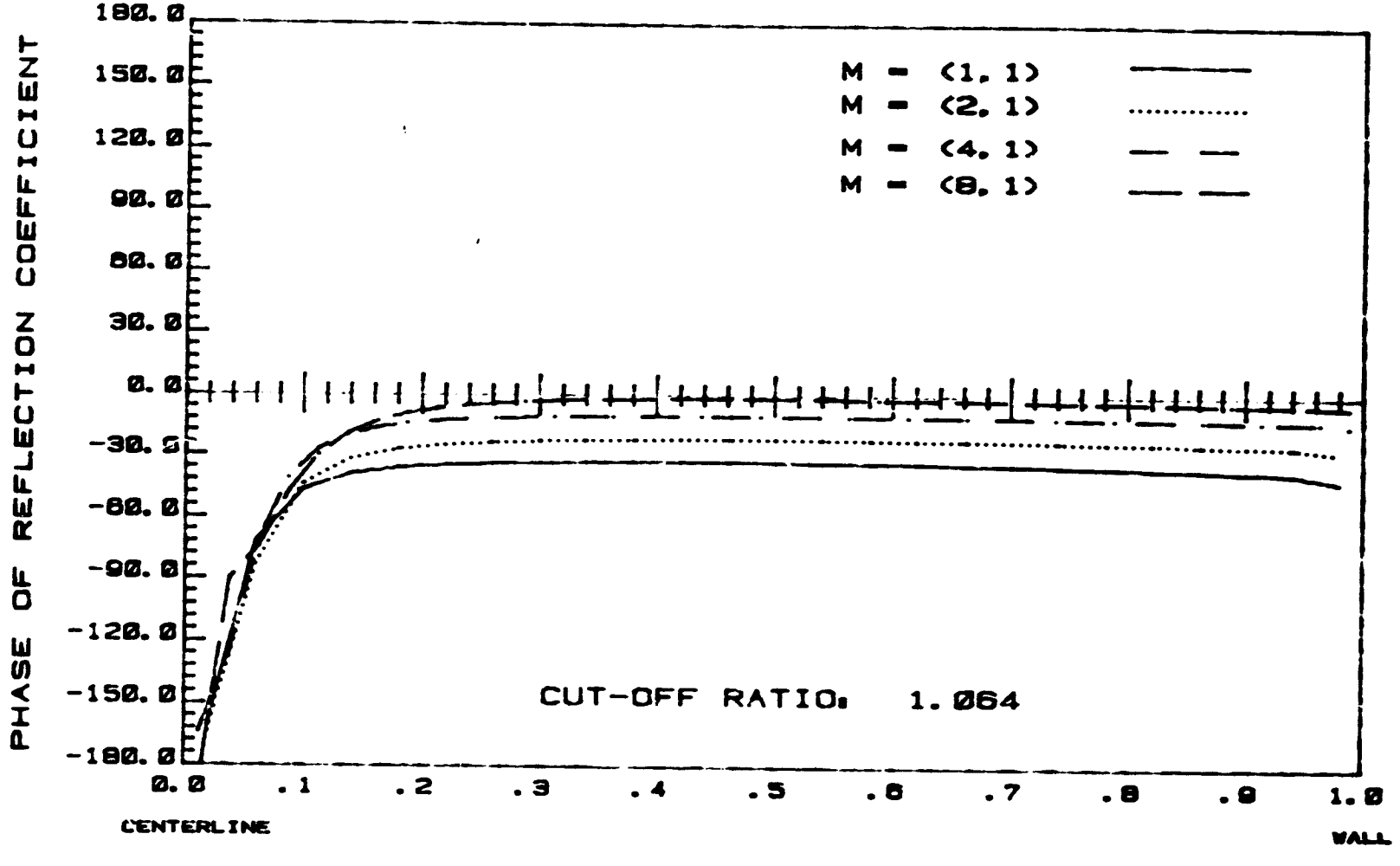

LANGLEY BELLMOUTH (Exit Plane)

Fig. 48b

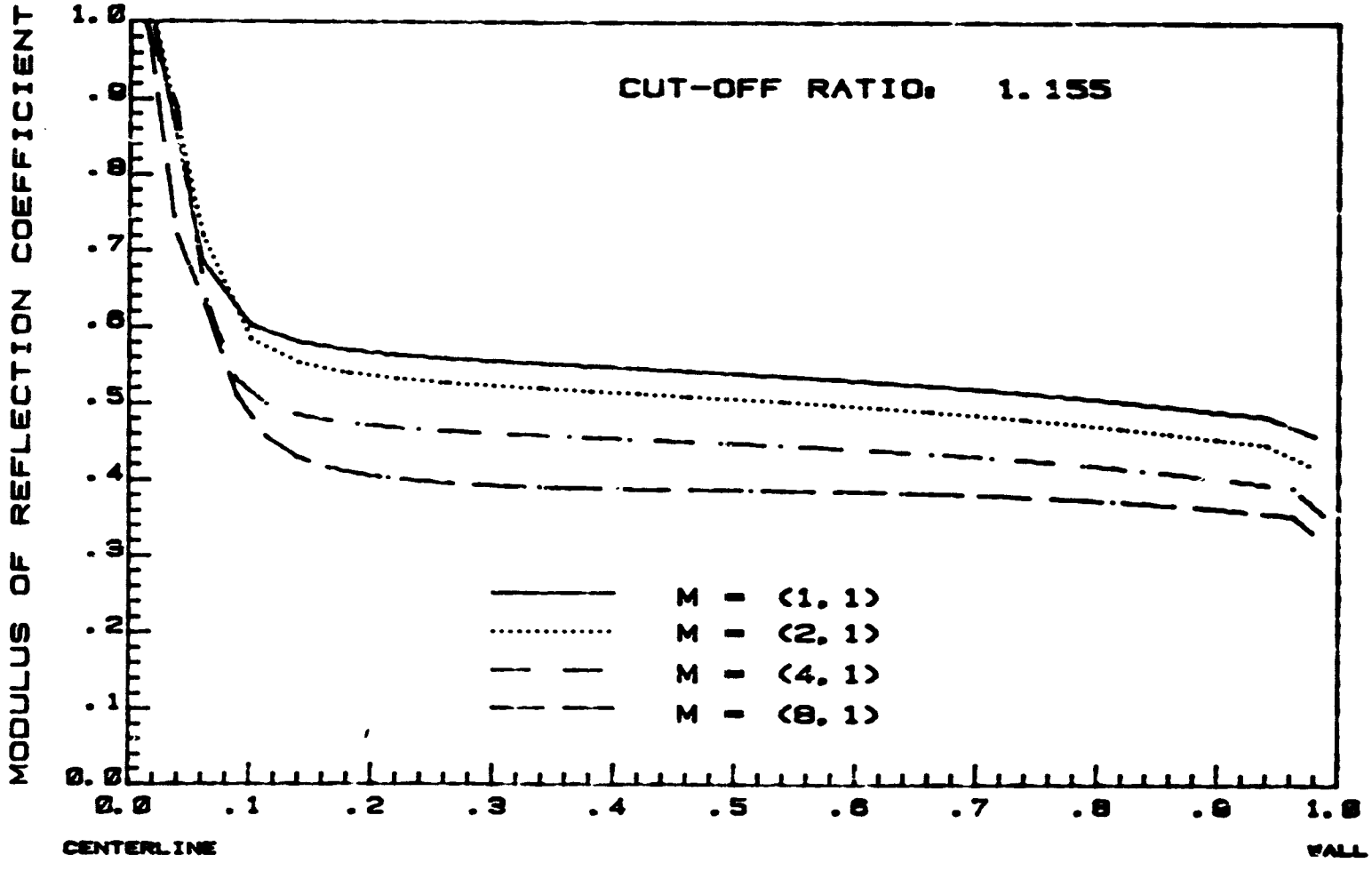

LANGLEY BELLMOUTH (Exit Plane)

Fig. 49a

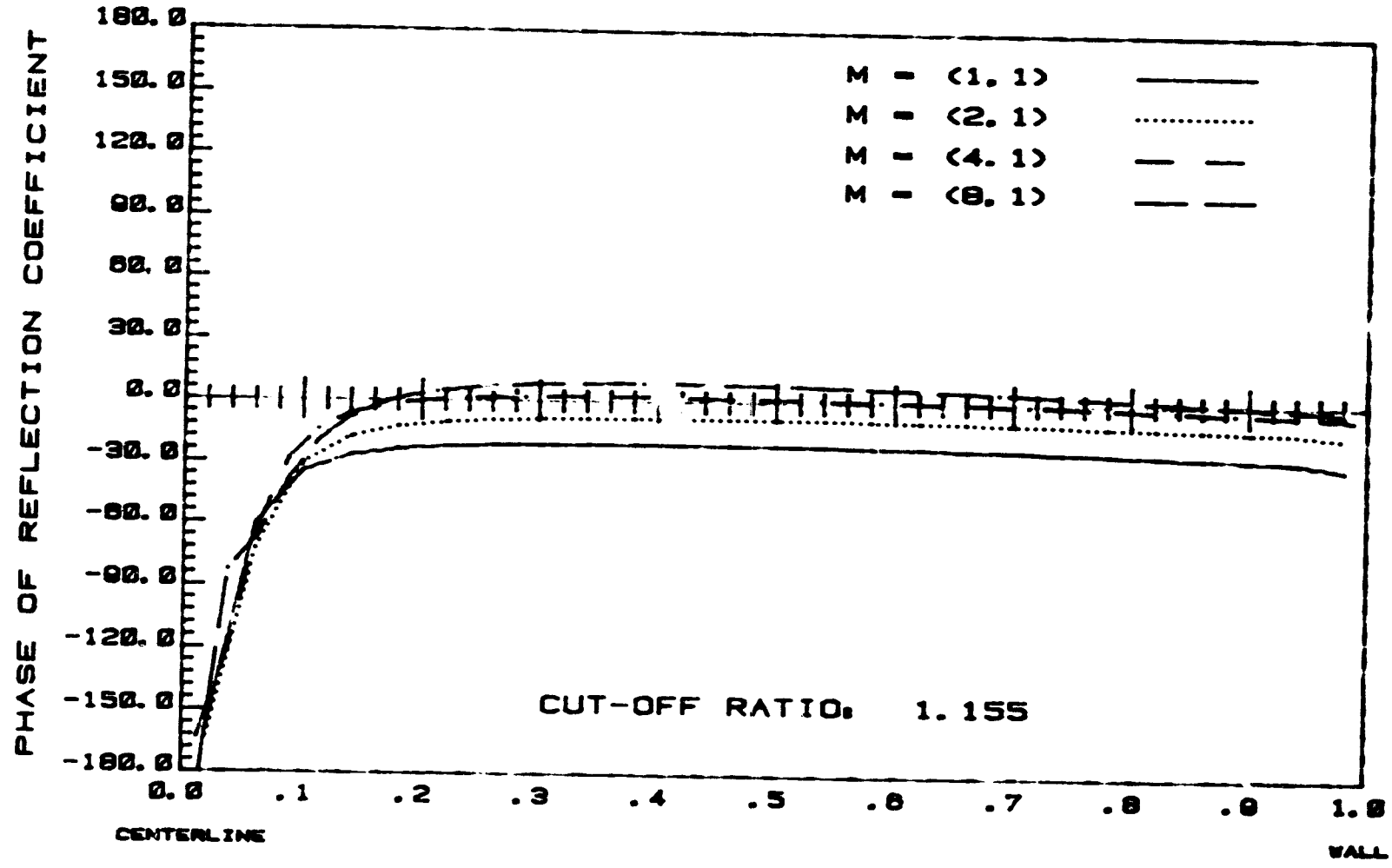

LANGLEY BELLMOUTH (Exit Plane)

Fig. 49b

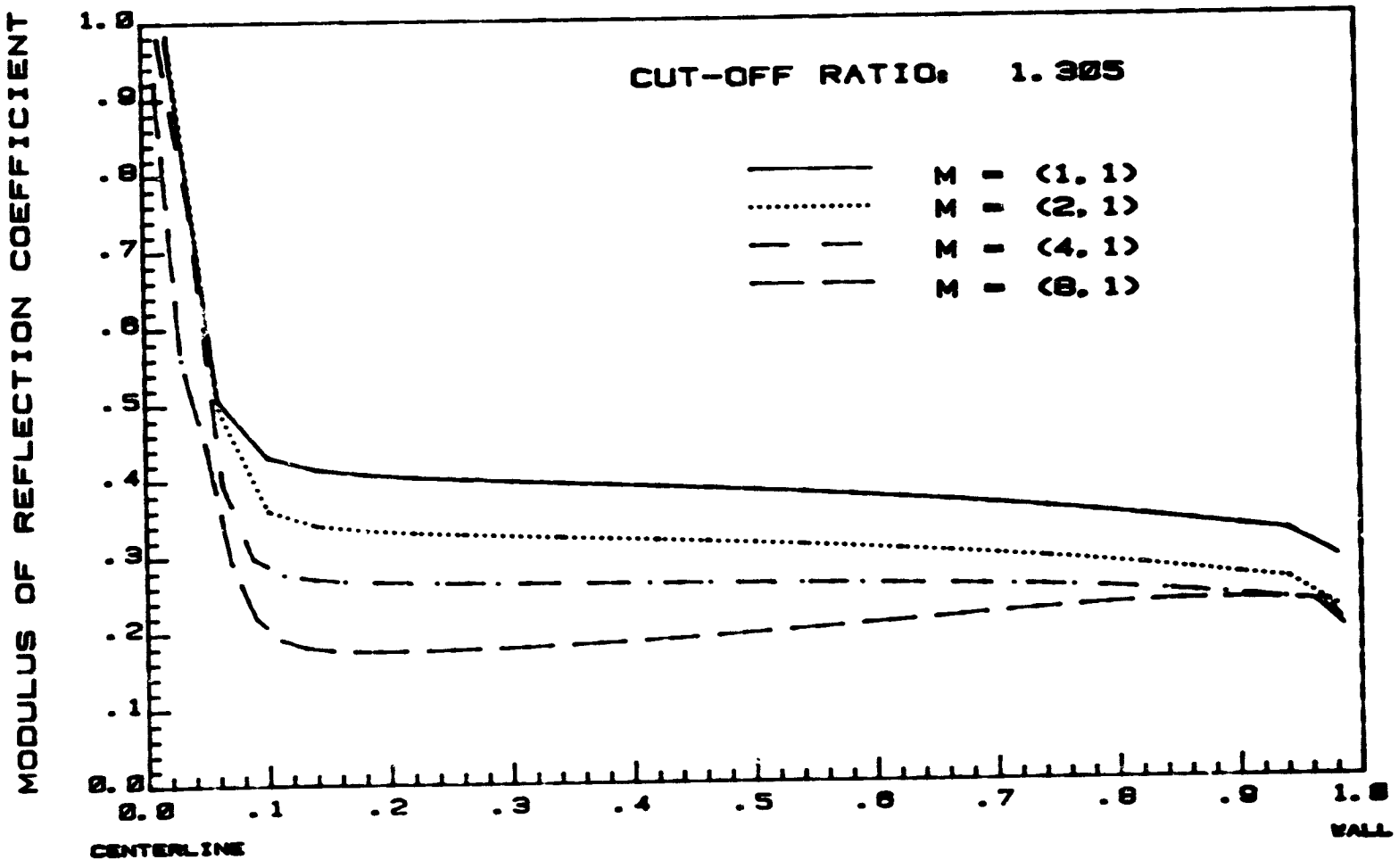

LANGLEY BELLMOUTH (Exit Plane)

Fig. 50a

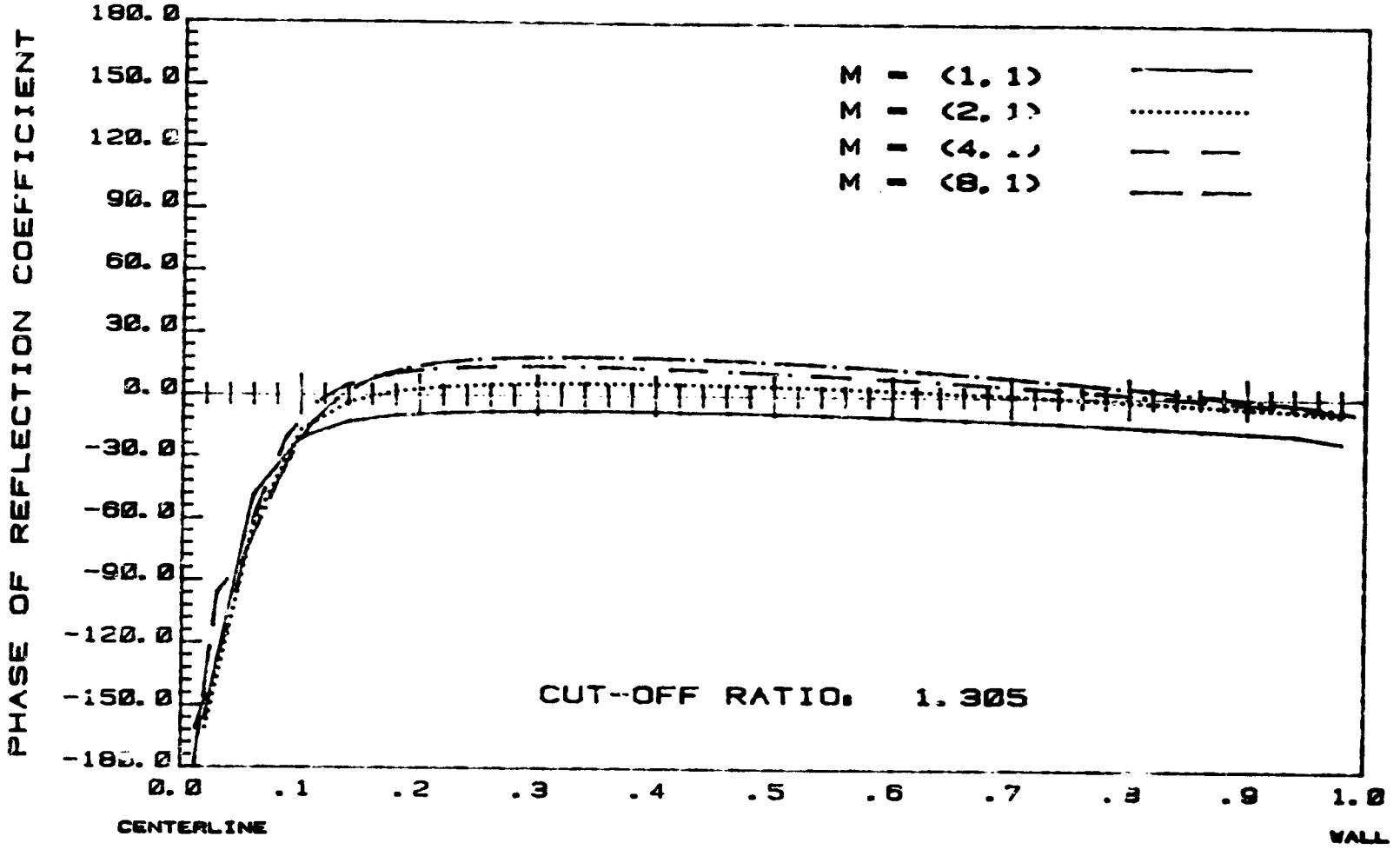

LANGLEY BELLMOUTH (ExitPlane)

Fig. 50b

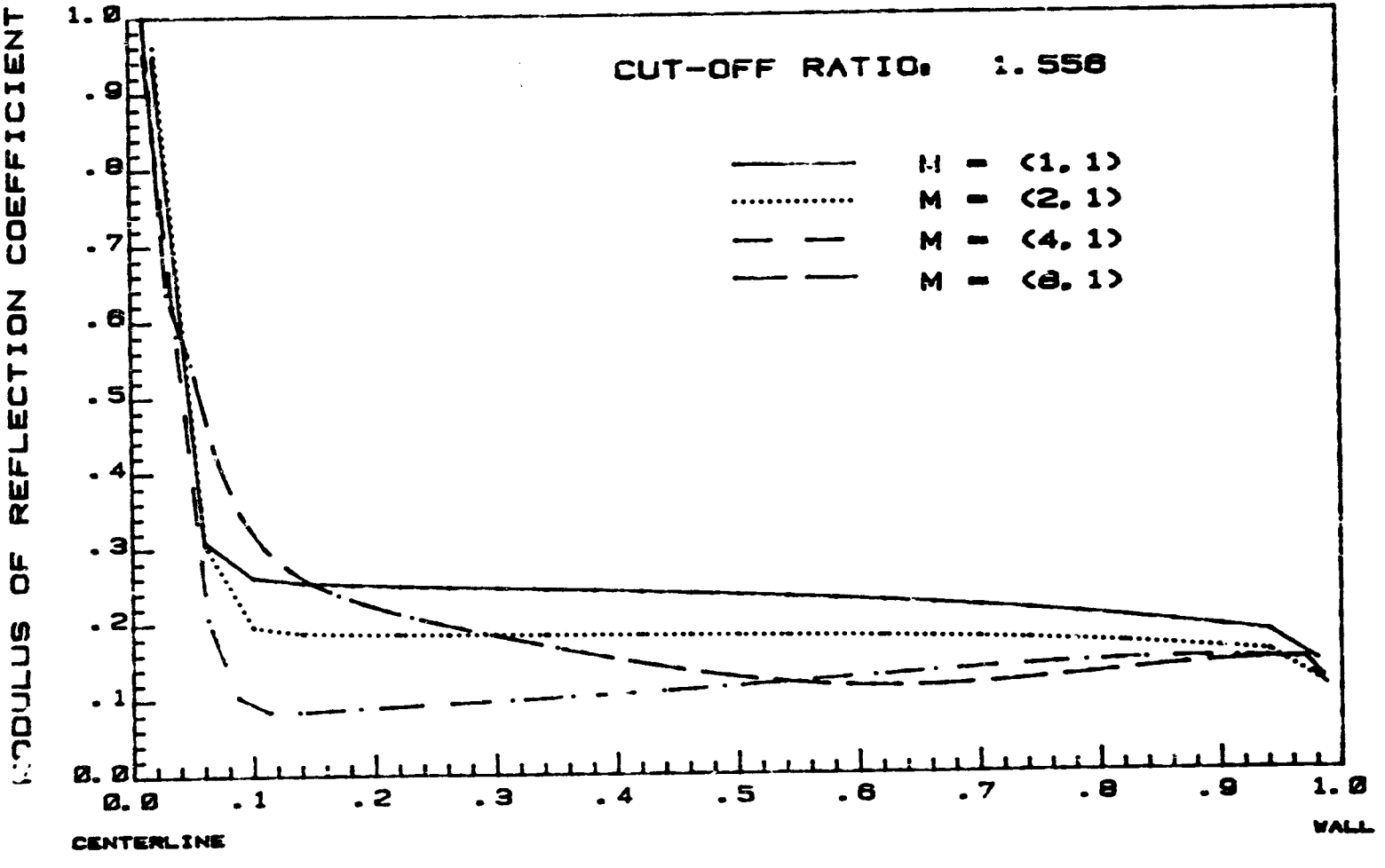

LANGLEY BELLMOUTH (Exit Plane)

Fig. 51a

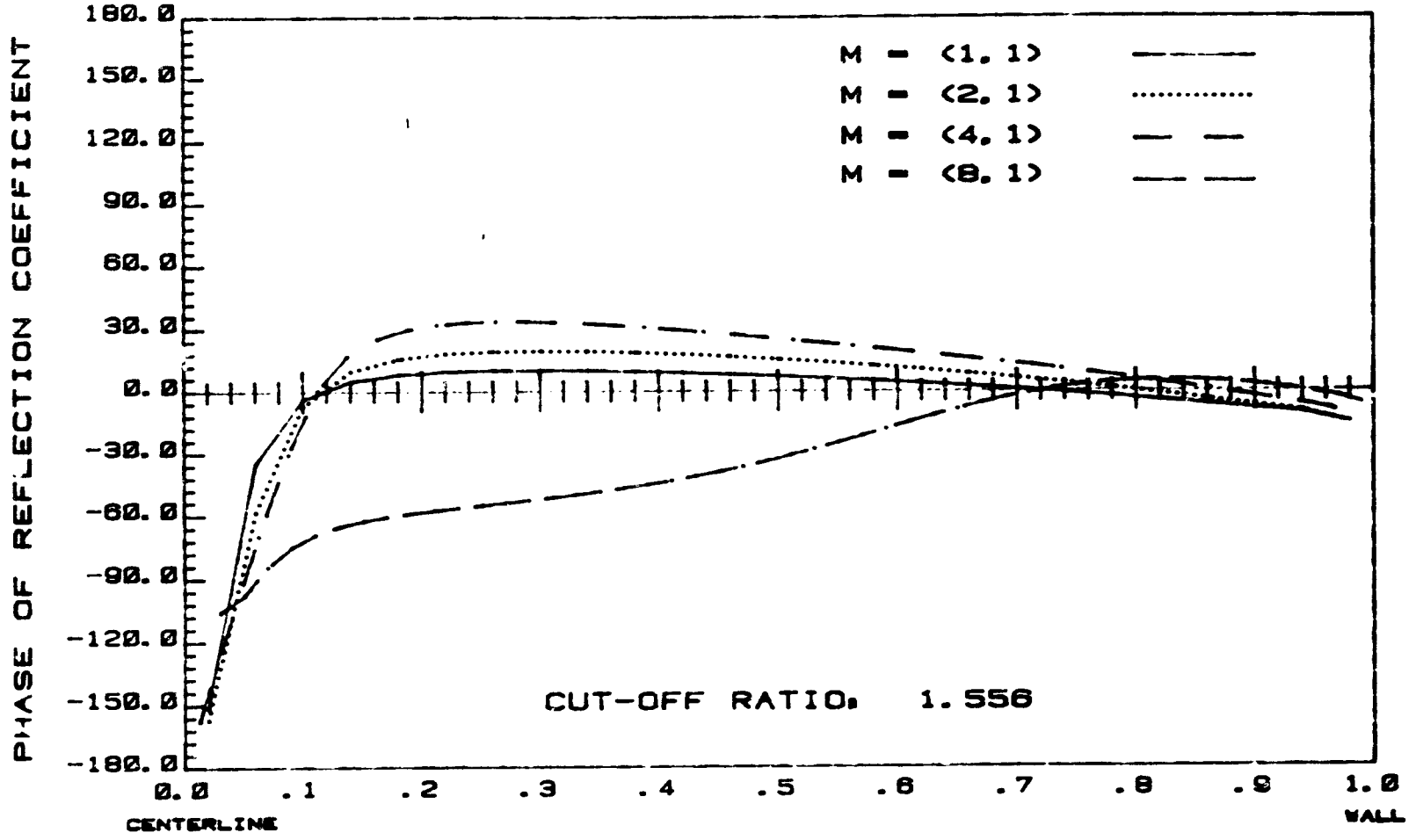

LANGLEY BELLMOUTH (Exit Plane)

Fig. 51b

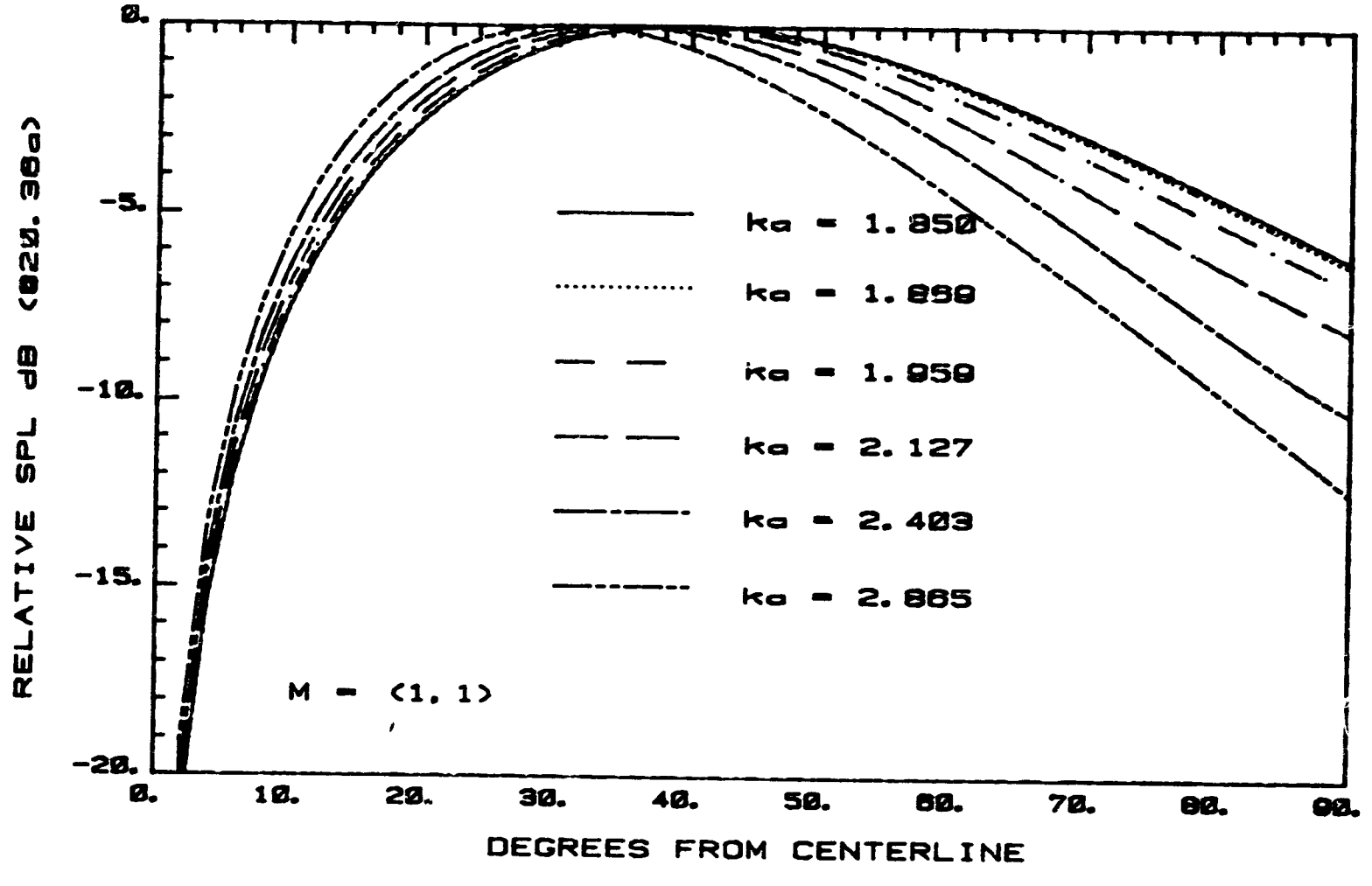

LANGLEY BELLMOUTH

Fig. 52a

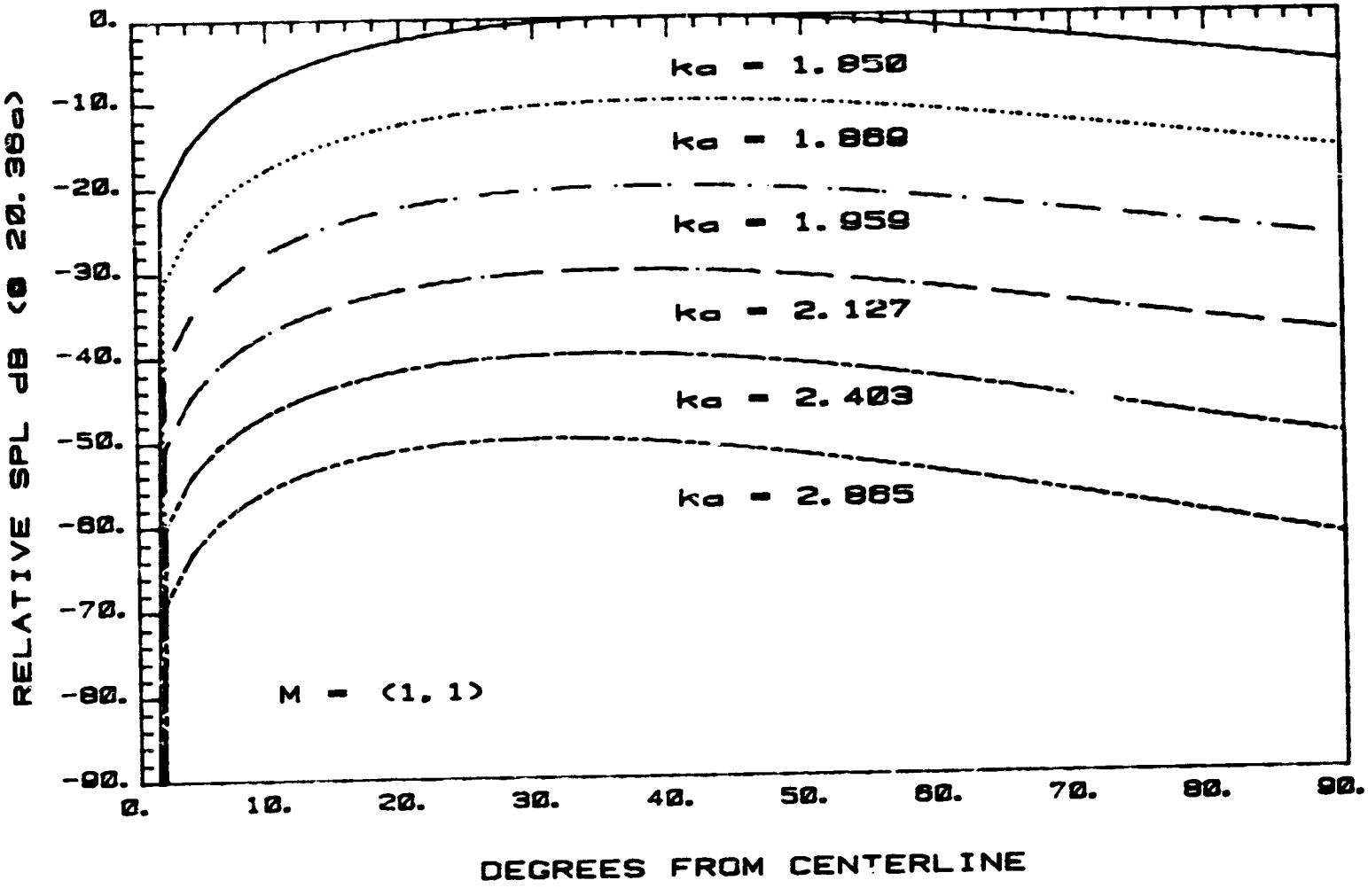

LANGLEY BELLMOUTH

Fig. 52b

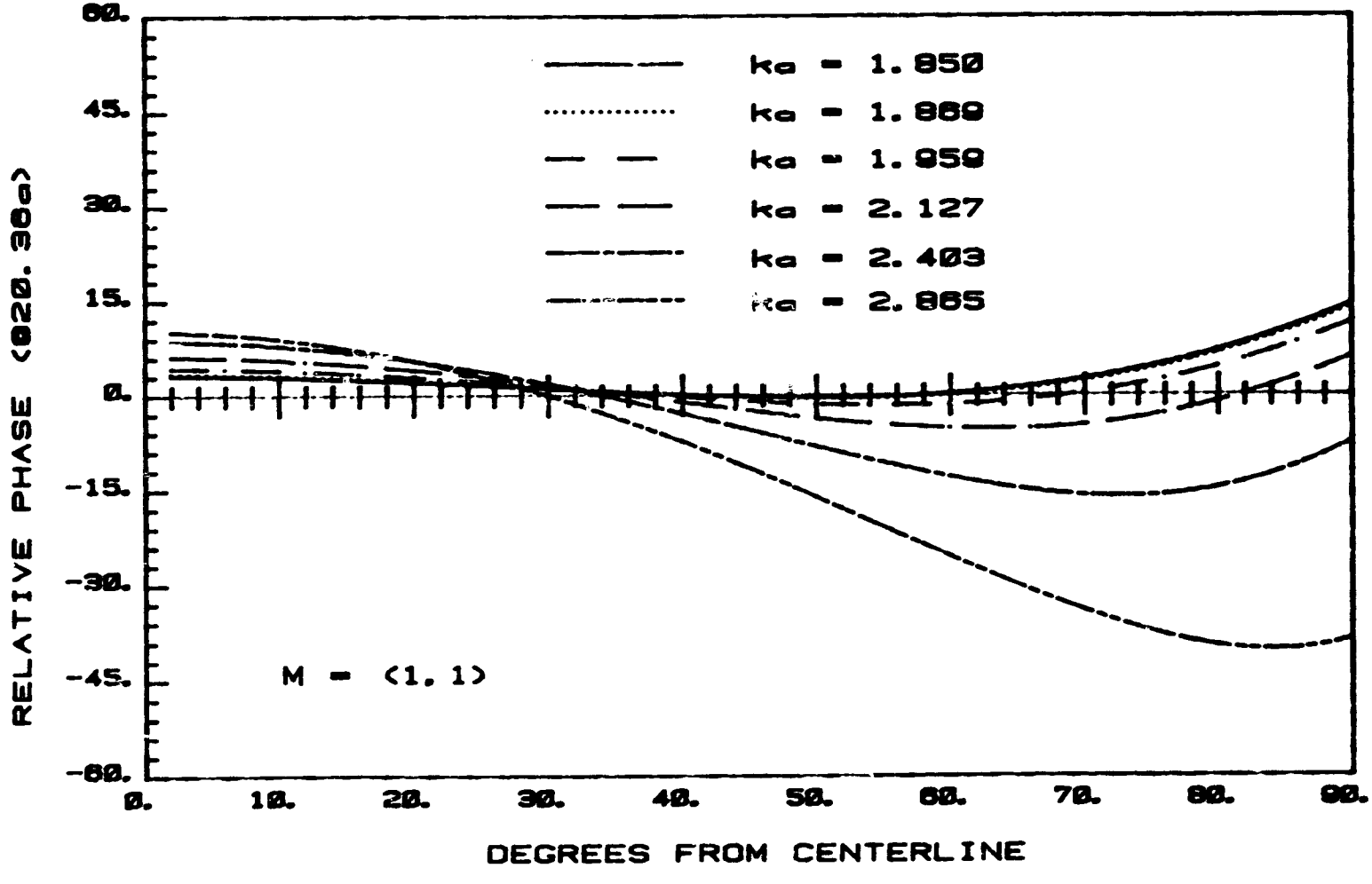

LANGLEY BELLMOUTH

Fig. 52c

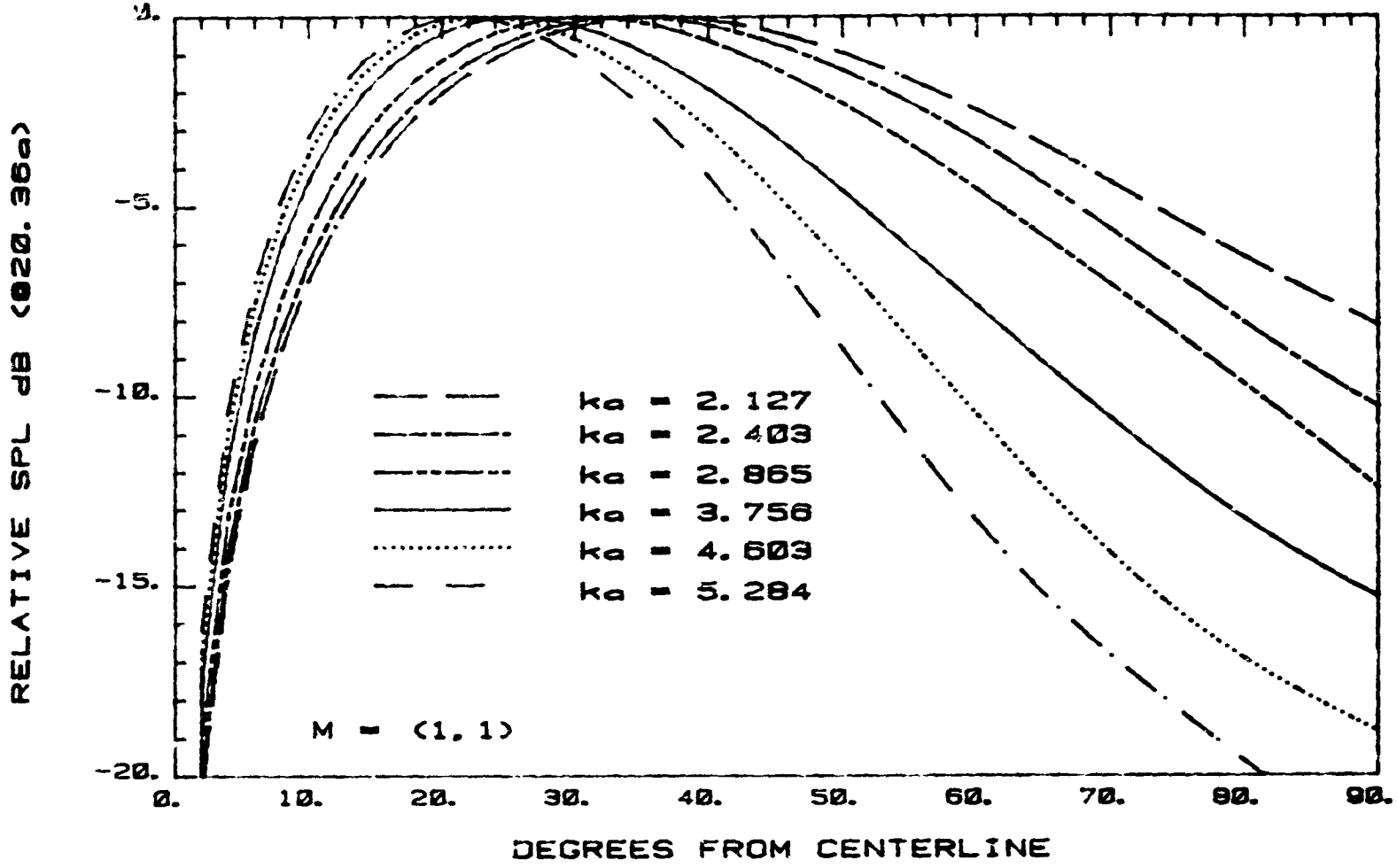

LANGLEY BELLMOUTH

Fig. 53a

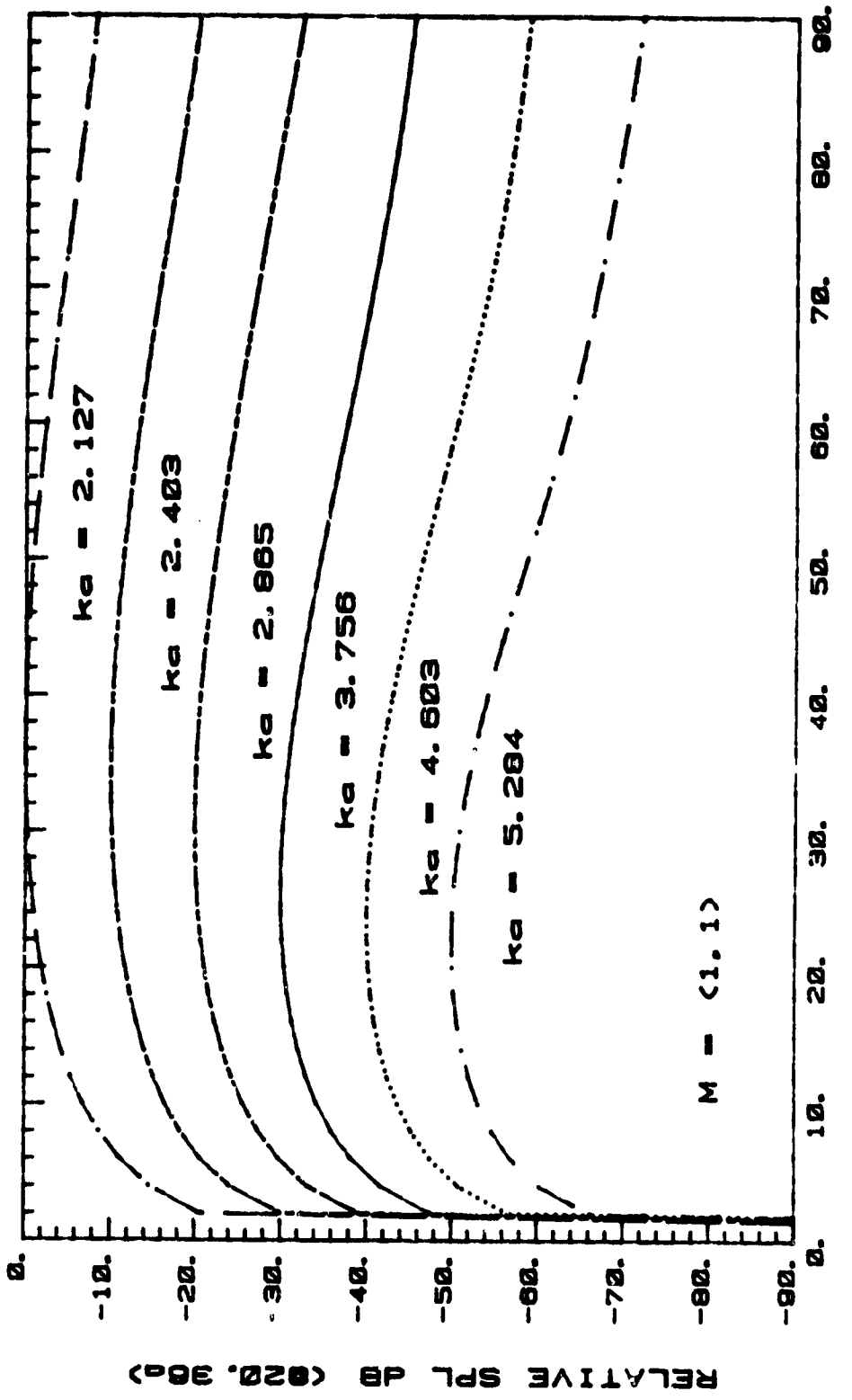
LANGLEY BELLMOUTH
RELATIVE SPL dB (020.30d)
DEGREES FROM CENTERLINE
ka = 2.127
ka = 2.403
ka = 2.865
ka = 3.756
ka = 4.603
ka = 5.284
M = (1.1)
0.
-10.
-20.
-30.
-40.
-50.
-60.
-70.
-80.
-90.
10.
20.
30.
40.
50.
60.
70.
80.
90.

Fig. 53b

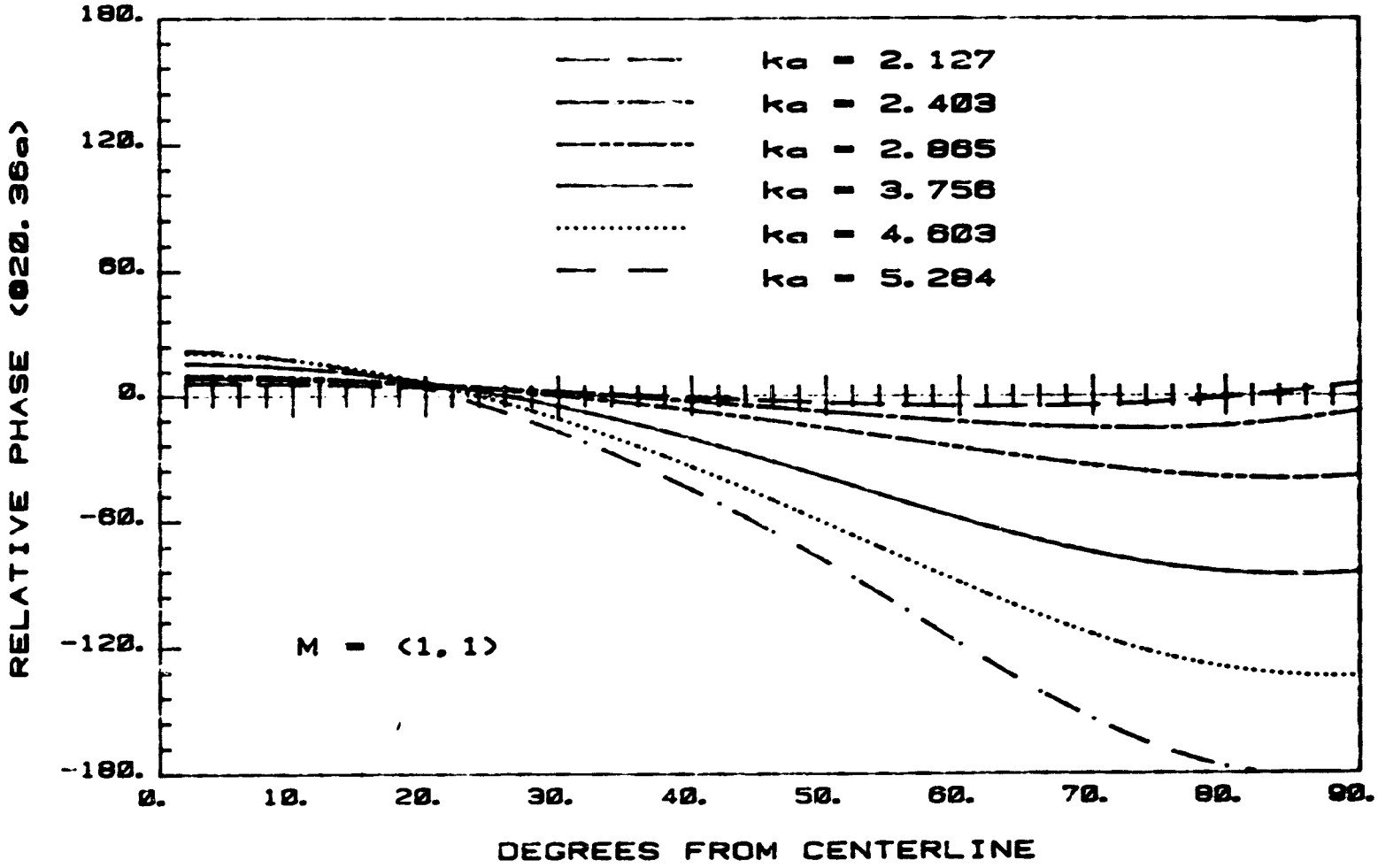

LANGLEY BELLMOUTH

Fig. 53c

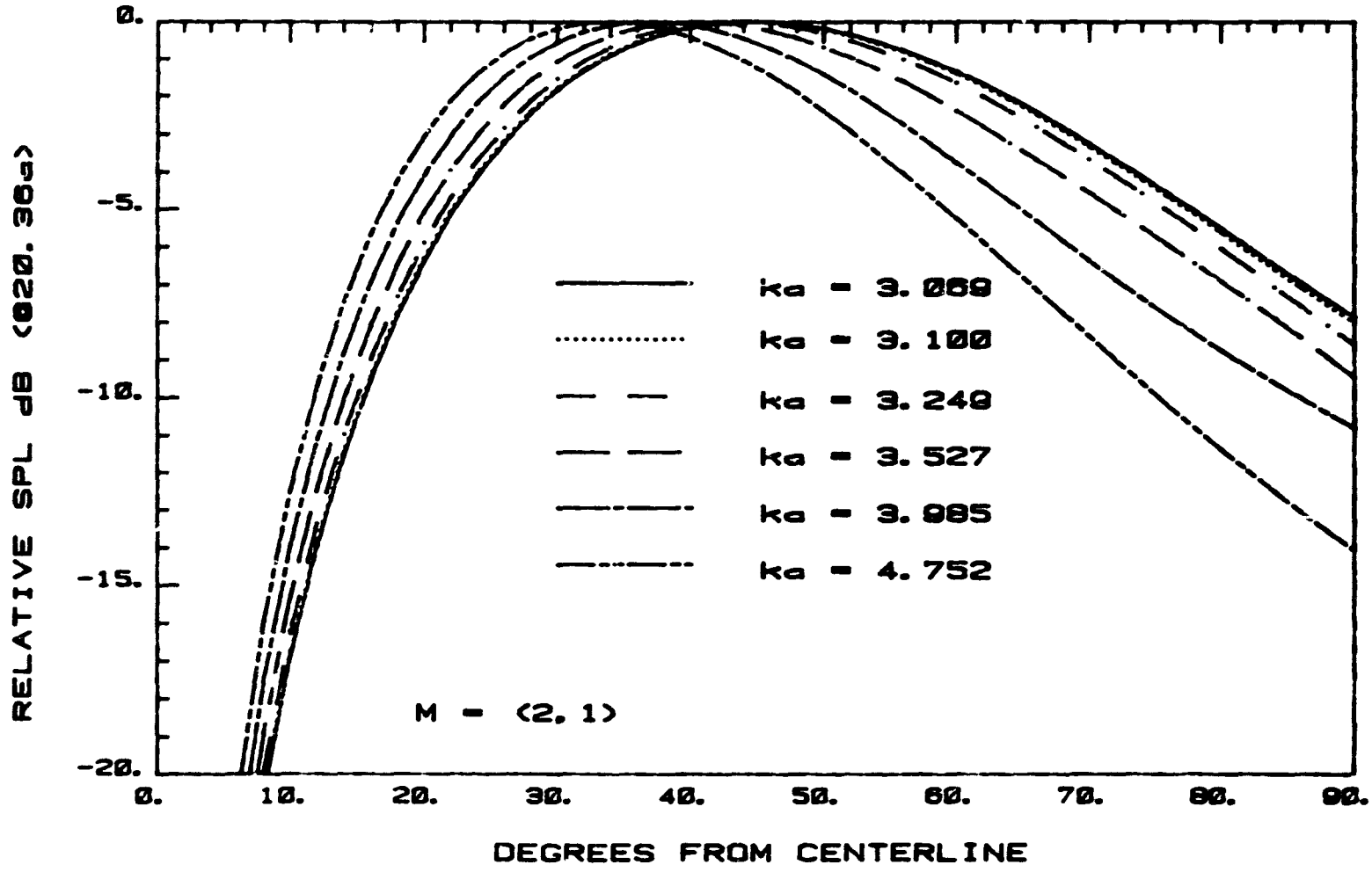

LANGLEY BELLMOUTH

Fig. 54a

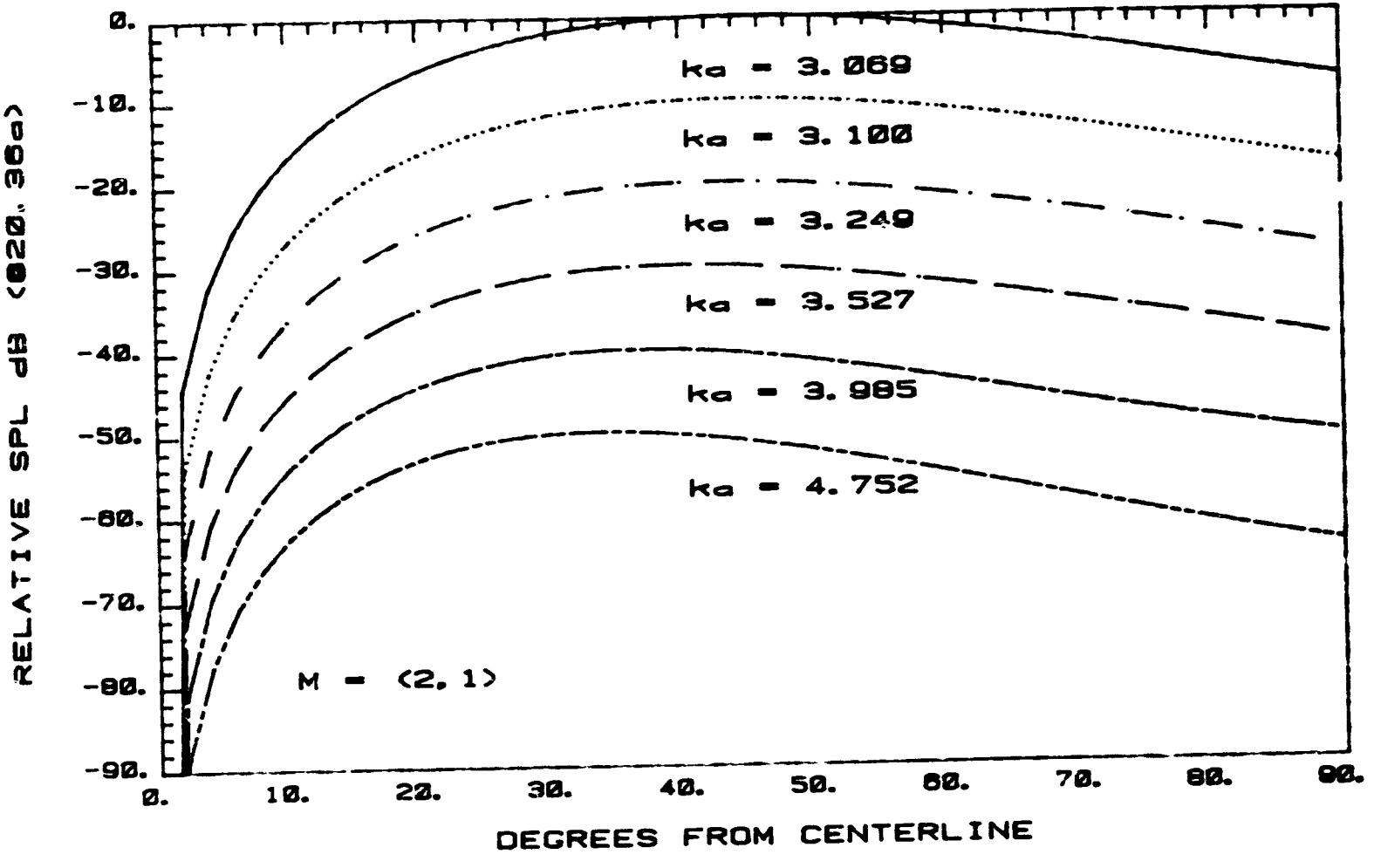

LANGLEY BELLMOUTH

Fig. 54b

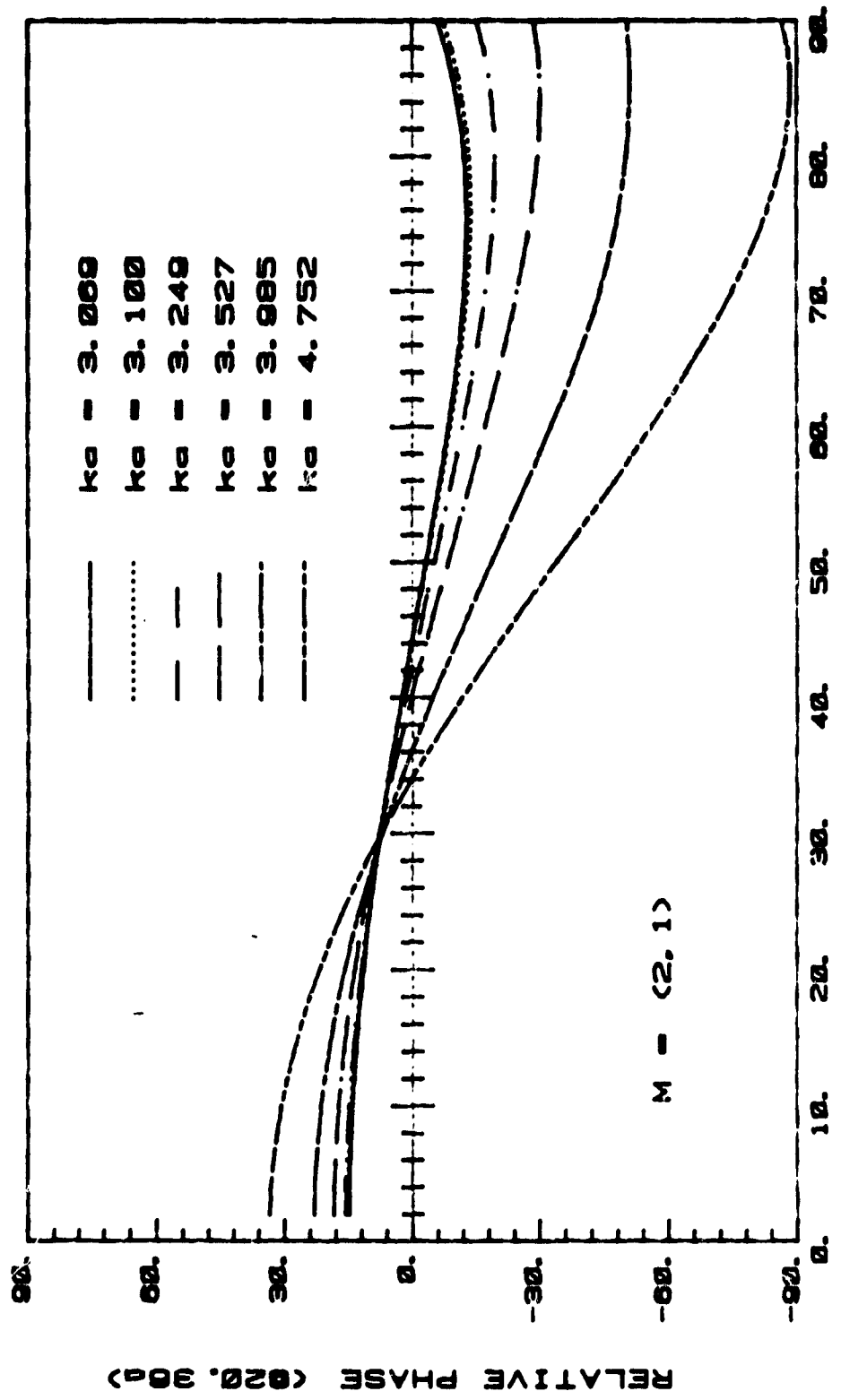
LANGLEY BELLMOUTH
RELATIVE PHASE (@20.30d)
DEGREES FROM CENTERLINE
M = (2,1)
ka = 3.009
ka = 3.100
ka = 3.240
ka = 3.527
ka = 3.985
ka = 4.752
90.
60.
30.
0.
-30.
-60.
-90.
0.
10.
20.
30.
40.
50.
60.
70.
80.
90.

Fig. 54c

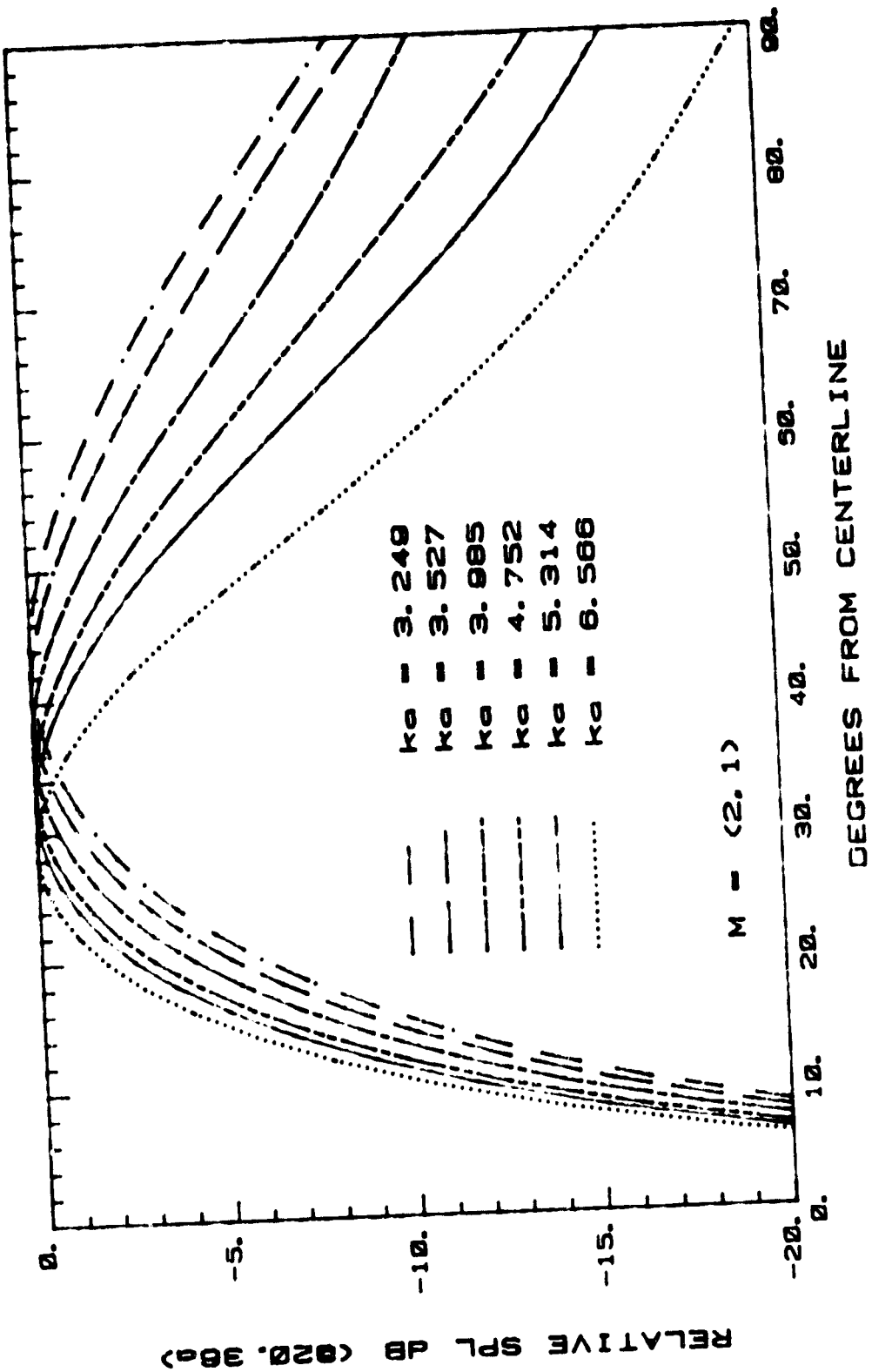
LANGLEY BELLMOUTH
RELATIVE SPL dB (020.36a)
0.
-5.
-10.
-15.
-20.
0.
10.
20.
30.
40.
50.
60.
70.
80.
90.
DEGREES FROM CENTERLINE
M = (2,1)
ka = 3.249
ka = 3.527
ka = 3.805
ka = 4.752
ka = 5.314
ka = 8.566

Fig. 55a

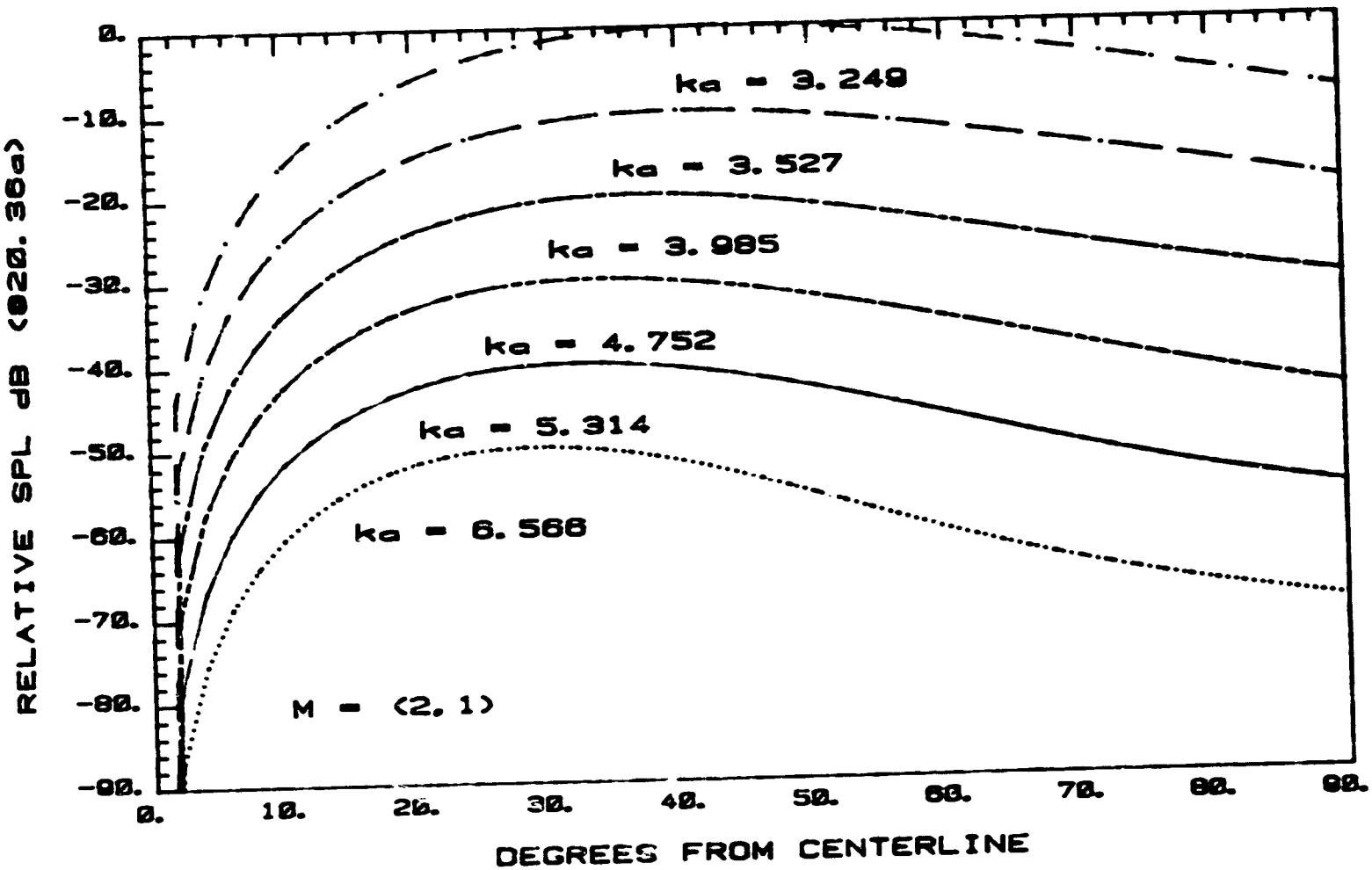

LANGLEY BELLMOUTH

Fig. 55b

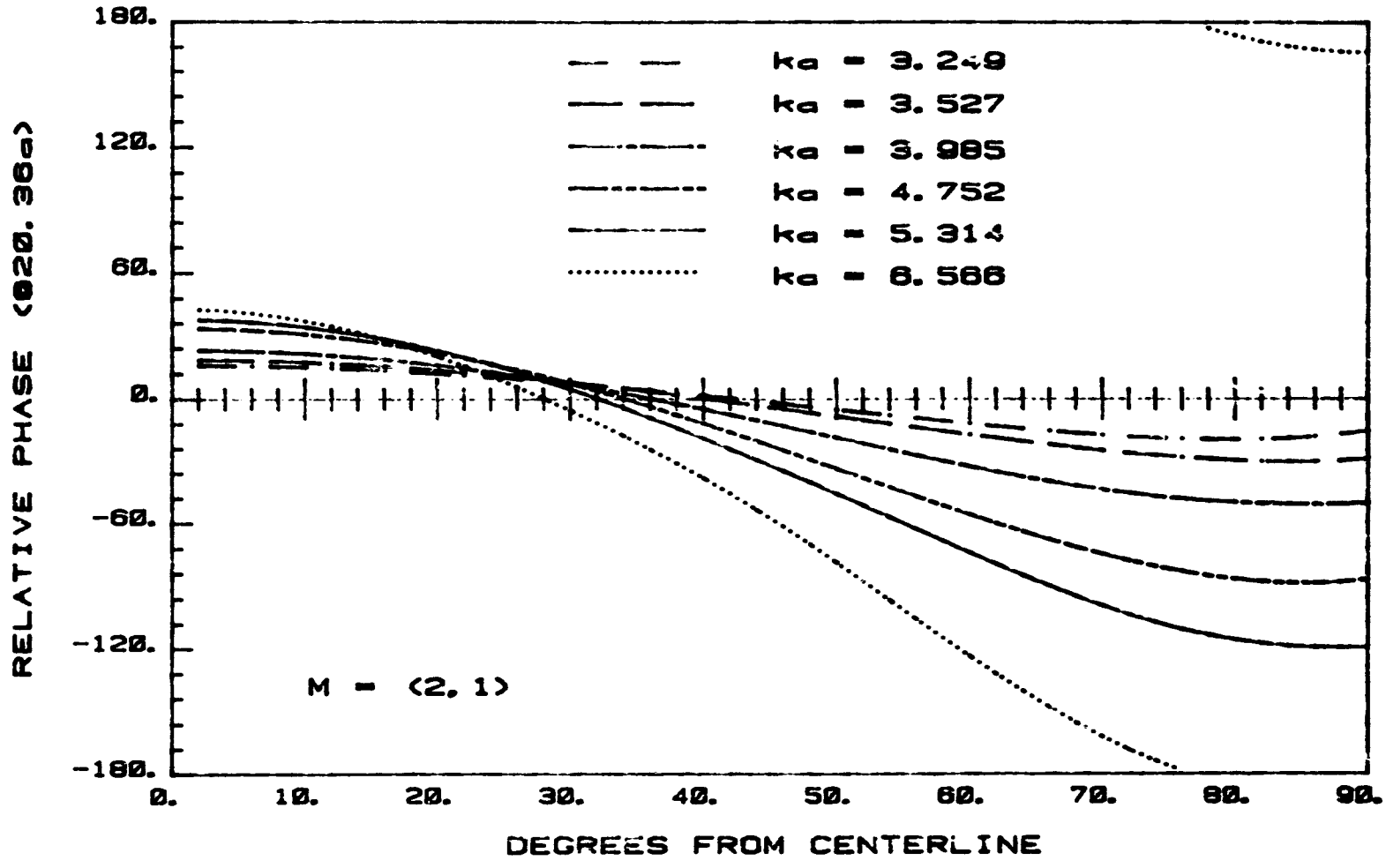

LANGLEY BELLMOUTH

Fig. 55c

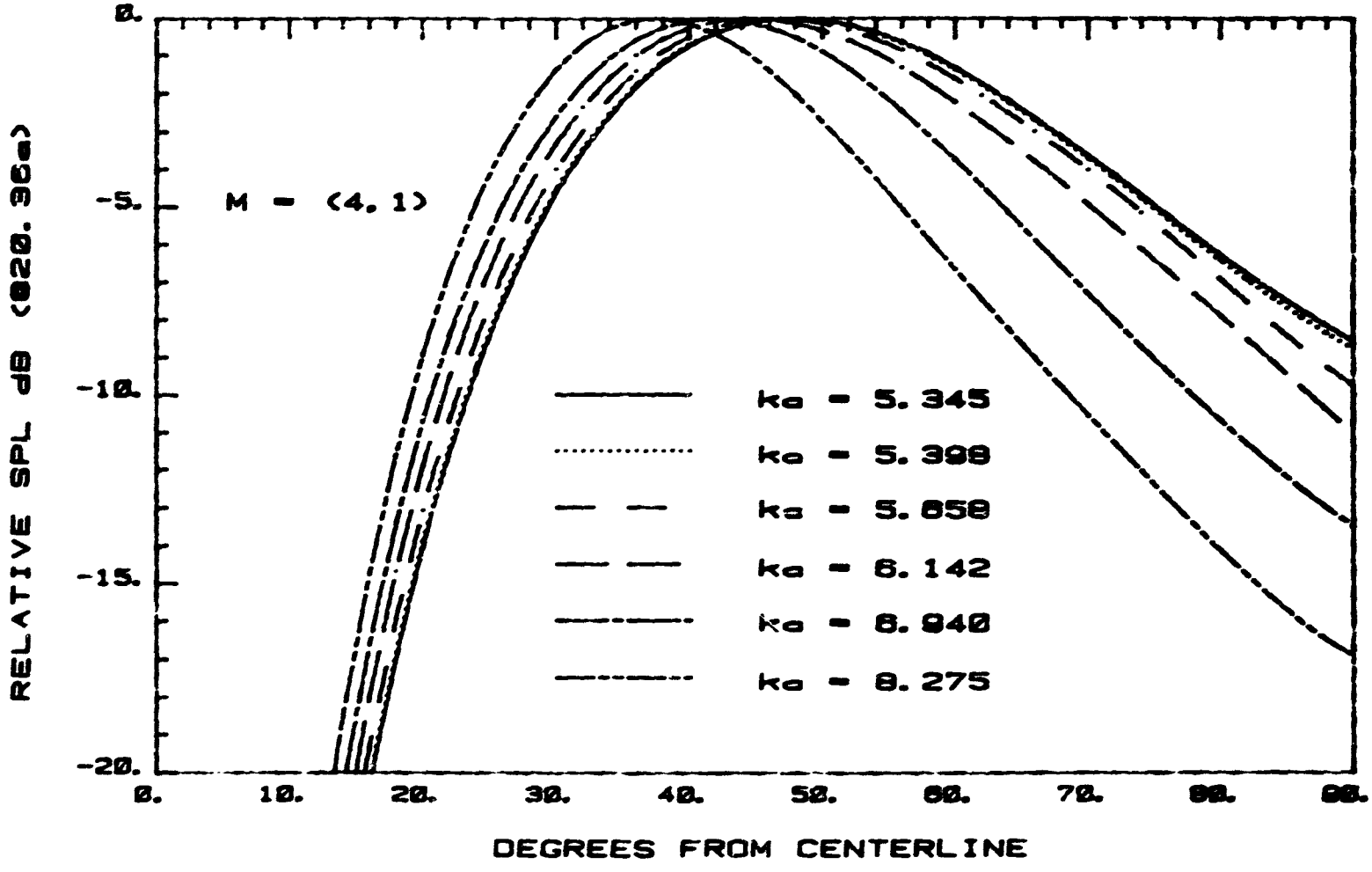

LANGLEY BELLMOUTH

Fig. 56a

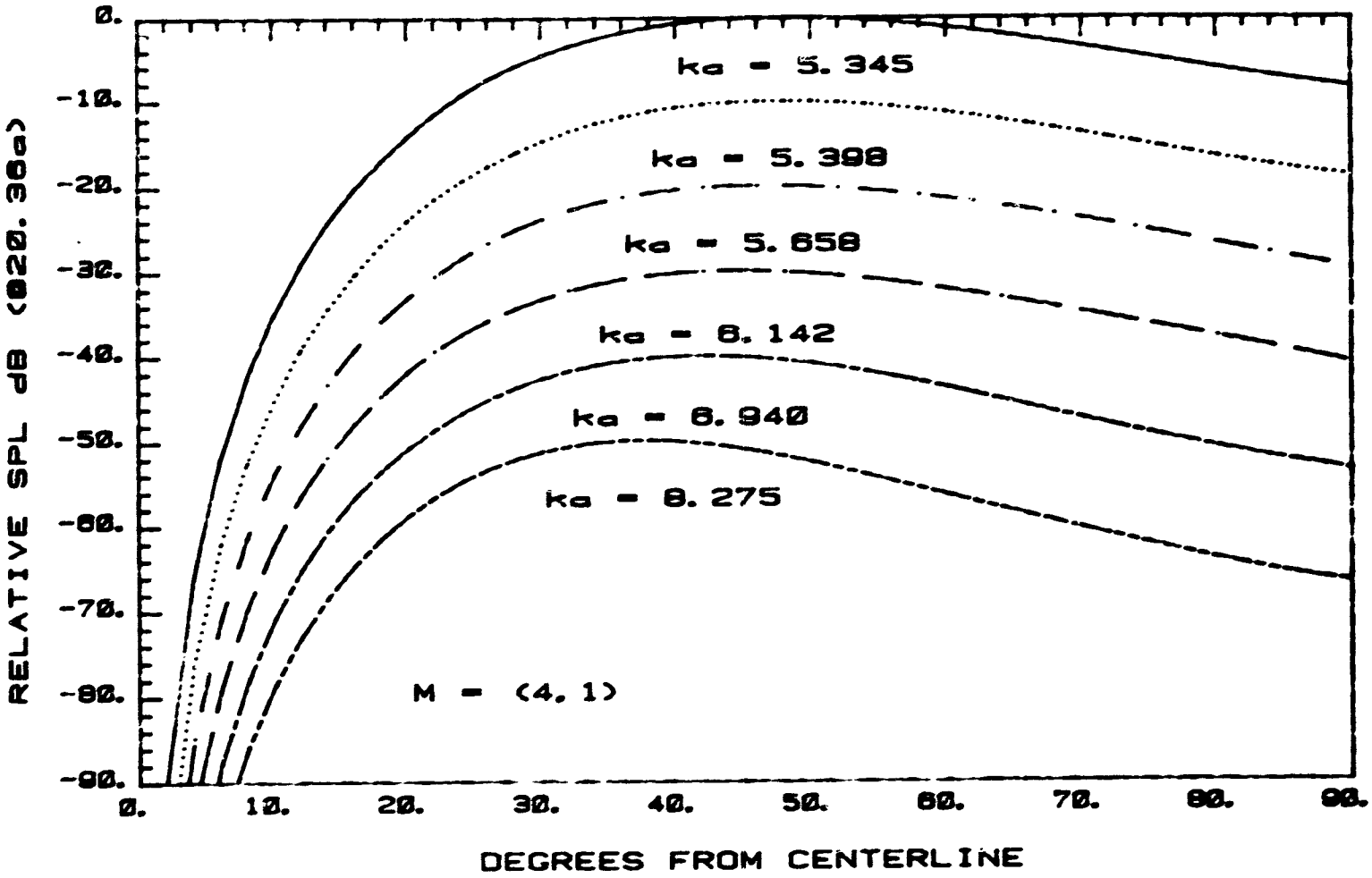

LANGLEY BELLMOUTH

Fig. 56b

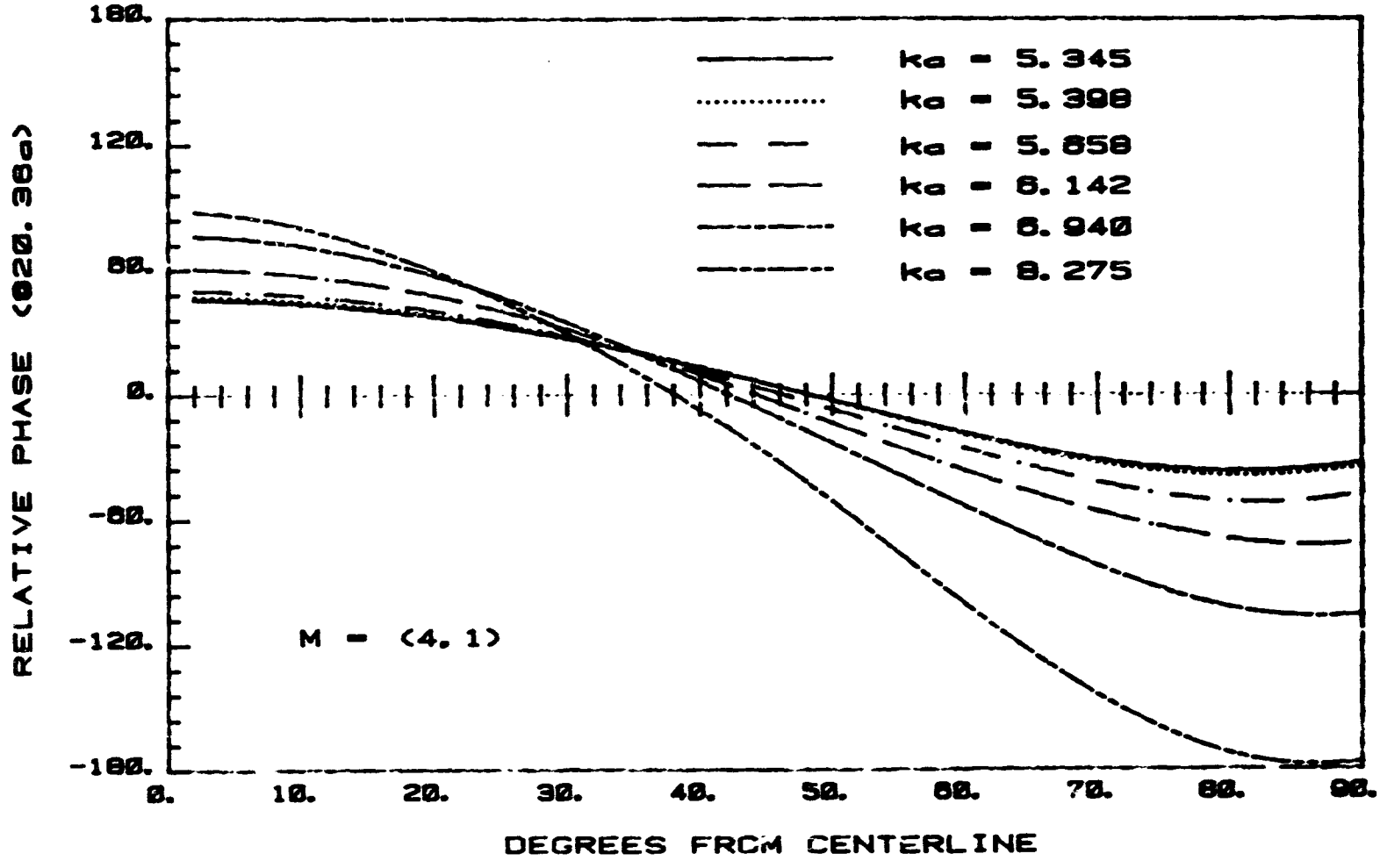

LANGLEY BELLMOUTH

Fig. 56c

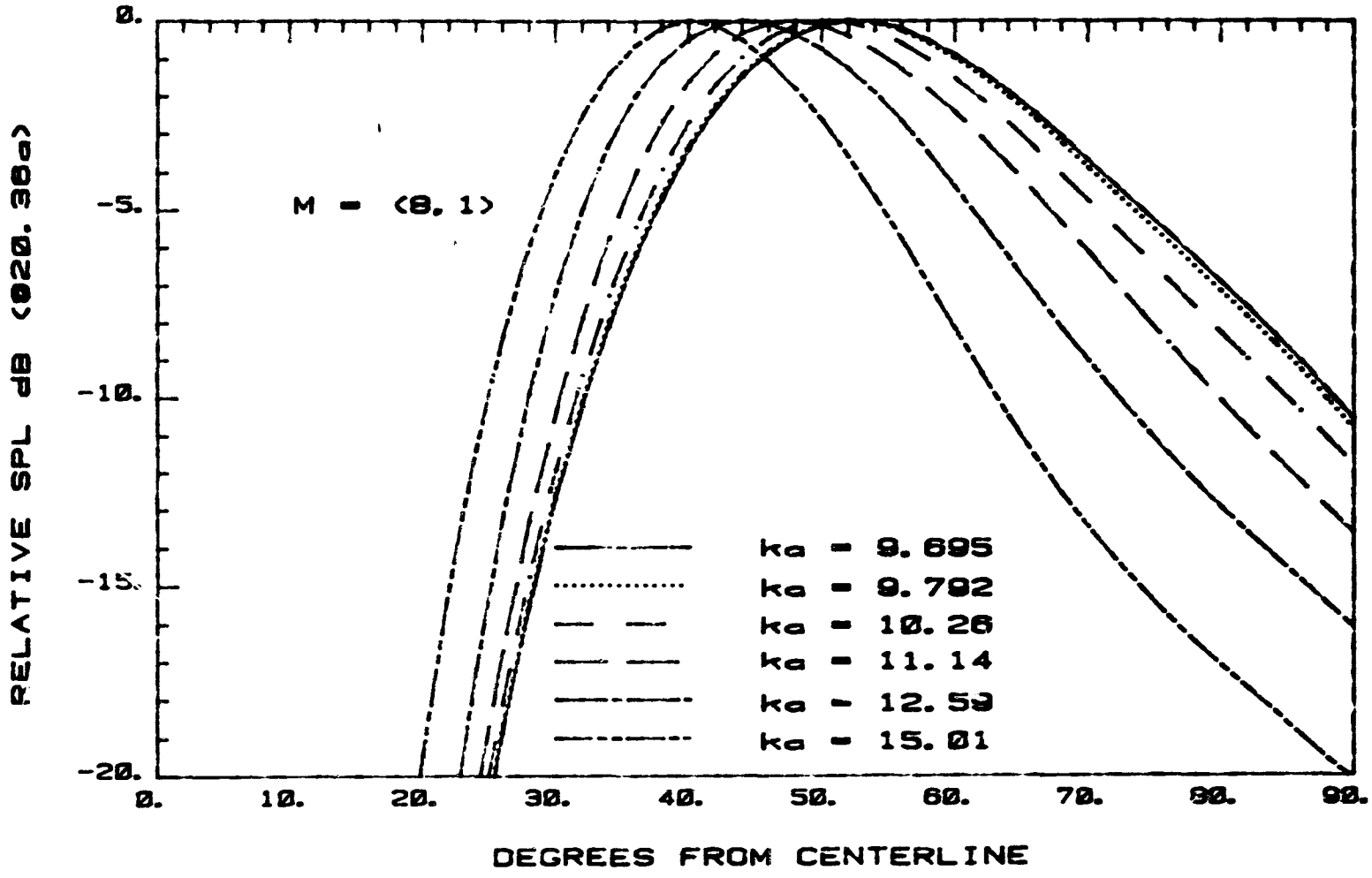

LANGLEY BELLMOUTH

Fig. 57a

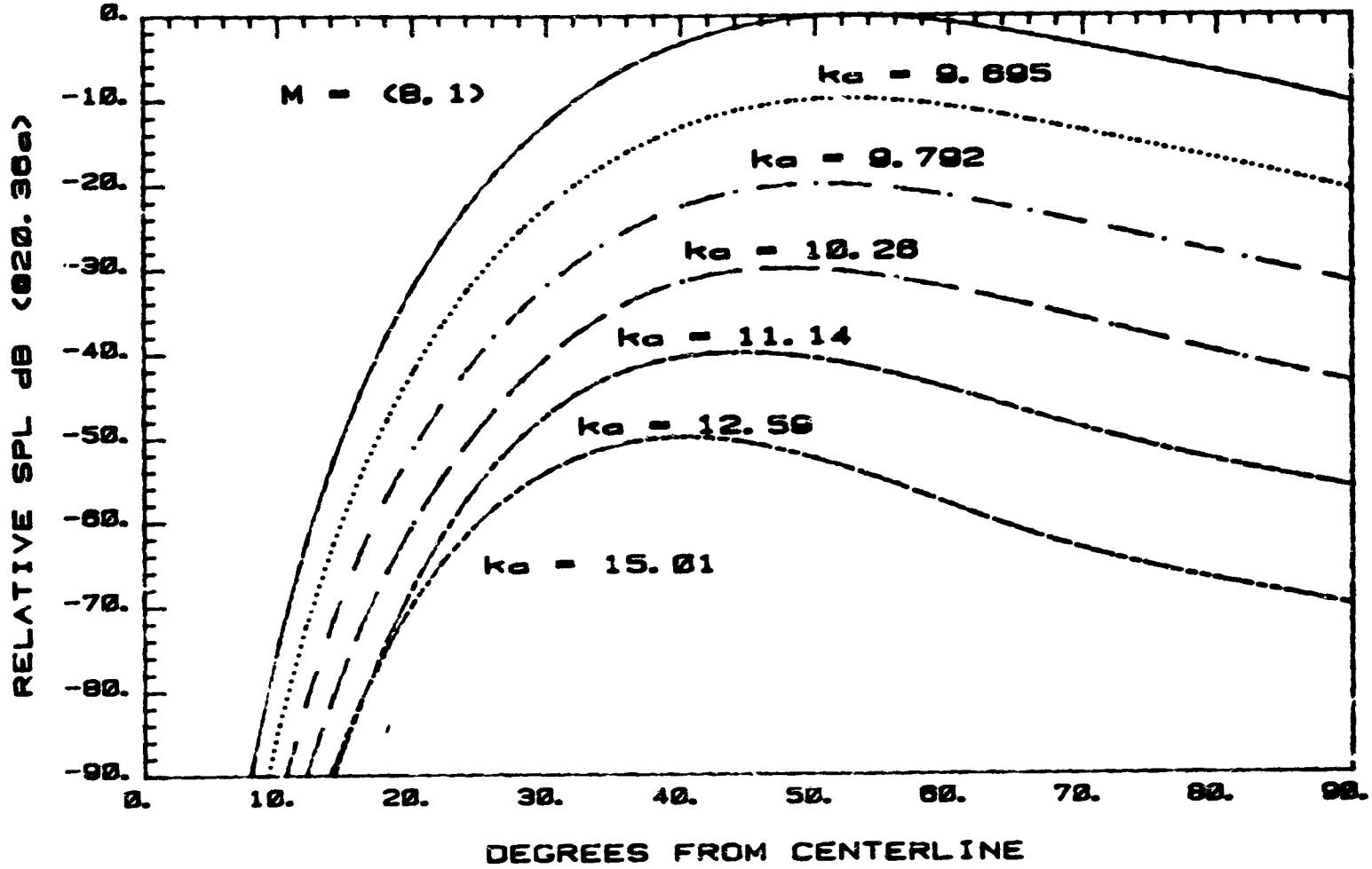

LANGLEY BELLMOUTH

Fig. 57b

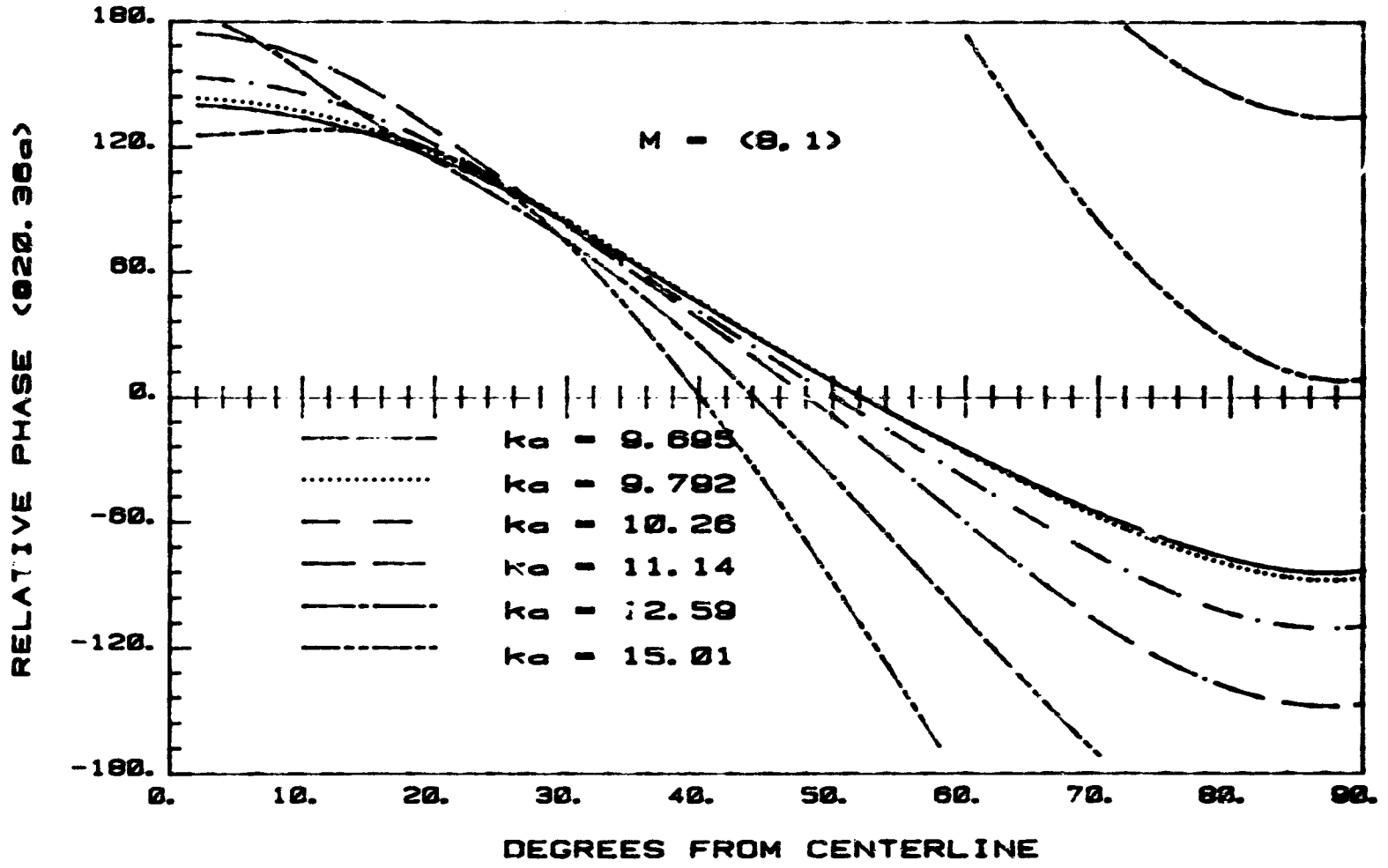

LANGLEY BELLMOUTH

Fig. 57c

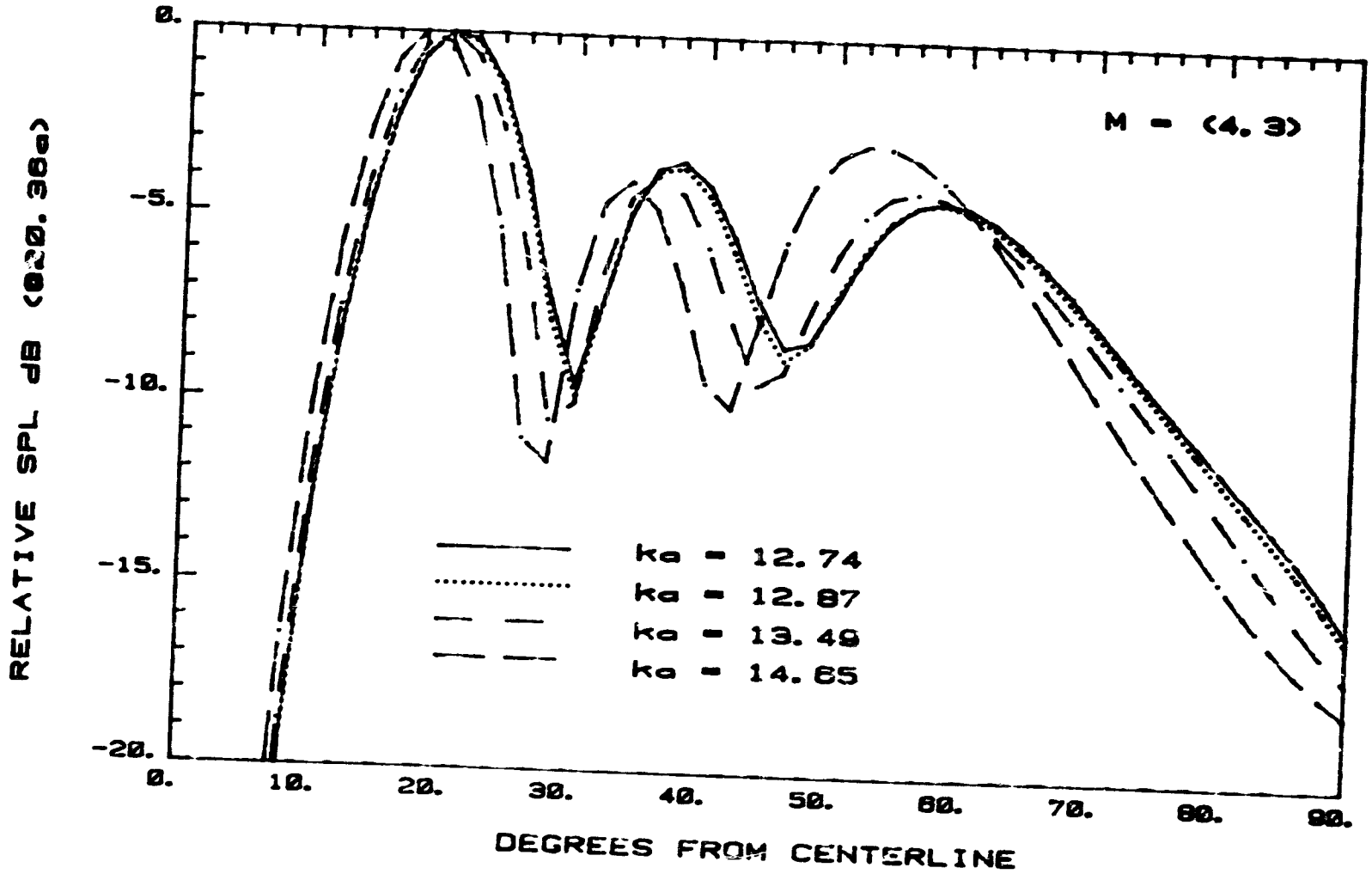

LANGLEY BELLMOUTH

Fig. 58a

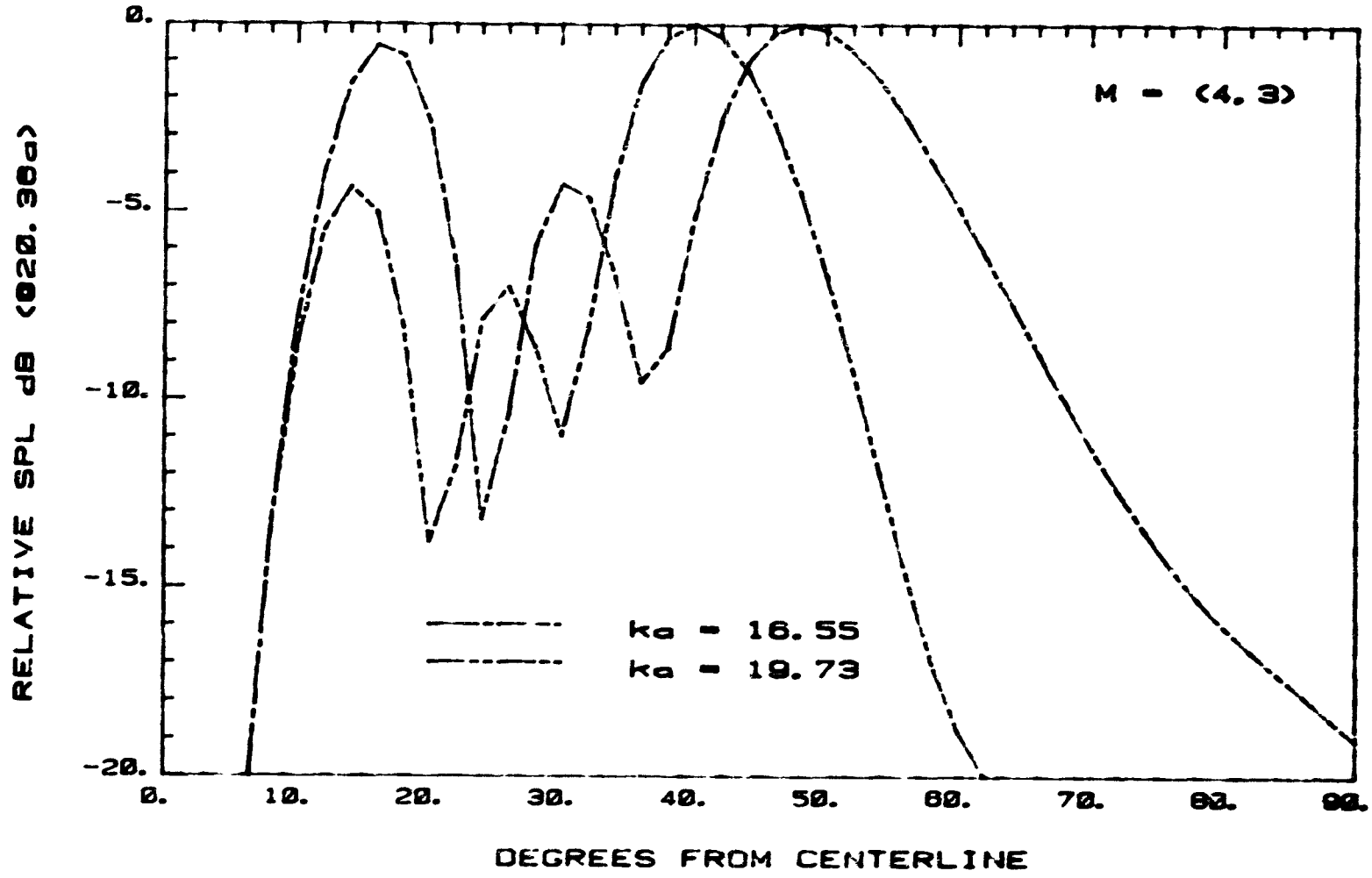

LANGLEY BELLMOUTH

Fig. 58b

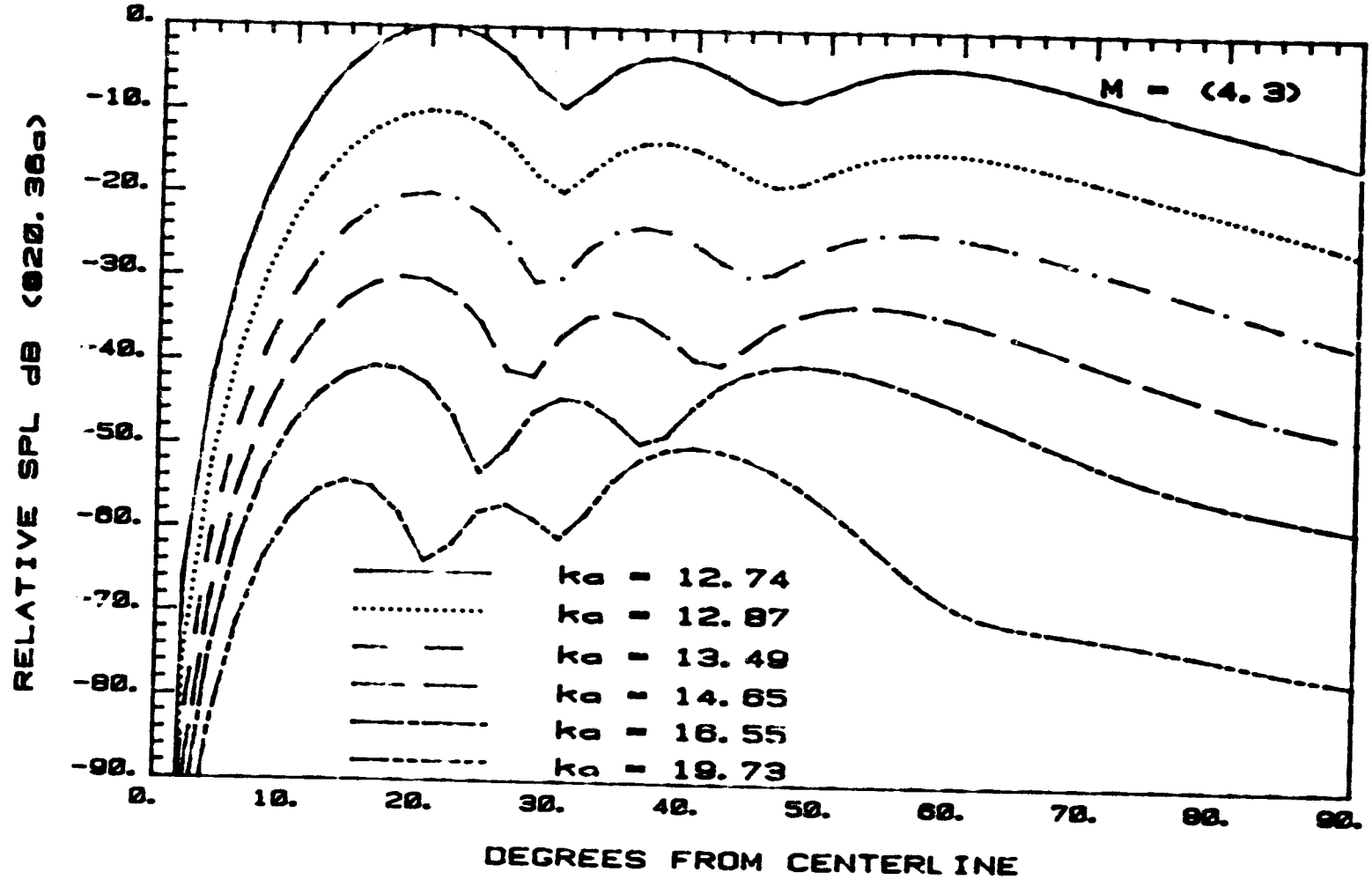

LANGLEY BELLMOUTH

Fig. 58c

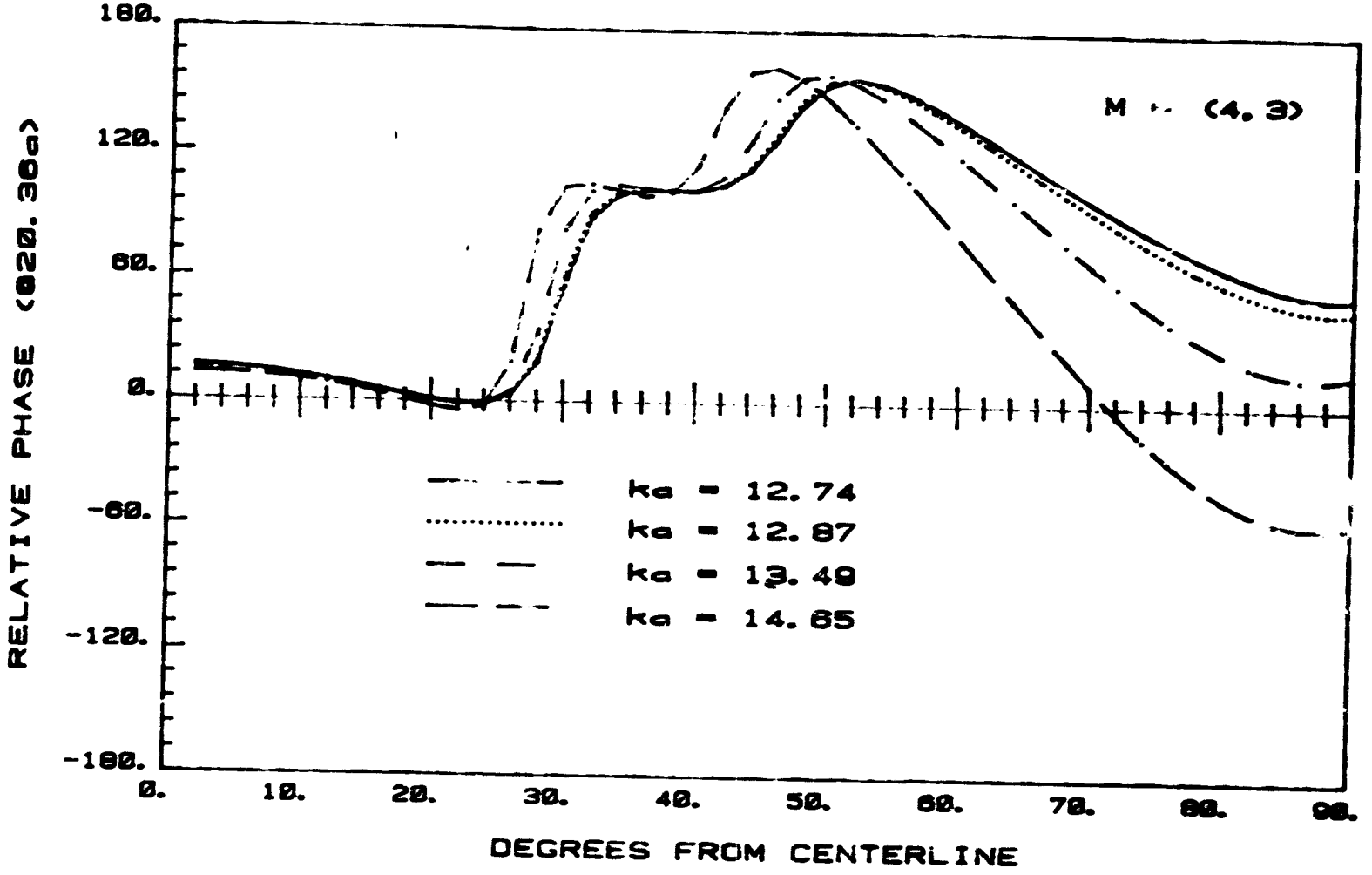

LANGLEY BELLMOUTH

Fig. 58d

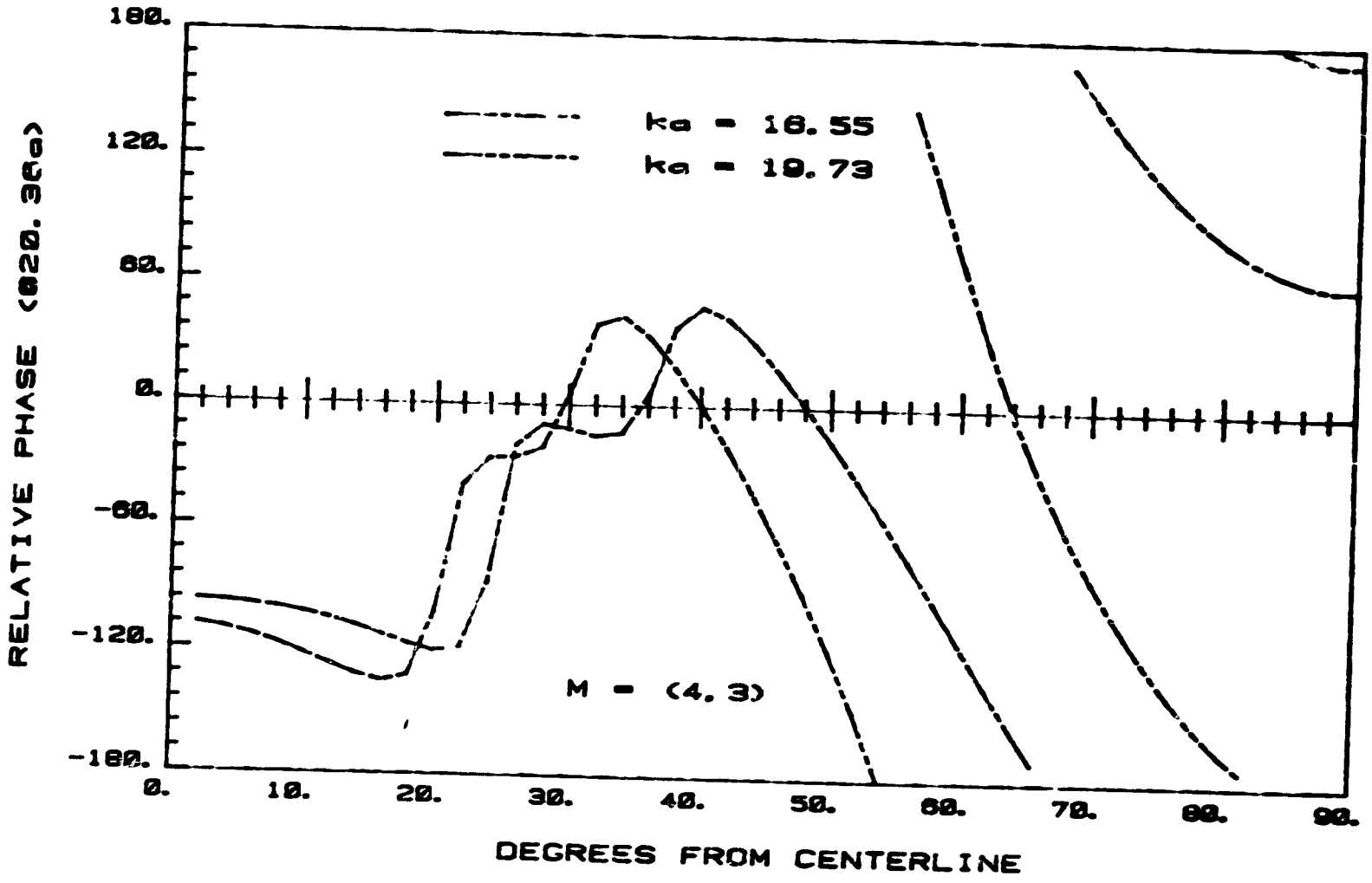

LANGLEY BELLMOUTH

Fig. 58e

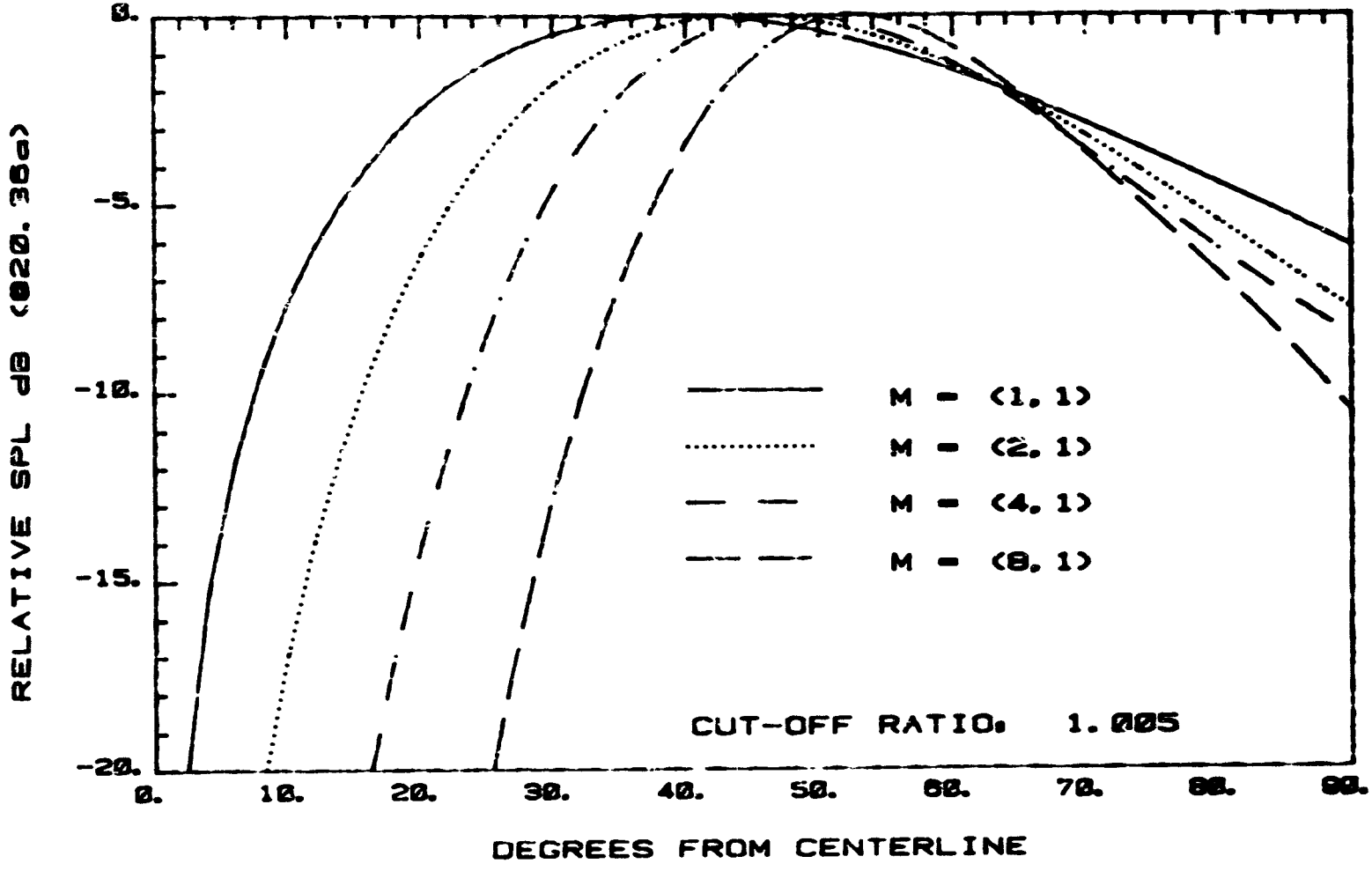

LANGLEY BELLMOUTH

Fig. 59a

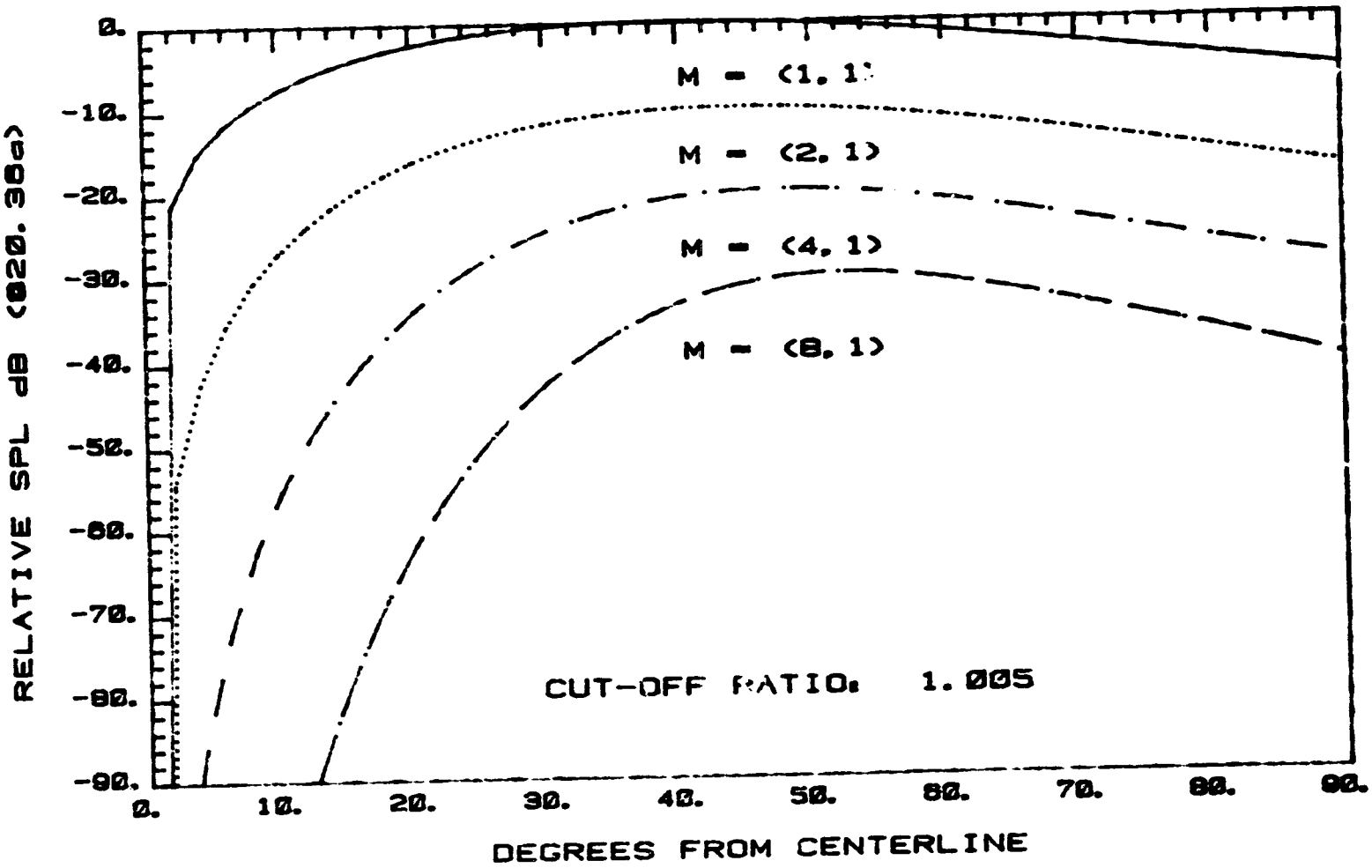

LANGLEY BELLMOUTH

Fig. 59b

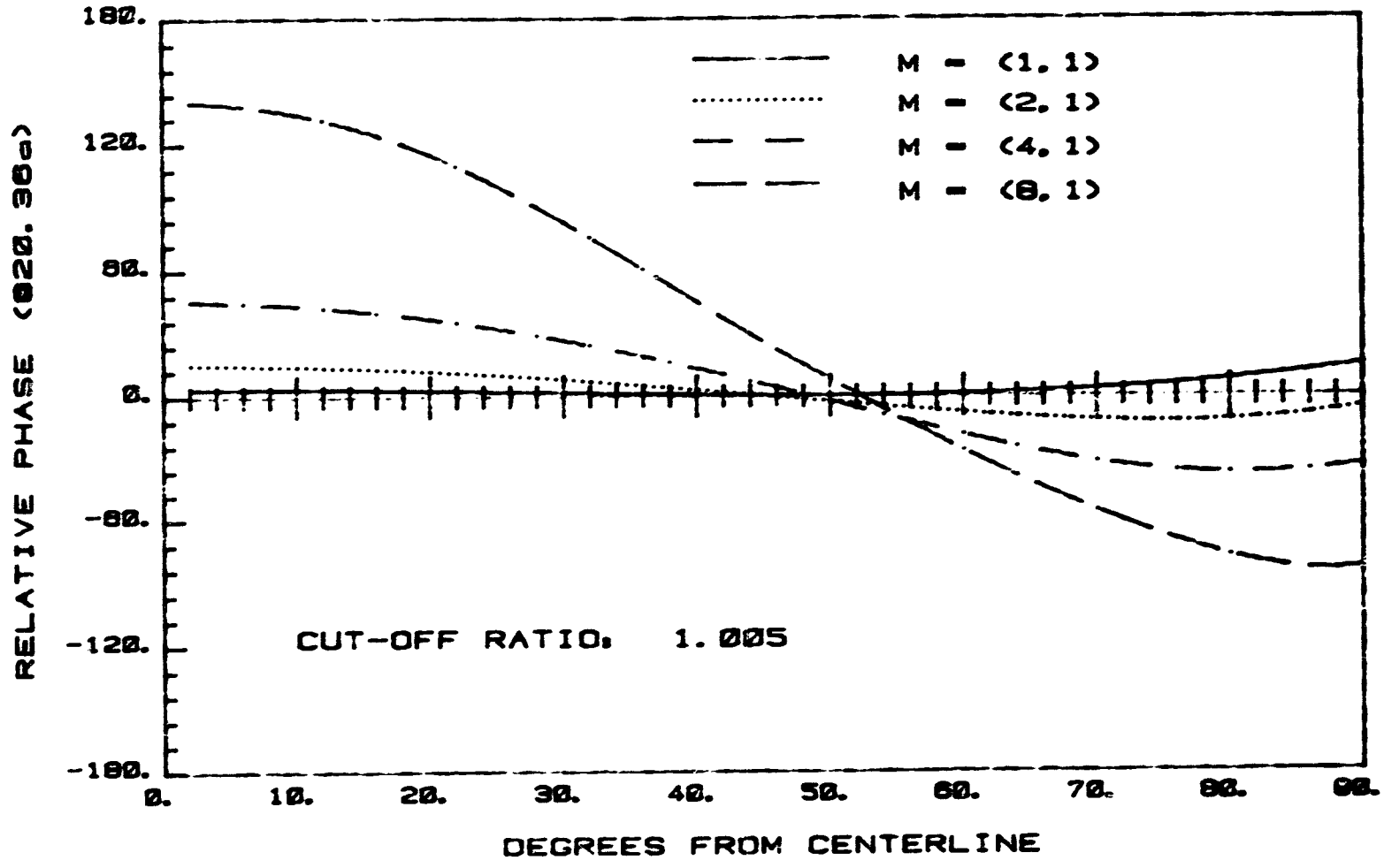

LANGLEY BELLMOUTH

Fig. 59c

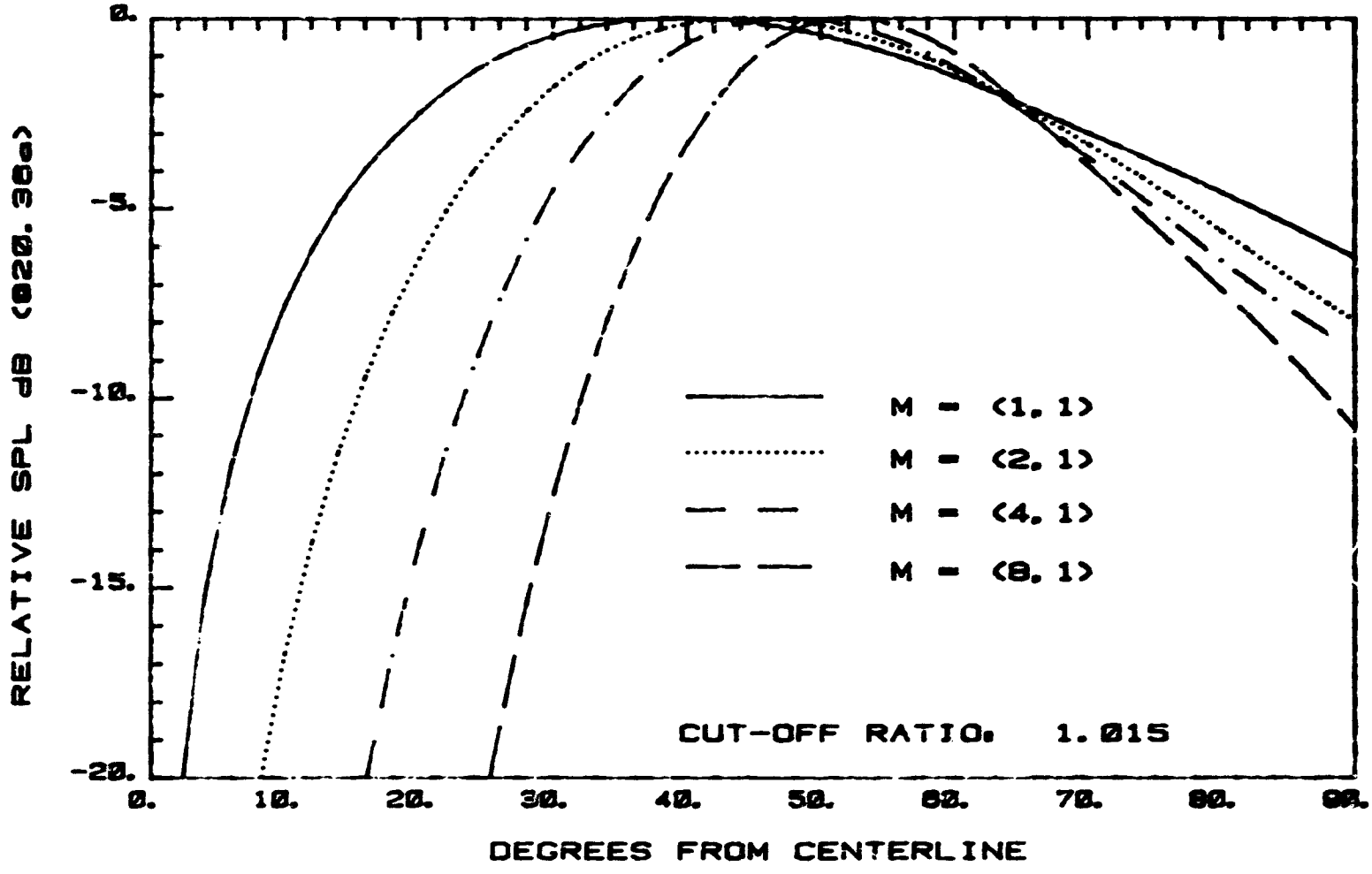

LANGLEY BELLMOUTH

Fig. 60a

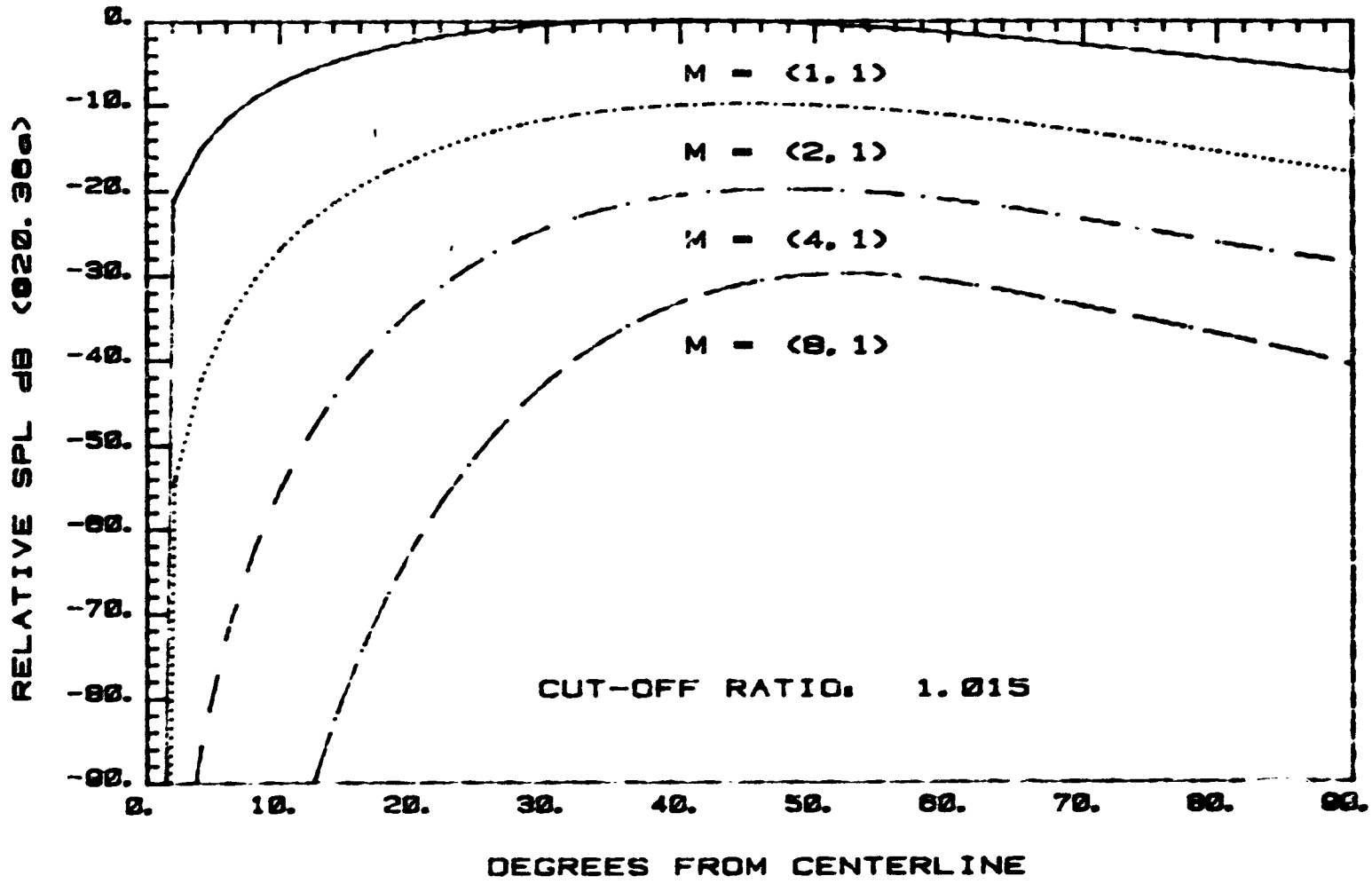

LANGLEY BELLMOUTH

Fig. 60b

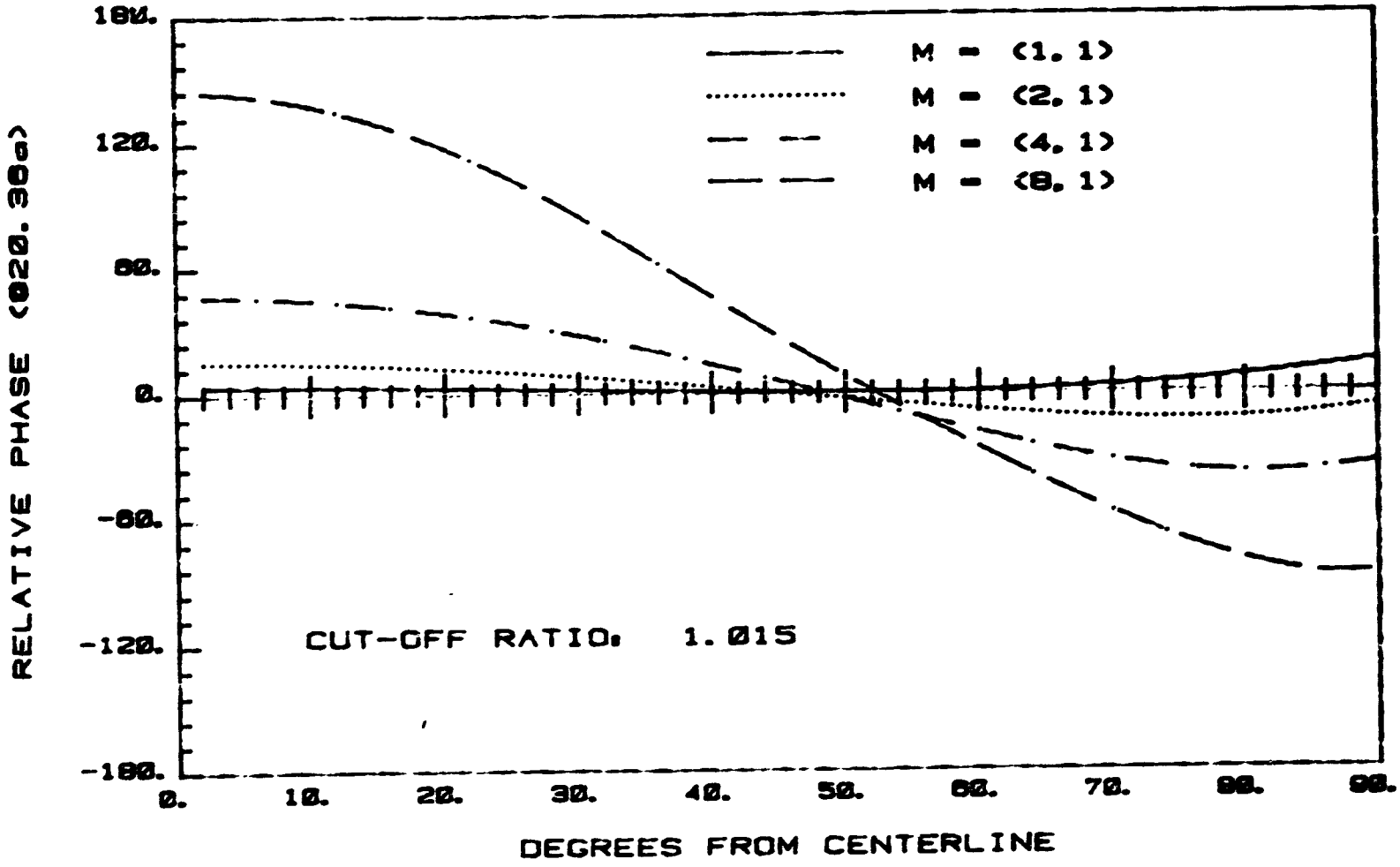

LANGLEY BELLMOUTH

Fig. 60c

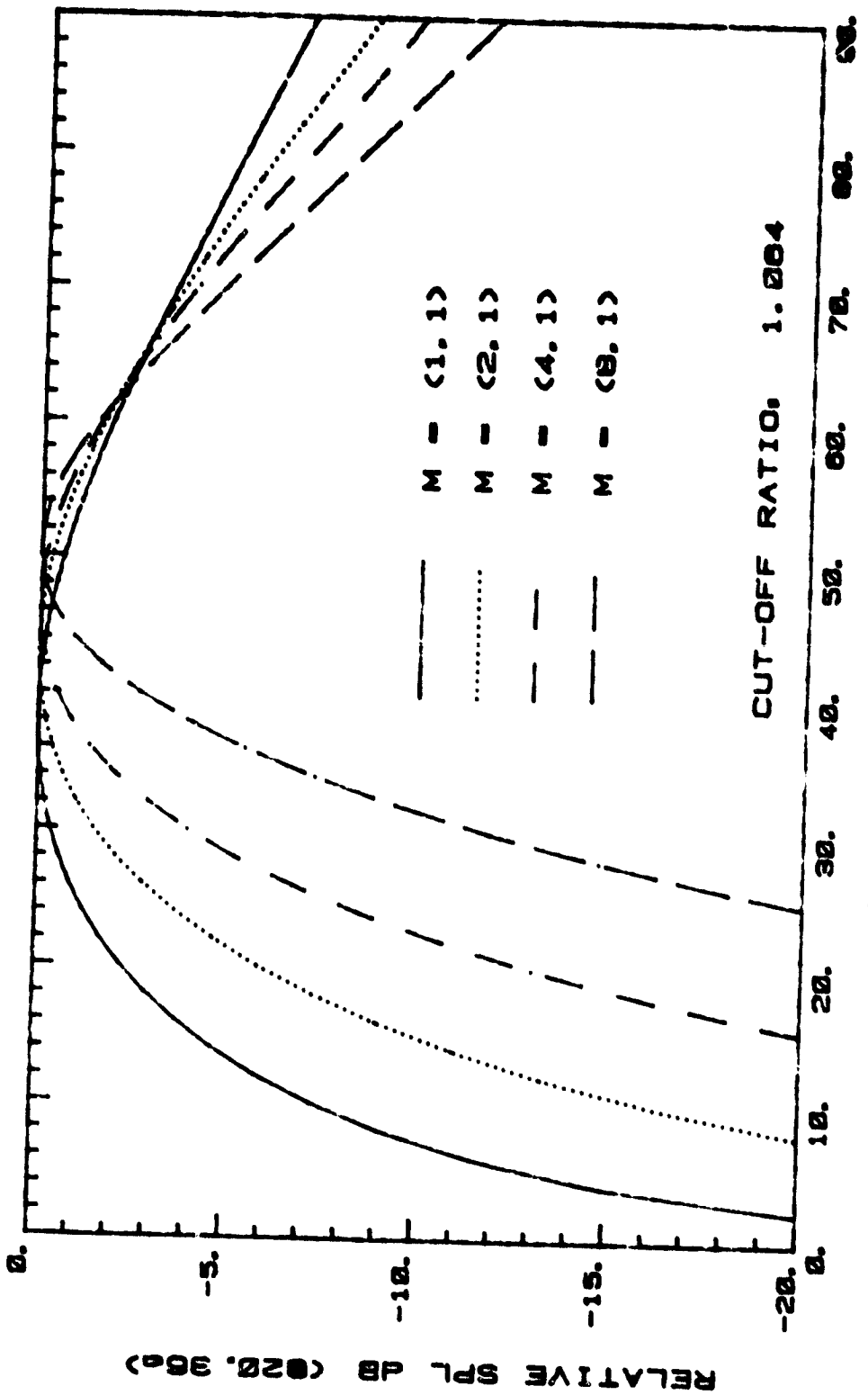

LANGLEY BELLMOUTH

Fig. 61a

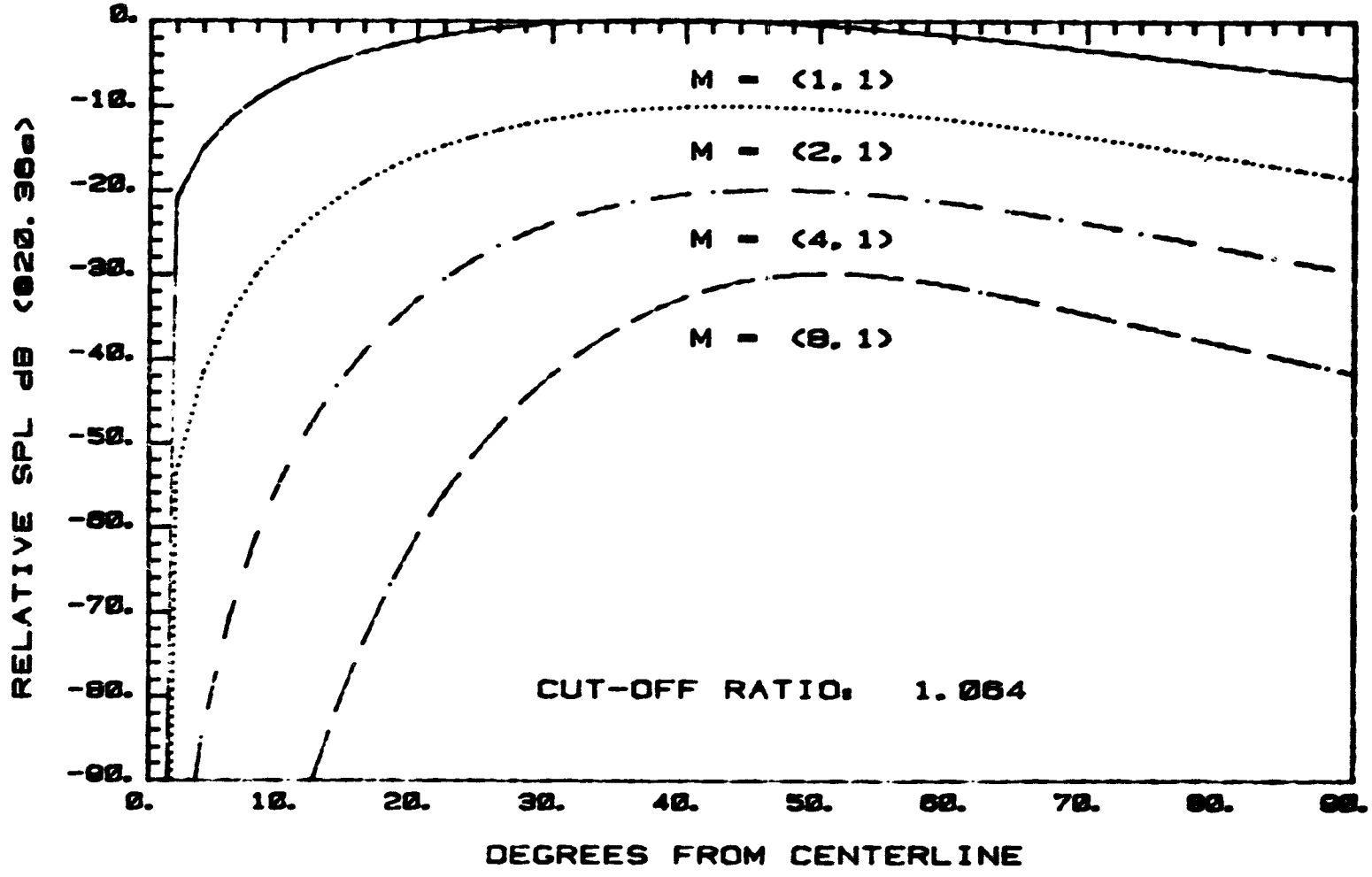

LANGLEY BELLMOUTH

Fig. 61b

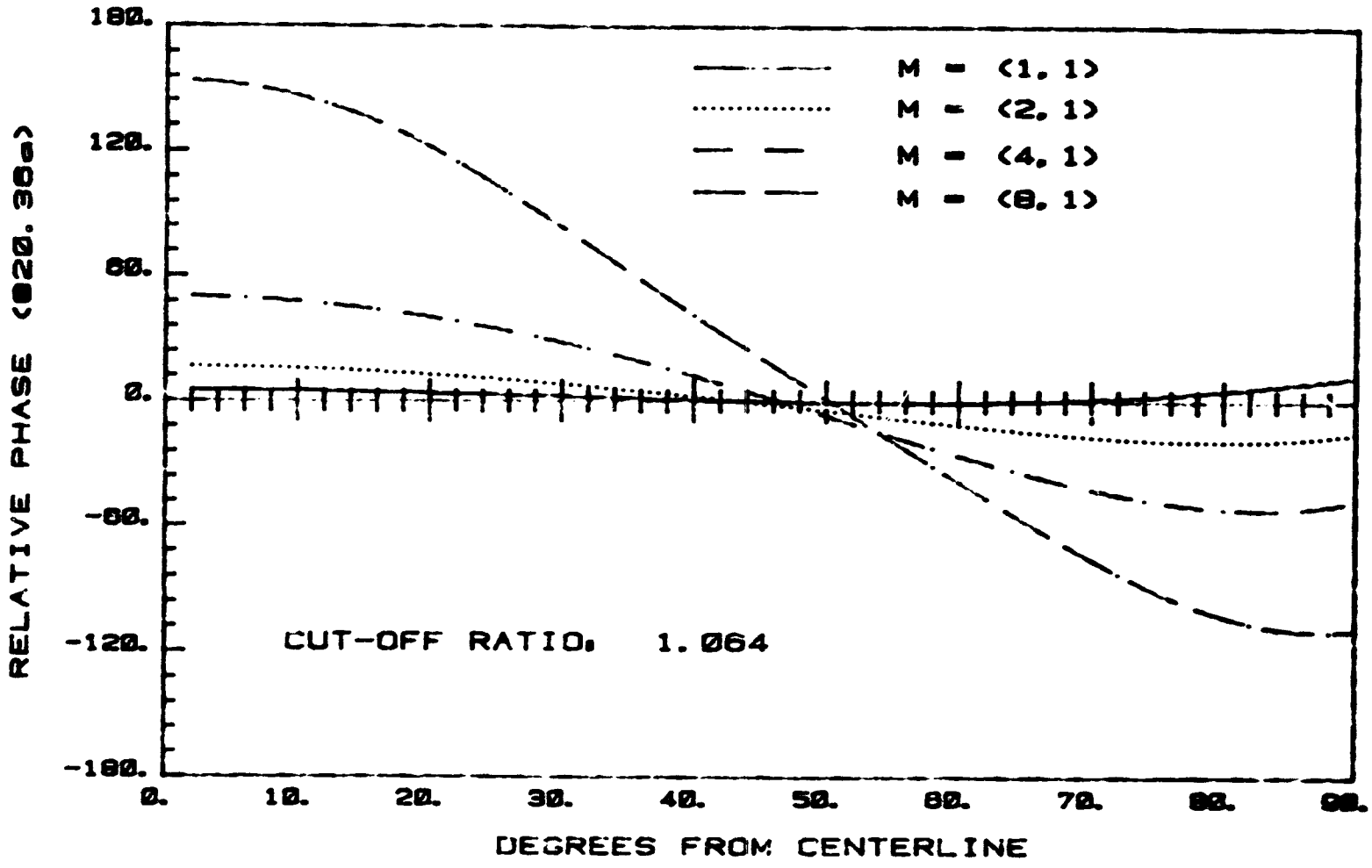

LANGLEY BELLMOUTH

Fig. 61c

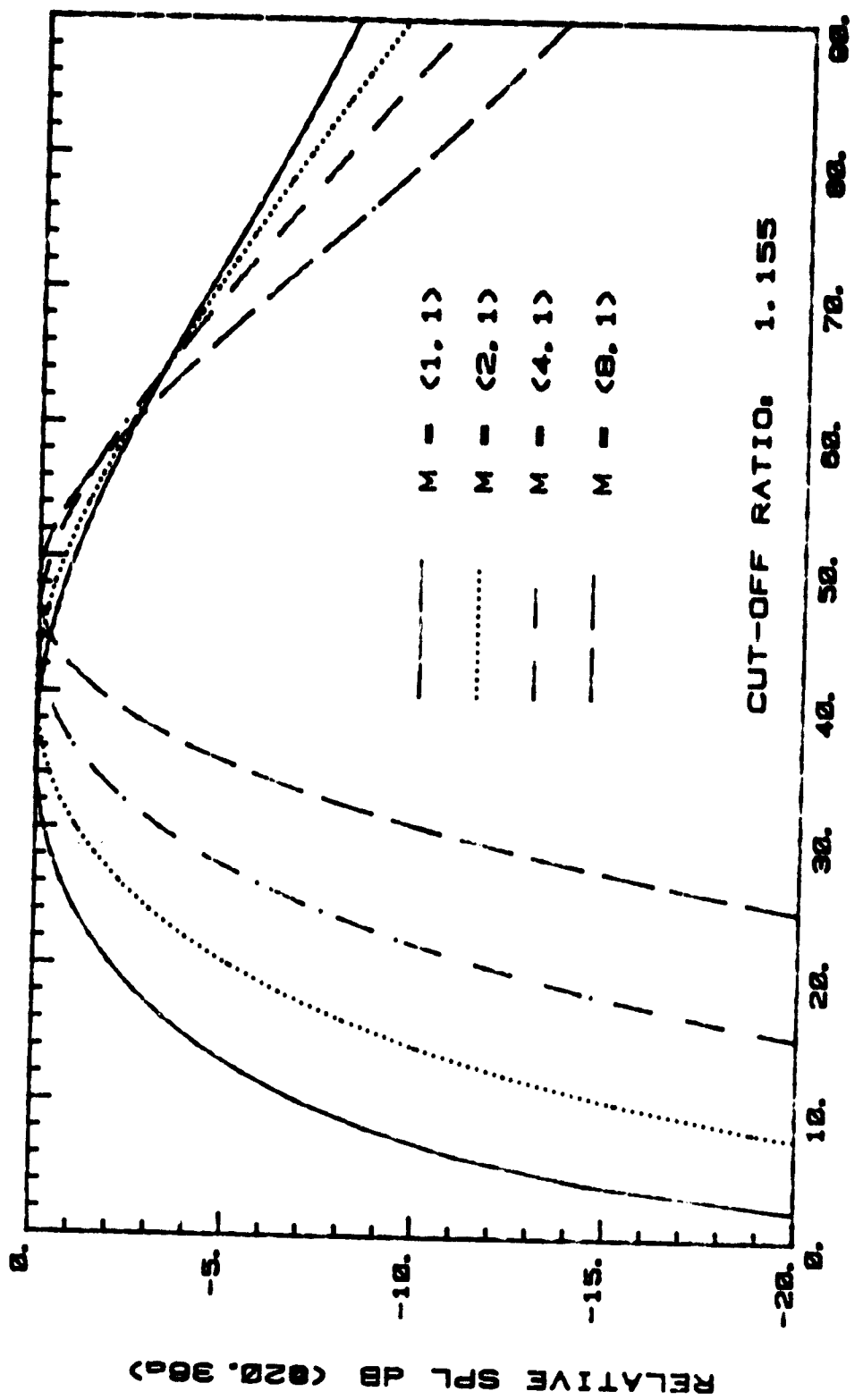

LANGLEY BELLMOUTH

Fig. 62a

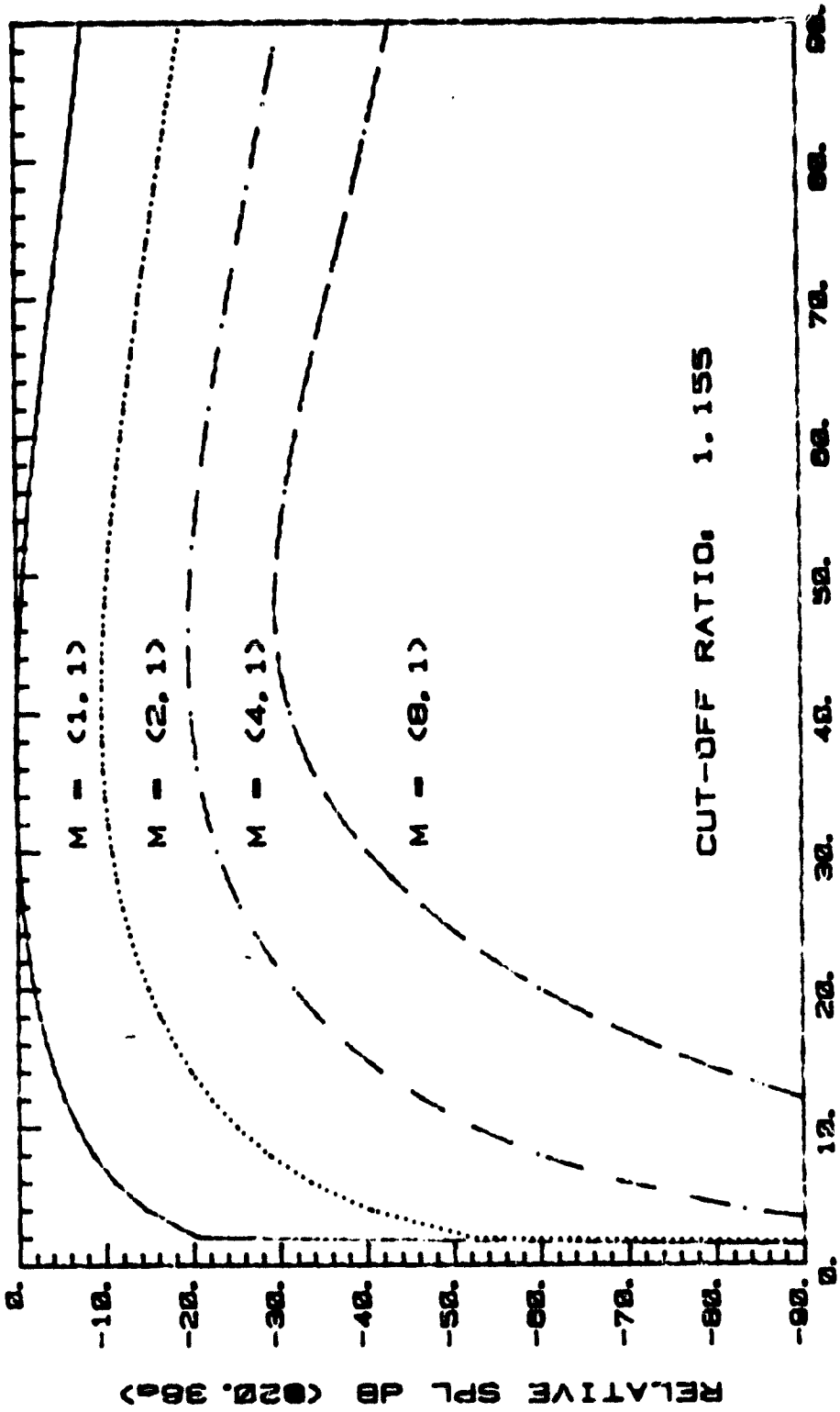

LANGLEY BELLMOUTH

Fig. 62b

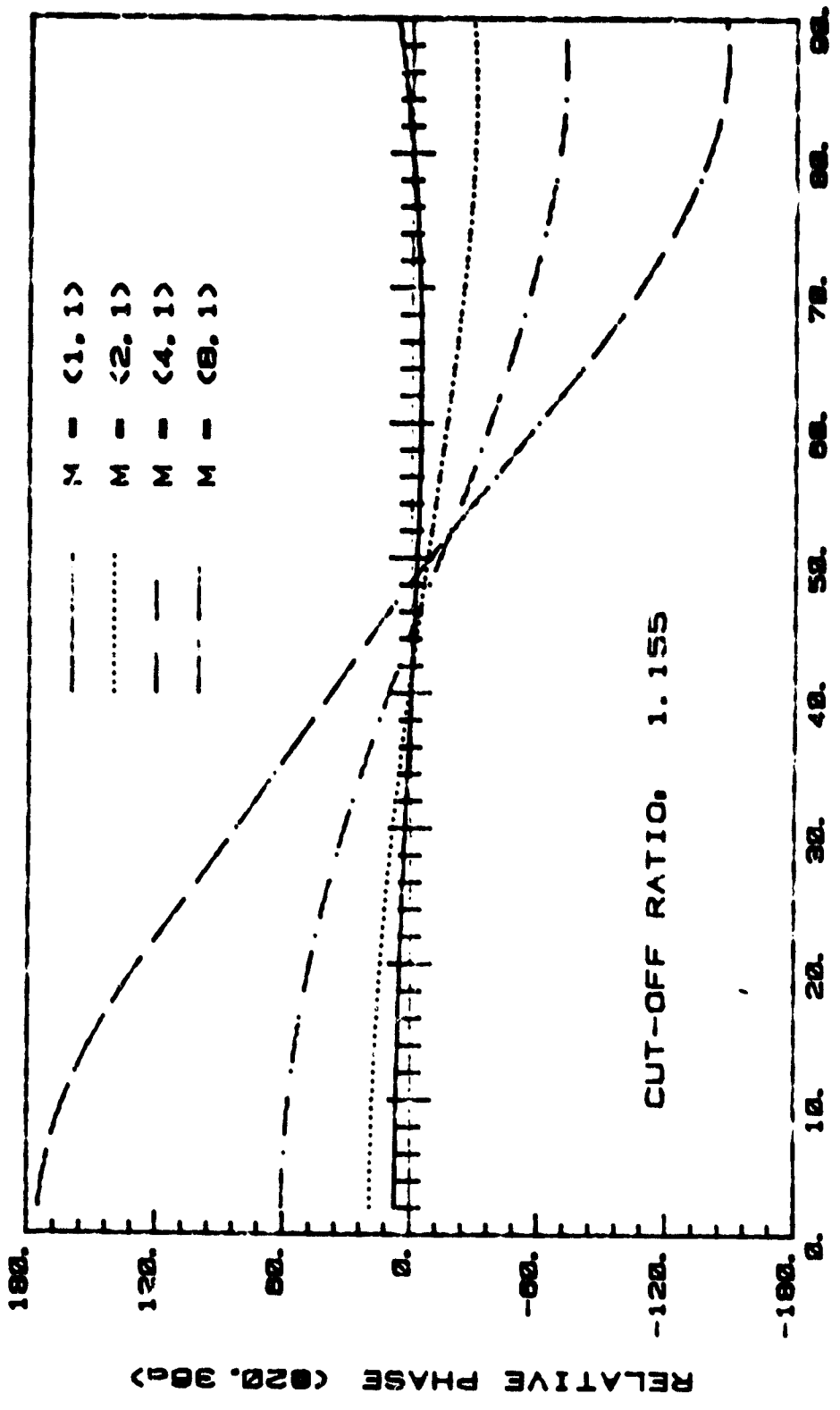

LANGLEY BELLMOUTH

Fig. 62c

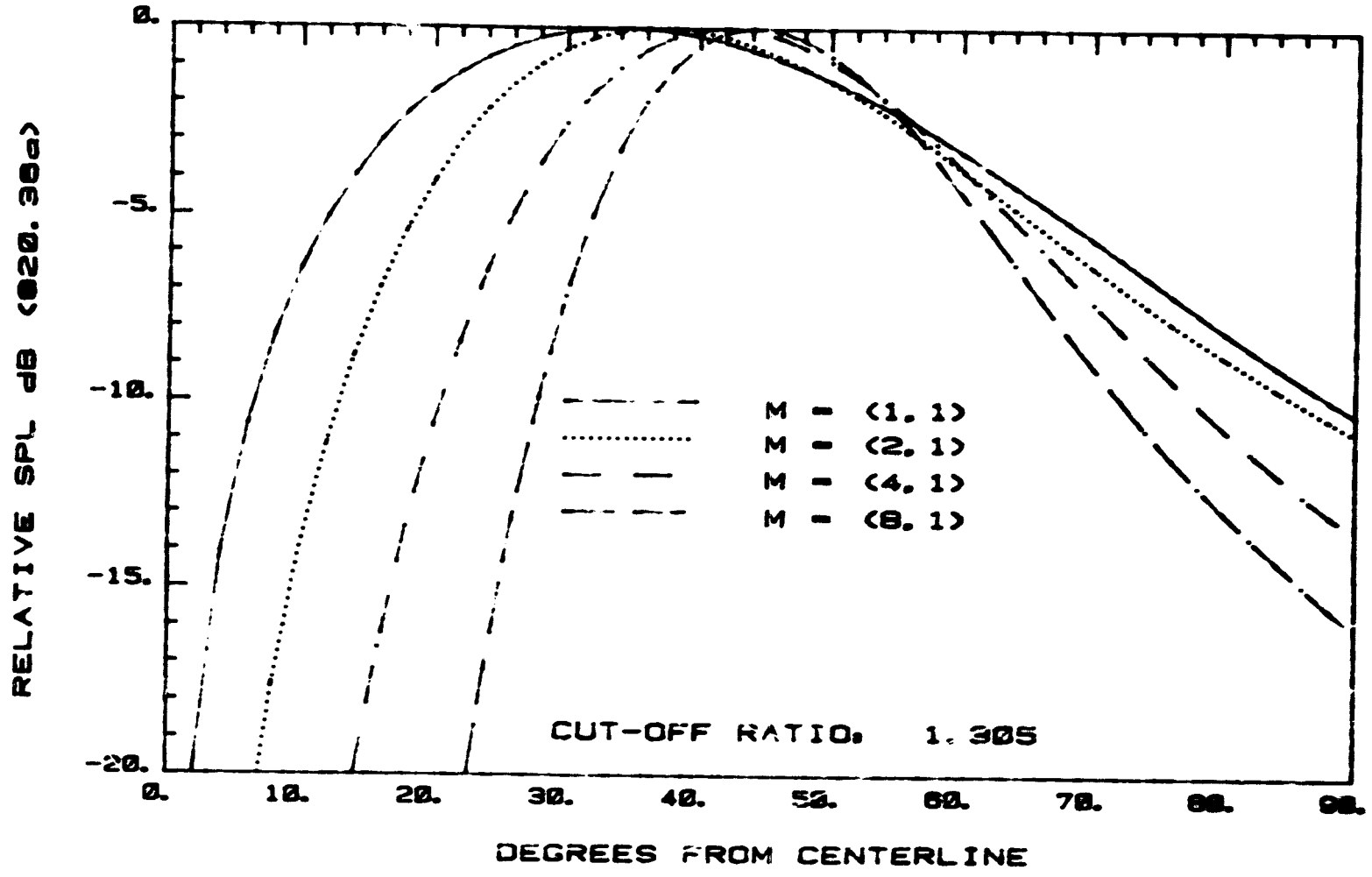

LANGLEY BELLMOUTH

Fig. 63a

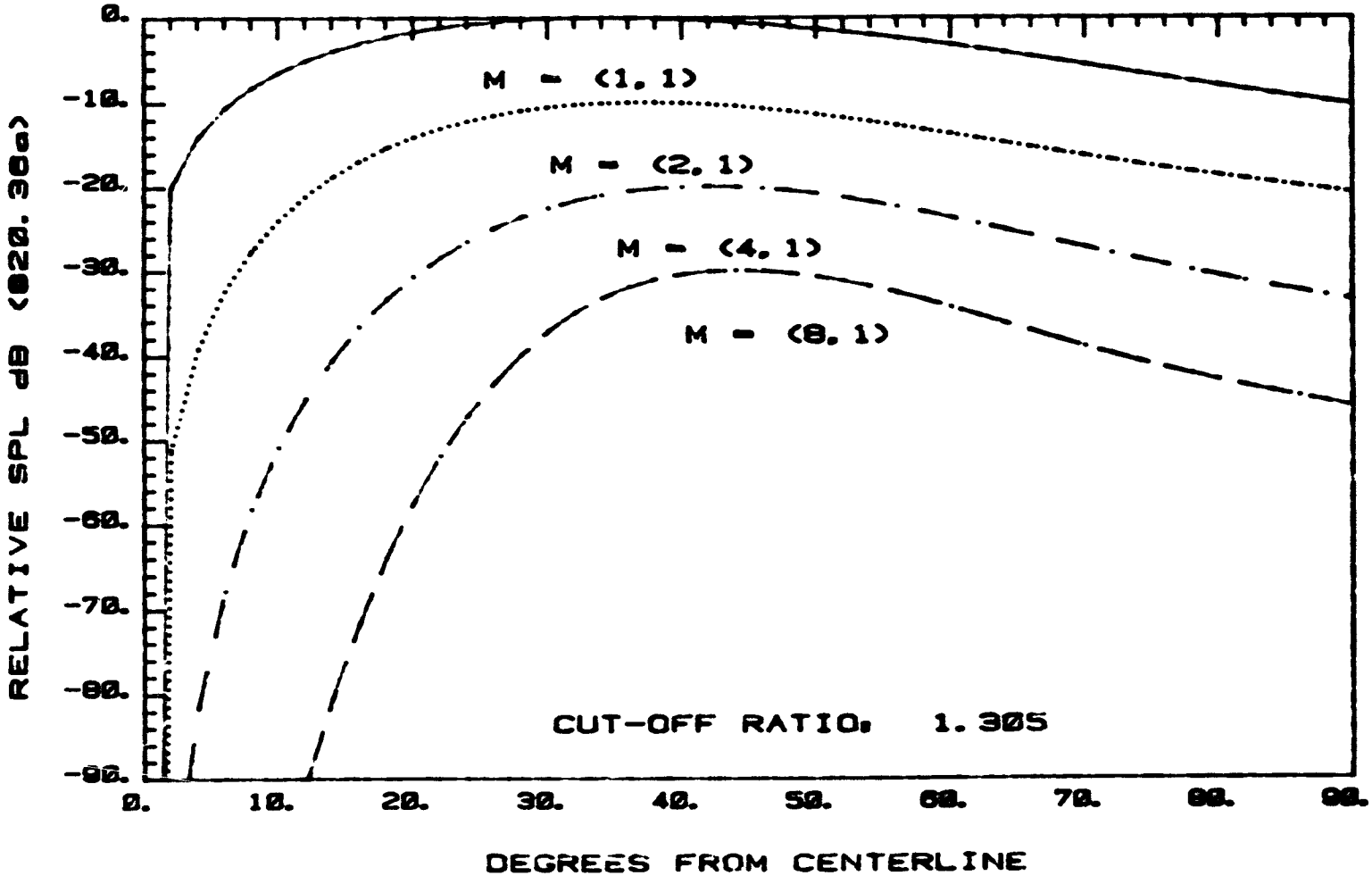

LANGLEY BELLMOUTH

Fig. 63b

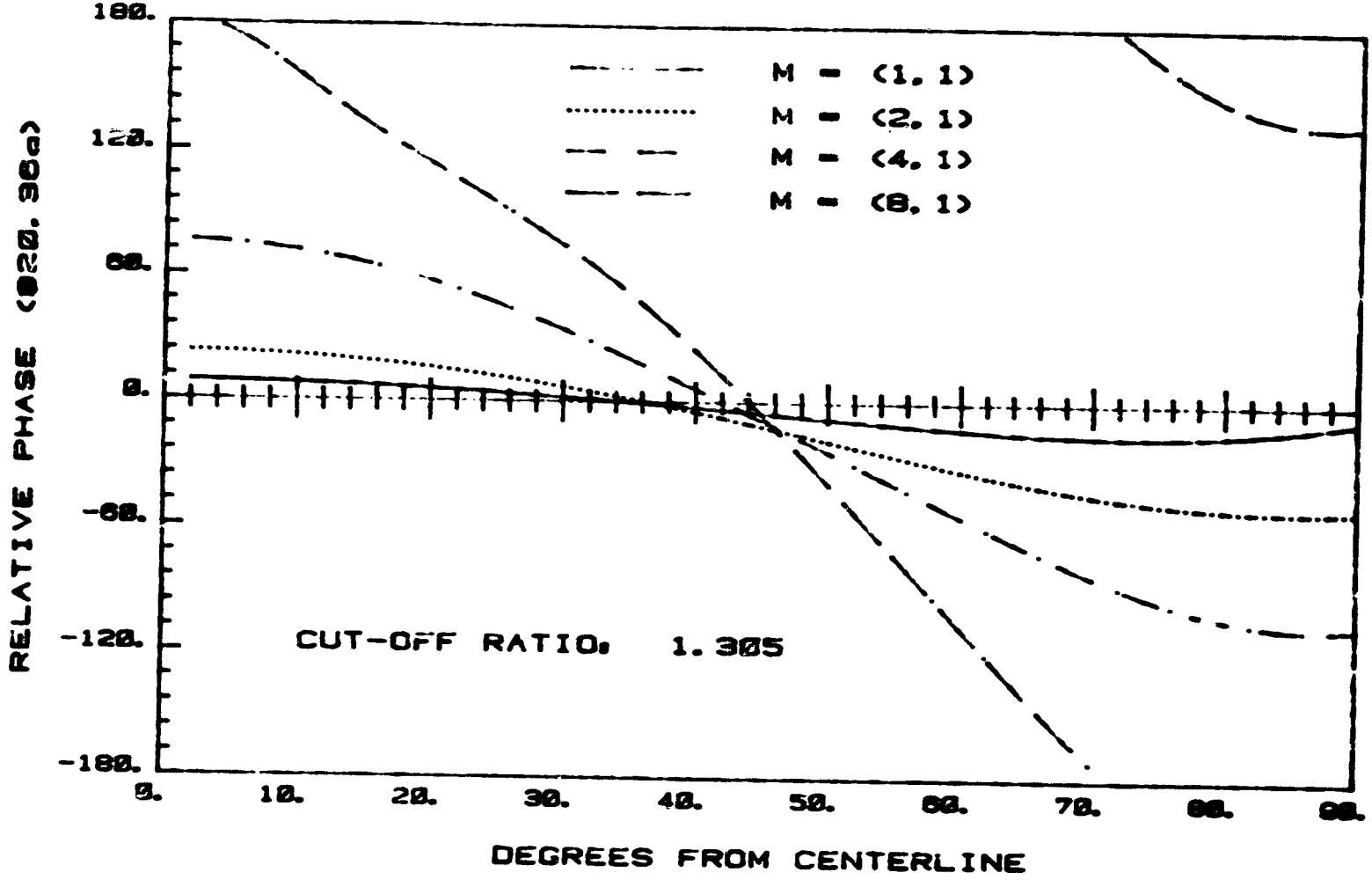

LANGLEY BELLMOUTH

Fig. 63c

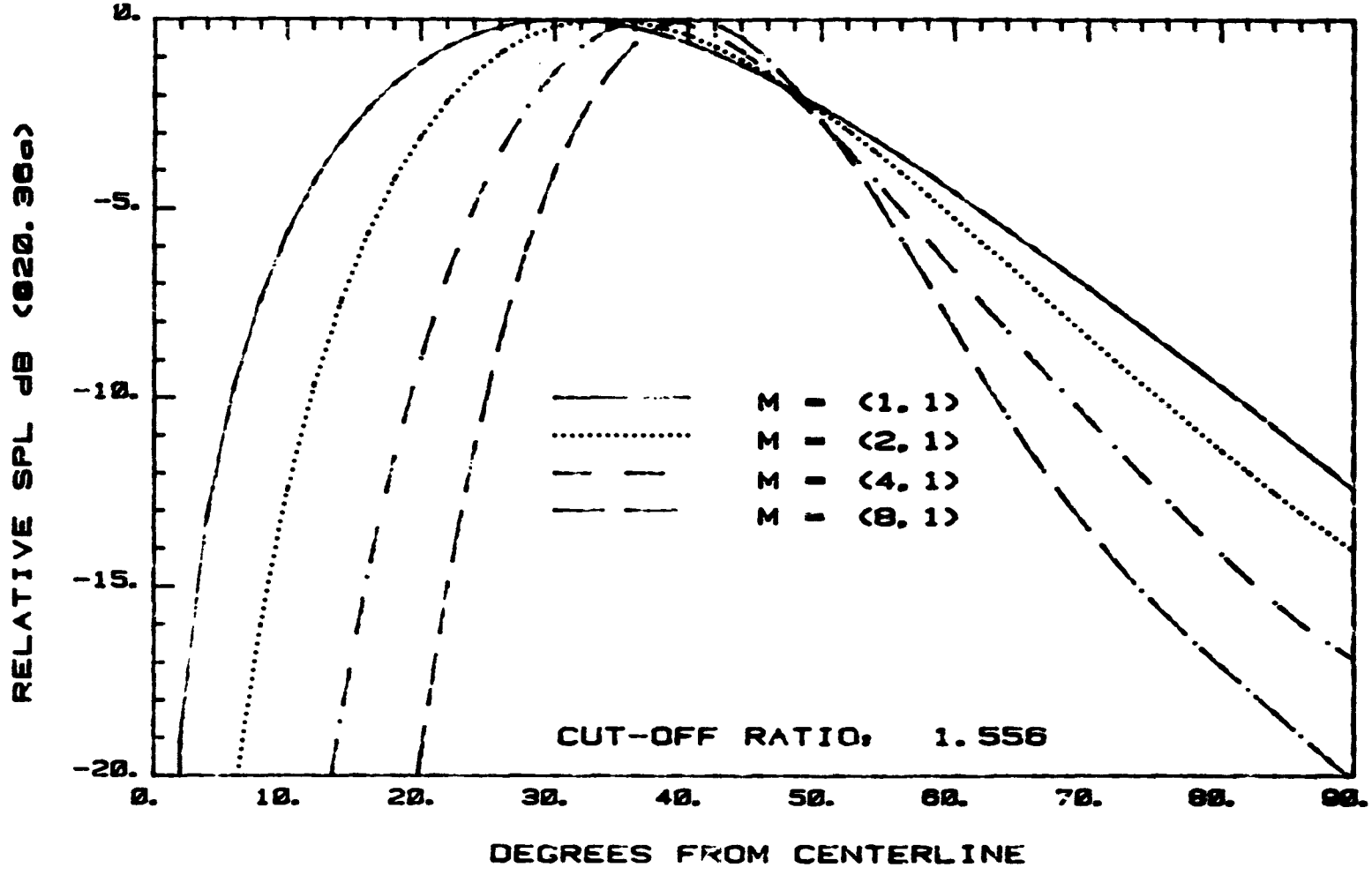

LANGLEY BELLMOUTH

Fig. 64a

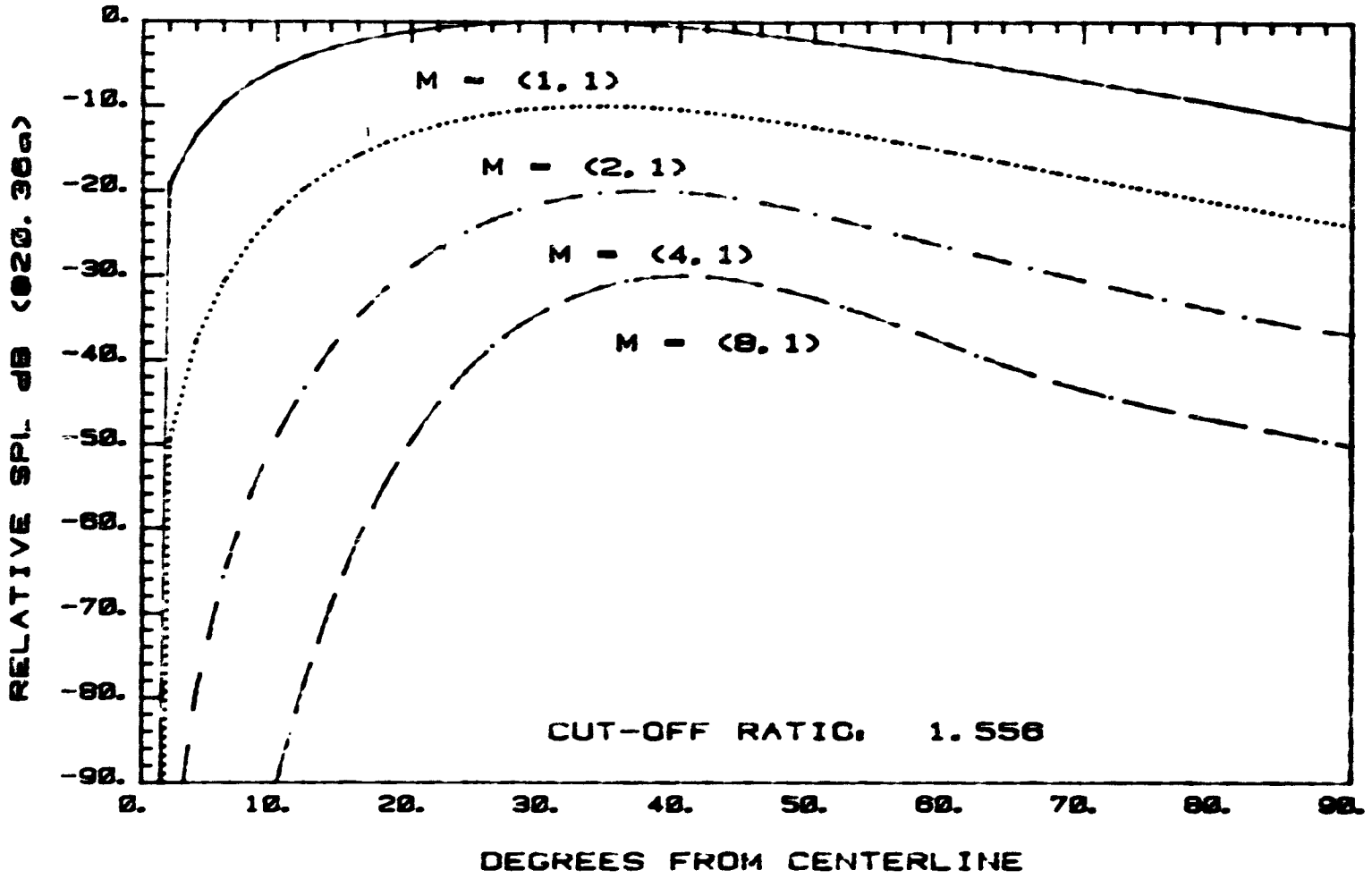

LANGLEY BELLMOUTH

Fig. 64b

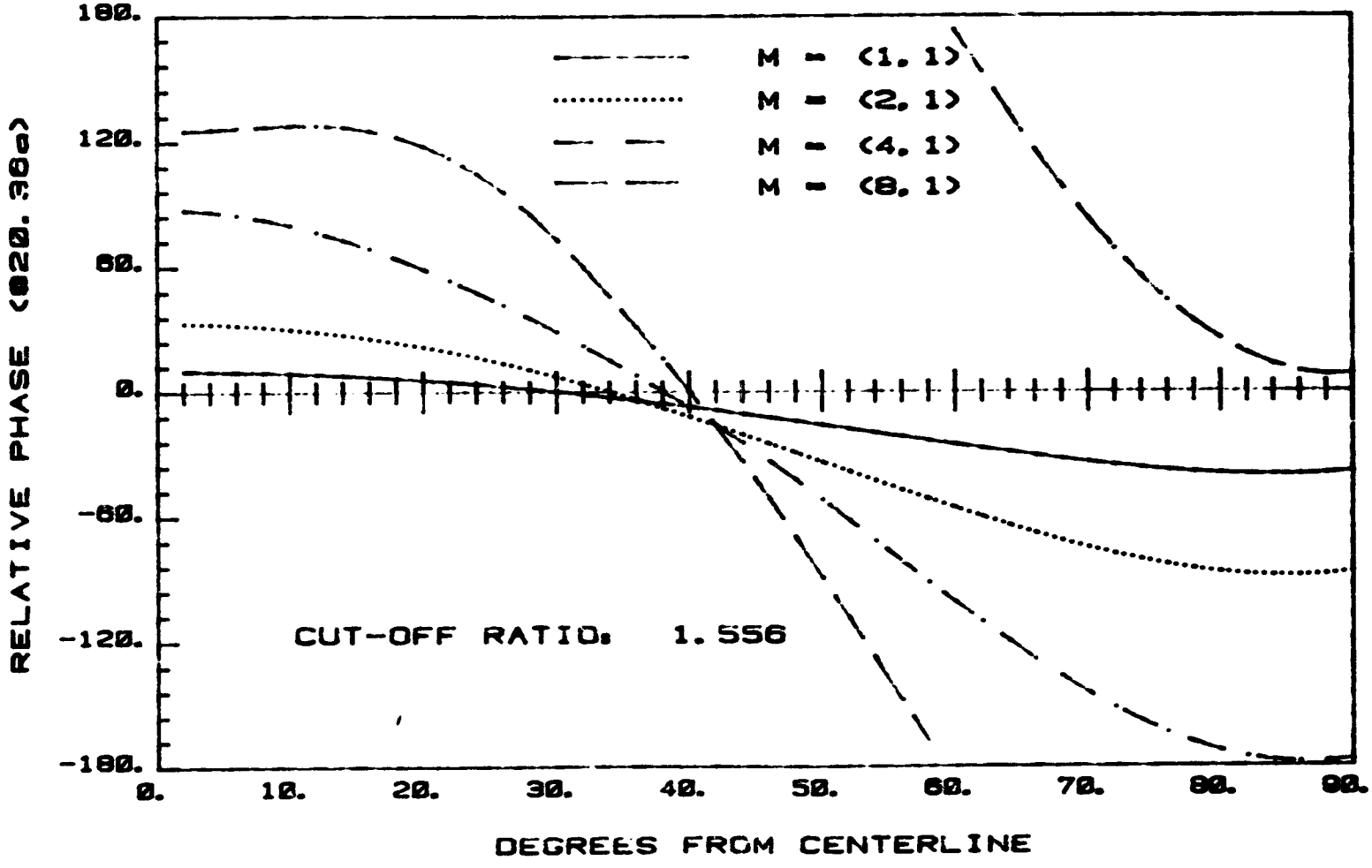

LANGLEY BELLMOUTH

Fig. 64c